

A general theory for anisotropic Kirchhoff-Love shells with in-plane bending of embedded fibers

Thang X. Duong^{a,b}, Vu N. Khiêm^b, Mikhail Itskov^{b,*}, and Roger A. Sauer^{a,c,d,*}

^aAachen Institute for Advanced Study in Computational Engineering Science (AICES), RWTH Aachen University, Templergraben 55, 52056 Aachen, Germany

^bDepartment of Continuum Mechanics, RWTH Aachen University, Templergraben 55, 52056 Aachen, Germany

^cFaculty of Civil and Environmental Engineering, Gdańsk University of Technology, ul. Narutowicza 11/12, 80-233 Gdańsk, Poland

^dDepartment of Mechanical Engineering, Indian Institute of Technology Kanpur, UP 208016, India

Published¹ in Mathematics and Mechanics of Solids, DOI: [10.1177/10812865221104427](https://doi.org/10.1177/10812865221104427)

Submitted on 12 October 2021; Last revised on 13 May 2022; Accepted on 14 May 2022

Abstract: This work presents a generalized Kirchhoff-Love shell theory that can explicitly capture fiber-induced anisotropy not only in stretching and out-of-plane bending, but also in in-plane bending. This setup is particularly suitable for heterogeneous and fibrous materials such as textiles, biomaterials, composites and pantographic structures. The presented theory is a direct extension of classical Kirchhoff-Love shell theory to incorporate the in-plane bending resistance of fibers. It also extends existing second-gradient Kirchhoff-Love shell theory for initially straight fibers to initially curved fibers. To describe the additional kinematics of multiple fiber families, a so-called in-plane curvature tensor – which is symmetric and of second order – is proposed. The effective stress tensor and the in-plane and out-of-plane moment tensors are then identified from the mechanical power balance. These tensors are all second order and symmetric in general. Constitutive equations for hyperelastic materials are derived from different expressions of the mechanical power balance. The weak form is also presented as it is required for computational shell formulations based on rotation-free finite element discretizations.

Keywords: anisotropic bending; fibrous composites; in-plane bending; Kirchhoff-Love shells; nonlinear gradient theory; textiles

List of important symbols

$\mathbf{1}$	identity tensor in \mathbb{R}^3
$\mathbf{a}_\alpha, \mathbf{a}^\alpha$	co- and contravariant tangent vectors at surface point $\mathbf{x} \in \mathcal{S}$; $\alpha = 1, 2$
$\mathbf{A}_\alpha, \mathbf{A}^\alpha$	co- and contravariant tangent vectors at surface point $\mathbf{X} \in \mathcal{S}_0$; $\alpha = 1, 2$
$\mathbf{a}_{\alpha,\beta}$	parametric derivative of \mathbf{a}_α w.r.t. ξ^β
$\mathbf{a}_{\alpha;\beta}$	covariant derivative of \mathbf{a}_α w.r.t. ξ^β
$a_{\alpha\beta}, a^{\alpha\beta}$	co- and contravariant surface metric at surface point $\mathbf{x} \in \mathcal{S}$
$A_{\alpha\beta}, A^{\alpha\beta}$	co- and contravariant surface metric at surface point $\mathbf{X} \in \mathcal{S}_0$
\mathbf{b}	out-of-plane curvature tensor of surface \mathcal{S} at surface point $\mathbf{x} \in \mathcal{S}$
$\bar{\mathbf{b}}$	in-plane curvature tensor at fiber point \mathbf{x} of fiber \mathcal{C} embedded in \mathcal{S}

* corresponding authors, email: itskov@km.rwth-aachen.de; sauer@aices.rwth-aachen.de

¹This pdf is the personal version of an article whose journal version is available at <https://journals.sagepub.com>

$b_{\alpha\beta}$	covariant components of tensor \mathbf{b} at surface point $\mathbf{x} \in \mathcal{S}$
$\bar{b}_{\alpha\beta}$	covariant components of tensor $\bar{\mathbf{b}}$ at fiber point $\mathbf{x} \in \mathcal{C} \subset \mathcal{S}$
\mathbf{b}_0	out-of-plane curvature tensor of surface \mathcal{S}_0 at surface point $\mathbf{X} \in \mathcal{S}_0$
$\bar{\mathbf{b}}_0$	in-plane curvature tensor of fiber \mathcal{C}_0 at fiber point $\mathbf{X} \in \mathcal{C}_0 \subset \mathcal{S}_0$
$B_{\alpha\beta}$	covariant components of tensor \mathbf{b}_0 at surface point $\mathbf{X} \in \mathcal{S}_0$
$\bar{B}_{\alpha\beta}$	covariant components of tensor $\bar{\mathbf{b}}_0$ at fiber point $\mathbf{X} \in \mathcal{C}_0 \subset \mathcal{S}_0$
β_\bullet	material parameters for fiber bending and torsion
\mathbf{c}	in-plane fiber director vector of fiber \mathcal{C} at fiber point $\mathbf{x} \in \mathcal{C} \subset \mathcal{S}$
\mathbf{c}_0	in-plane fiber director vector of fiber \mathcal{C}_0 at fiber point $\mathbf{X} \in \mathcal{C}_0 \subset \mathcal{S}_0$
c_α, c^α	co- and contravariant components of vector \mathbf{c} at fiber point $\mathbf{x} \in \mathcal{C} \subset \mathcal{S}$
$c_{\alpha;\beta}, c^\alpha_{;\beta}$	covariant derivatives of c_α and c^α
\mathbf{C}	right Cauchy-Green tensor of the shell mid-surface
\mathcal{C}	a curve representing a fiber embedded in shell surface \mathcal{S}
\mathcal{C}_0	initial configuration of fiber curve \mathcal{C} embedded in shell surface \mathcal{S}_0
\mathbf{D}	rate of surface deformation tensor
$\delta\dots$	variation of ...
δ_α^β	surface Kronecker delta
ϵ_\bullet	material parameters for fiber stretching and shearing
\mathbf{E}	Green-Lagrange strain tensor of the shell mid-surface
\mathbf{f}	prescribed surface loads
f^α	in-plane components of \mathbf{f}
\mathbf{F}	deformation gradient of the shell mid-surface
γ_{ij}	nominal angle between current fiber configurations \mathcal{C}_i and \mathcal{C}_j in \mathcal{S} ; $i \neq j$
γ_{ij}^0	nominal angle between reference fiber configurations \mathcal{C}_{0i} and \mathcal{C}_{0j} in \mathcal{S}_0 ; $i \neq j$
$\hat{\gamma}_{ij}$	absolute angle between fiber \mathcal{C}_i and \mathcal{C}_j ; $i \neq j$
G_{in}	inertial virtual work
G_{ext}	external virtual work
G_{int}	internal virtual work
$\Gamma_{\alpha\beta}^\gamma$	surface Christoffel symbols of the second kind on \mathcal{S}
$\bar{\Gamma}_{\alpha\beta}^\gamma$	surface Christoffel symbols of the second kind on \mathcal{S}_0
$\Gamma_{\alpha\beta}^c$	projection of vectors $\mathbf{a}_{\alpha,\beta}$ in direction \mathbf{c}
$\Gamma_{\alpha\beta}^\ell$	projection of vectors $\mathbf{a}_{\alpha,\beta}$ in direction ℓ
\mathbf{H}	collective symbol for various structural tensors
H	mean curvature of surface \mathcal{S} at surface point $\mathbf{x} \in \mathcal{S}$
$h^{\alpha\beta}$	collective symbol for components of various structural tensors
i	fiber index; added to all fiber-related quantities in case of multiple fibers
\mathbf{i}	surface identity tensor on \mathcal{S}
\mathbf{I}	surface identity tensor on \mathcal{S}_0
I_1	first invariant of \mathbf{C}
\mathcal{I}	parametrized interface obtained by cutting through \mathcal{S}
j	fiber index; added to all fiber-related quantities in case of multiple fibers
J	surface area change
k_n	absolute change in normal curvature κ_n at point \mathbf{x} of fiber $\mathcal{C} \subset \mathcal{S}$
k_g	absolute change in geodesic curvature κ_g at point \mathbf{x} of fiber $\mathcal{C} \subset \mathcal{S}$
k_n	stretch-excluded change in normal curvature κ_n at point \mathbf{x} of fiber $\mathcal{C} \subset \mathcal{S}$
k_g	stretch-excluded change in geodesic curvature κ_g at point \mathbf{x} of fiber $\mathcal{C} \subset \mathcal{S}$
κ	Gaussian curvature of surface \mathcal{S} at surface point $\mathbf{x} \in \mathcal{S}$
κ_n	normal curvature of current fiber configuration \mathcal{C} at $\mathbf{x} \in \mathcal{C} \subset \mathcal{S}$
κ_n^0	normal curvature of reference fiber configuration \mathcal{C}_0 at $\mathbf{X} \in \mathcal{C}_0 \subset \mathcal{S}_0$
κ_g	geodesic curvature of current fiber configuration \mathcal{C} at $\mathbf{x} \in \mathcal{C} \subset \mathcal{S}$

κ_g^0	geodesic curvature of reference fiber configuration \mathcal{C}_0 at $\mathbf{X} \in \mathcal{C}_0 \subset \mathcal{S}_0$
κ_g^Γ	contribution of the Christoffel symbol to geodesic curvature κ_g of fiber \mathcal{C}
κ_g^L	contribution of the gradient of \mathbf{L} to geodesic curvature κ_g of fiber \mathcal{C}
κ_p	principal curvature of fiber \mathcal{C} at fiber point $\mathbf{x} \in \mathcal{C} \subset \mathcal{S}$
K	kinetic energy of surface \mathcal{S}
K_n	nominal change in normal curvature κ_n at point \mathbf{x} of fiber $\mathcal{C} \subset \mathcal{S}$
K_g	nominal change in geodesic curvature κ_g at point \mathbf{x} of fiber $\mathcal{C} \subset \mathcal{S}$
\mathbf{K}	relative change of the out-of-plane curvature tensor
$\bar{\mathbf{K}}$	relative change of the in-plane curvature tensor
ℓ	normalized tangent vector of fiber \mathcal{C} at fiber point $\mathbf{x} \in \mathcal{C} \subset \mathcal{S}$
ℓ_α, ℓ^α	co- and contravariant components of ℓ in \mathcal{S} ; $\alpha = 1, 2$
$\ell^{\alpha\beta}$	contravariant components of structural tensor $\ell \otimes \ell$ in \mathcal{S}
$\ell_{\alpha;\beta}, \ell^\alpha_{;\beta}$	covariant derivatives of ℓ_α and ℓ^α
λ	stretch of fiber \mathcal{C} at fiber point $\mathbf{x} \in \mathcal{C} \subset \mathcal{S}$
\mathbf{L}	normalized tangent vector of fiber \mathcal{C}_0 at fiber point $\mathbf{X} \in \mathcal{C}_0 \subset \mathcal{S}_0$
L_α, L^α	co- and contravariant components of \mathbf{L} ; $\alpha = 1, 2$
$L^{\alpha\beta}$	contravariant components of structural tensor $\mathbf{L} \otimes \mathbf{L}$
$\hat{L}^\alpha_{;\beta}, \hat{L}_{\alpha;\beta}$	parametric derivatives $L^\alpha_{;\beta}$ and $L_{\alpha;\beta}$ scaled by inverted fiber stretch λ^{-1}
Λ	$= \lambda^2$; square of stretch of fiber $\mathcal{C} \subset \mathcal{S}$
$\hat{\mathbf{m}}$	moment vector acting on a cut \mathcal{I} normal to $\boldsymbol{\nu}$
$\hat{\mathbf{m}}^\alpha$	moment vector acting on a cut \mathcal{I} normal to \mathbf{a}^α
\mathbf{m}	component of $\hat{\mathbf{m}}$ causing out-of-plane bending and twisting
$\bar{\mathbf{m}}$	component of $\hat{\mathbf{m}}$ causing in-plane bending
$m^{\alpha\beta}$	components of moment tensor $\hat{\boldsymbol{\mu}}$ with basis $\mathbf{a}_\alpha \otimes \mathbf{a}_\beta$
\bar{m}^α	components of moment tensor $\hat{\boldsymbol{\mu}}$ with basis $\mathbf{a}_\alpha \otimes \mathbf{n}$
m_τ, m_ν, \bar{m}	components of moment vector $\hat{\mathbf{m}}$ in directions $\boldsymbol{\tau}$, $\boldsymbol{\nu}$, and \mathbf{n}
μ	surface shear modulus
$\bar{\mu}$	component of tensor $\hat{\boldsymbol{\mu}}_{\text{fib}}$ with basis $\ell \otimes \mathbf{n}$, causing in-plane bending of fiber \mathcal{C}
$\bar{\mu}_0$	moment component $\bar{\mu}$ scaled by J
$\boldsymbol{\mu}$	stress couple tensor associated with out-of-plane bending and twisting
$\boldsymbol{\mu}_0$	stress couple tensor obtained by the pull-back of tensor $J\boldsymbol{\mu}$.
$\bar{\boldsymbol{\mu}}$	stress couple tensor associated with in-plane bending of fiber \mathcal{C}
$\bar{\boldsymbol{\mu}}_0$	stress couple tensor obtained by the pull-back of tensor $J\bar{\boldsymbol{\mu}}$.
$\hat{\boldsymbol{\mu}}$	(total) internal moment tensor at $\mathbf{x} \in \mathcal{S}$
$\hat{\boldsymbol{\mu}}_{\text{fib}}$	(total) internal moment tensor within fiber \mathcal{C}
\mathbf{M}	stress couple vector associated with out-of-plane bending at cut $\mathcal{I} \perp \boldsymbol{\nu}$
\mathbf{M}^α	stress couple vectors associated with out-of-plane bending at cut $\mathcal{I} \perp \mathbf{a}^\alpha$
$\bar{\mathbf{M}}$	stress couple vector associated with in-plane bending of fiber \mathcal{C} at cut $\mathcal{I} \perp \boldsymbol{\nu}$
$\bar{\mathbf{M}}^\alpha$	stress couple vectors associated with in-plane bending at cut $\mathcal{I} \perp \mathbf{a}^\alpha$
$M^{\alpha\beta}$	contravariant components of stress couple tensor $-\boldsymbol{\mu}$
$M_0^{\alpha\beta}$	stress couple components $M^{\alpha\beta}$ scaled by J
$\bar{M}^{\alpha\beta}$	contravariant components of stress couple tensor $-\bar{\boldsymbol{\mu}}$
$\bar{M}_0^{\alpha\beta}$	stress couple components $\bar{M}^{\alpha\beta}$ scaled by J
$\bar{M}_{0\gamma}^{\alpha\beta}$	stress couple components for in-plane bending in second-gradient shell theory
\mathbf{n}	unit surface normal vector of \mathcal{S} at surface point $\mathbf{x} \in \mathcal{S}$
\mathbf{n}_p	principal normal vector of fiber \mathcal{C} at fiber point $\mathbf{x} \in \mathcal{C} \subset \mathcal{S}$
n_f	number of fiber families
\mathbf{N}	unit surface normal vector of \mathcal{S}_0 at surface point $\mathbf{X} \in \mathcal{S}_0$
$N^{\alpha\beta}$	in-plane contravariant components of Cauchy stress tensor $\boldsymbol{\sigma}$
$\nabla_s \bullet$	$= \bullet_{,\alpha} \otimes \mathbf{a}^\alpha$; surface gradient operator

$\bar{\nabla}_s \bullet$	$= \mathbf{i} \nabla_s \bullet$; projected surface gradient operator
$\boldsymbol{\nu}$	unit normal on cut \mathcal{I}
ν_α, ν^α	co- and contravariant components of $\boldsymbol{\nu}$
ξ^α	curvilinear coordinates; $\alpha = 1, 2$
\dot{w}_{int}	internal stress power per current area
\mathbf{P}	first Piola-Kirchhoff stress tensor of the shell surface
$P_{\text{int}}, P_{\text{ext}}$	surface internal and external power
\mathcal{P}	parametric domain spanned by ξ^1 and ξ^2
$\mathcal{R}, \mathcal{R}_0$	arbitrary simply-connected sub-region of surface \mathcal{S} or \mathcal{S}_0
q_i	Lagrange multiplier for the inextensibility constraint for fiber \mathcal{C}_i
ρ	areal mass density of surface \mathcal{S}
s	parameter coordinate of fiber \mathcal{C}
\mathcal{S}	current configuration of the shell surface
\mathcal{S}_0	reference configuration of the shell surface
$\partial\mathcal{S}$	boundary of \mathcal{S}
\mathbf{S}	second Piola-Kirchhoff stress tensor of the shell surface
S^α	contravariant, out-of-plane shear stress components
$S_{\alpha\beta}^\gamma$	change in Christoffel symbols from \mathcal{S}_0 to \mathcal{S}
$\boldsymbol{\sigma}$	Cauchy stress tensor within the shell
$\boldsymbol{\sigma}_{\text{fib}}$	Cauchy stress tensor within fiber \mathcal{C}
$\tilde{\sigma}^{\alpha\beta}$	effective membrane stress associated with in-plane curvature measure $c^\beta \ell_{\beta;\alpha}$
$\sigma^{\alpha\beta}$	effective membrane stress associated with in-plane curvature measure κ_g or $\bar{b}_{\alpha\beta}$
t	time variable
t_g	absolute change in geodesic torsion τ_g at point \mathbf{x} of fiber $\mathcal{C} \subset \mathcal{S}$
t_g	stretch-excluded change in geodesic torsion τ_g at point \mathbf{x} of fiber $\mathcal{C} \subset \mathcal{S}$
T_g	nominal change in geodesic torsion τ_g at point \mathbf{x} of fiber $\mathcal{C} \subset \mathcal{S}$
\mathbf{T}	traction vector acting on cut \mathcal{I} normal to $\boldsymbol{\nu}$
\mathbf{T}^α	traction vectors acting on cut \mathcal{I} normal to \mathbf{a}^α
T^α	in-plane contravariant components of traction vector \mathbf{T}
T^3	component of traction vector \mathbf{T} in direction \mathbf{n}
$\boldsymbol{\tau}$	unit vector along cut \mathcal{I}
$\boldsymbol{\tau}^\alpha$	effective stress vector work-conjugate to $\dot{\mathbf{a}}_\alpha$ in second-gradient shell theory
$\hat{\boldsymbol{\tau}}$	Kirchhoff stress tensor of the shell surface
τ_g	geodesic torsion of current fiber configuration \mathcal{C} at $\mathbf{x} \in \mathcal{C} \subset \mathcal{S}$
τ_g^0	geodesic torsion of reference fiber configuration \mathcal{C}_0 at $\mathbf{X} \in \mathcal{C}_0 \subset \mathcal{S}_0$
τ_α, τ^α	co- and contravariant components of vector $\boldsymbol{\tau}$
$\tau^{\alpha\beta}$	contravariant components of Kirchhoff stress tensor $\hat{\boldsymbol{\tau}}$ of the shell
\mathbf{v}	velocity, i.e. the material time derivative of \mathbf{x}
\mathcal{V}	space of admissible variations $\delta\mathbf{x}$
W	strain energy density function per reference area
\mathbf{x}	current position of a surface point on the current shell surface \mathcal{S}
\mathbf{x}_c	function describing curve \mathcal{C}
\mathbf{X}	initial position of \mathbf{x} on the reference shell surface \mathcal{S}_0
$\dot{\bullet}$	material time derivative

1 Introduction

Fiber reinforced composites have become an important material in the sports, automotive, marine, and aerospace industry owing to their high specific stiffness-to-weight ratio, which allows

for lightweight designs. To produce such composites, fabric sheets are formed by warp and weft yarns (i.e. in a bundle of fibers) loosely linked together by different technologies, resulting for example in woven fabrics or non-crimp fabrics. The fabrics are then draped (molded) into desired shapes before injecting liquid resin (adhesives). After the resin solidifies, the fibers are strongly bonded together in the final product.

In this work, we are interested in continuum models for fabric sheets both with and without matrix material. Such models are required for the description and simulation of fiber-reinforced shell structures and draping processes. Geometrically, fabric structures can be modeled by a surface with embedded curves representing yarns. From the microscopic point of view, the resistance (in-plane and out-of-plane) of fabrics results from the deformation of yarns and their interaction, i.e. their linkage and contact. In particular, axial stretching of fibers is associated with (anisotropic) membrane resistance, and the linkage between yarns offers shear resistance. Twisting of a yarn can be assumed to be fully associated with the second fundamental form of the yarn-embedding surface (Steigmann and Dell’Isola, 2015). Bending of a yarn can have both in-plane and out-of-plane components and is characterized by the corresponding curvatures. The out-of-plane curvature is associated with the second fundamental form, while the in-plane curvature is associated with the gradient of the surface metric.

Fabric sheets can be modeled as thin shells from the macroscopic point of view, and Kirchhoff-Love kinematics together with plane stress conditions are usually adopted. Membrane deformation is characterized by stretching and shearing, while out-of-plane deformation is characterized by bending and twisting. In Kirchhoff-Love shell models, two kinematical quantities – the surface metric and the second fundamental form – are used for the two deformation types. In the literature, the general case of arbitrarily large deformations and nonlinear material behavior of shells has been treated extensively. See e.g. the texts of Naghdi (1982); Pietraszkiewicz (1989); Libai and Simmonds (1998) and references therein. Here, we refer to this nonlinear case as classical Kirchhoff-Love shell theory. Note that although Kirchhoff-Love shell theory is mostly discussed for solids, its application can also be extended to liquid shells (Steigmann, 1999a). The incorporation of material anisotropy in classical Kirchhoff-Love shells due to embedded fibers – for both stretching and out-of-plane bending – is straightforward, see e.g. Tepole et al. (2015), Wu et al. (2018) and references therein. As shown by Roohbakhshan and Sauer (2017), classical Kirchhoff-Love shell theory also admits complex anisotropic bending models, e.g. due to fibers not located at the mid-surface.

While classical Kirchhoff-Love shell theory can also be regarded as a special case of Cosserat theory (Steigmann, 1999b)², it has its own development history and has the advantage of simplicity and intuitiveness when following its argument structure. Therefore, it facilitates building corresponding computational as well as physically-based constitutive models. This motivated Sauer and Duong (2017) to provide a unified formulation for both liquid and solid shells (within the framework of classical Kirchhoff-Love shell theory). Their work aimed at providing a concise, yet general theoretical framework for corresponding computational rotation-free shell formulations (Duong et al., 2017; Sauer et al., 2017).

It should be noted that most existing shell models, including classical Kirchhoff-Love shell theory, focus on out-of-plane bending, while the in-plane response is still based on the classical Cauchy continuum. That is, one assumes that there is no moment (or stress couple) causing in-plane bending at a material point. This assumption is usually sufficient when only the overall material behavior is of interest, as e.g. in the draping simulations of Khiêm et al. (2018). However, it fails to capture deformations governed by in-plane fiber bending, which are important

²From another point of view, classical Kirchhoff-Love shell theory also falls in the category of high gradient theories due to the high gradient term in the bending energy.

for obtaining accurate and convergent numerical results. An example of these are the localized shear bands (Ferretti et al., 2014; Boisse et al., 2017) in the bias-extension test. In this case, simulations with finite element shell models based on the in-plane Cauchy continuum will fail to converge to a finite width of the shear band under mesh refinement. Another example is the asymmetric deformation of woven fabrics with different in-plane fiber bending stiffness for different fiber families (Madeo et al., 2016; Barbagallo et al., 2017).

Similar effects of the in-plane bending stiffness can also be found in pantographic structures (Dell’Isola et al., 2016; Placidi et al., 2016; Dell’Isola et al., 2019) and fibrous composites, such as biological tissues (Gasser et al., 2006). Thus, a more general model that considers the in-plane bending response is required for fabrics, fibrous composites and pantographic structures.

The first theoretical work considering in-plane bending was presented by Wang and Pipkin (1986, 1987) to model cloth and cable networks. Their theory is a special form of finite-deformation fibrous plate theory with inextensible fibers that contain bending couples that are proportional to their curvature. Since in-plane bending is related to the in-plane components of the second displacement gradient, it can be captured by more general continuum theories, such as Cosserat theories (see e.g. Mindlin and Tiersten (1962); Koiter (1963); Toupin (1964)), and gradient theories (see e.g. Green and Rivlin (1964); Mindlin (1964, 1965); Germain (1973)). For 3D fiber-reinforced solids, Spencer and Soldatos (2007) introduced explicitly the bending resistance of embedded fibers in the context of nonlinear second-gradient theory. A computational model based on Spencer and Soldatos (2007) has been developed by Asmanoglu and Menzel (2017). Starting from Cosserat theory, Steigmann (2012) derives a fiber-reinforced solid model that includes fiber bending, twisting, and stretching.

Concerned with in-plane bending for thin structures, Steigmann and Dell’Isola (2015) presented a continuum model for woven fabric sheets modeled as orthotropic plates, which treats fibers as Kirchhoff-Love rods that are distributed continuously across the sheet. Although the concept of stress couples from Cosserat theory is used, the model of Steigmann and Dell’Isola (2015) can be categorized as second-gradient theory, since their material model depends on the first and second displacement gradients. Following this, Steigmann (2018) further developed a second-gradient shell model that explicitly includes general fiber bending, twisting, and stretching. There, a concise set of equilibrium equations, boundary conditions, and material symmetries are discussed. However, to the best of our knowledge, the theory has not yet been fully formulated for the general case of more than two fiber families with initially curved fibers.

Focusing on Kirchhoff-Love shells, Balabanov et al. (2019) presented a new shell model derived from the second displacement gradient theory of Mindlin (1964). A corresponding computational formulation was also discussed in Balabanov et al. (2019). However, explicit in-plane fiber bending is not considered and the weak form requires at least C^2 -continuity of the geometry. Recently, Schulte et al. (2020) applied the second-gradient theory of Steigmann (2018) directly to Kirchhoff-Love shells, and presented the first rotation-free computational shell formulation accounting for in-plane bending using C^1 -continuous discretization.

In this contribution, we propose a general Kirchhoff-Love shell theory that explicitly incorporates fiber bending (both in-plane and out-of-plane), geodesic fiber twisting, and stretching. Unlike the existing approaches that derive the Kirchhoff-Love shell from a more general theory, here our theory is constructed directly from Kirchhoff-Love thin shell assumptions without introducing extra degrees-of-freedom, such as independent directors or micro-displacements. It is shown that the in-plane fiber bending contribution can be formulated analogously to its out-of-plane counterpart. All the definitions of stresses and moments, and the equilibrium equations thus follow in the same manner as in classical Kirchhoff-Love shell theory. Unlike the second-gradient theory of Steigmann (2018), the stress couple (or double force) in our theory is fully

equivalent to the bending moment under Kirchhoff-Love assumptions.

Our approach provides several advantages over existing second-gradient shell theories, such as those of [Steigmann and Dell’Isola \(2015\)](#) and [Steigmann \(2018\)](#). In particular, it allows us to identify work-conjugated pairs of symmetric stress and symmetric strain measures for all terms, including a new in-plane stress couple and corresponding in-plane curvature tensor. Instead of using third order tensors for in-plane bending, as is done in current second-gradient shell theories, the stress and strain tensors in our theory are all of second order. Their invariants thus can be easily identified and geometrically interpreted, which is advantageous for constructing constitutive models. Furthermore, our theory admits a wide range of constitutive models for straight as well as initially curved fibers without limitation on the number of fiber families and the angles between them.

Besides, the presented work also aims at providing a general formulation that is suitable for a straightforward isogeometric finite element implementation ([Duong et al., 2022](#)). Since the in-plane bending term in our theory is analogous to the out-of-plane bending term, existing finite element formulations for out-of-plane bending can be easily extended to in-plane bending. As for existing formulations, the corresponding weak form requires at least C^1 -continuous surface discretizations in the framework of rotation-free finite element formulations. For the purpose of verifying finite element implementations, we further provide the analytical solution for several nonlinear benchmark examples. Here, we are restricting ourselves to hyperelastic material models for the fabrics. Inelastic behavior, e.g. due to inter- and intra-ply fiber sliding, will be considered in future work.

In summary, our approach contains the following novelties and merits compared to earlier works:

- A concise shell theory with in-plane bending that is a direct extension of classical Kirchhoff-Love thin shell theory,
- a general theory that can admit a wide range of constitutive models for straight or initially curved fibers with no limitation on the number of fiber families and the angles between them,
- the introduction of a new symmetric in-plane curvature tensor,
- the identification of work-conjugated pairs of symmetric stress and symmetric strain measures,
- the weak form as it is required for rotation-free finite element formulations,
- the analytical solution for several nonlinear benchmark examples that include different modes of fiber deformation and are useful for verifying computational formulations.

The following presentation is structured as follows: [Sec. 2](#) summarizes the kinematics of thin shells with embedded curves and introduces the in-plane curvature tensor to capture the in-plane curvature of fibers. With this, the balance laws are presented in [Sec. 3](#). Different choices of work-conjugated pairs are then discussed in [Sec. 4](#). [Sec. 5](#) gives some examples of constitutive models for the proposed theory. [Sec. 6](#) then presents the weak form. Several analytical benchmark examples supporting the proposed theory are presented in [Sec. 7](#). The paper is concluded by [Sec. 8](#).

2 Kinematics for thin shells with embedded curves

In this section, nonlinear Kirchhoff-Love shell kinematics ([Naghdi, 1982](#)) is extended to deforming surfaces with embedded curves. The extended kinematics allows to capture not only

stretching and out-of-plane bending, but also in-plane bending of the embedded curves. Fiber-induced anisotropy is allowed in all these modes of deformation. The description is presented fully in the general framework of curvilinear coordinates. The variation of different kinematical quantities can be found in Appendix A.

2.1 Geometric description

The mid-surface of a thin shell at time t is modeled in three dimensional space as a 2D manifold, denoted by \mathcal{S} . In curvilinear coordinates, \mathcal{S} is described by the one-to-one mapping of a point (ξ^1, ξ^2) in parameter space \mathcal{P} to the point $\mathbf{x} \in \mathcal{S}$ as

$$\mathbf{x} = \mathbf{x}(\xi^\alpha, t), \quad \text{with } \alpha = 1, 2. \quad (1)$$

The (covariant) tangent vectors along the convective coordinate curves ξ^α at any point $\mathbf{x} \in \mathcal{S}$ can be defined by

$$\mathbf{a}_\alpha := \frac{\partial \mathbf{x}}{\partial \xi^\alpha} = \mathbf{x}_{,\alpha}, \quad (2)$$

where the comma denotes the parametric derivative. The unit normal vector can then be defined by

$$\mathbf{n} := \frac{\mathbf{a}_1 \times \mathbf{a}_2}{\|\mathbf{a}_1 \times \mathbf{a}_2\|}. \quad (3)$$

From the tangent vectors \mathbf{a}_α in Eq. (2), the so-called dual tangent vectors, denoted by \mathbf{a}^α , are defined by

$$\mathbf{a}^\alpha \cdot \mathbf{a}_\beta = \delta_\beta^\alpha, \quad (4)$$

with δ_β^α being the Kronecker delta. The covariant and dual tangent vectors are related to each other by³ $\mathbf{a}_\alpha = a_{\alpha\beta} \mathbf{a}^\beta$ and $\mathbf{a}^\alpha = a^{\alpha\beta} \mathbf{a}_\beta$, where

$$a_{\alpha\beta} := \mathbf{a}_\alpha \cdot \mathbf{a}_\beta, \quad a^{\alpha\beta} := \mathbf{a}^\alpha \cdot \mathbf{a}^\beta \quad (5)$$

denote the co- and contravariant surface metric, respectively.

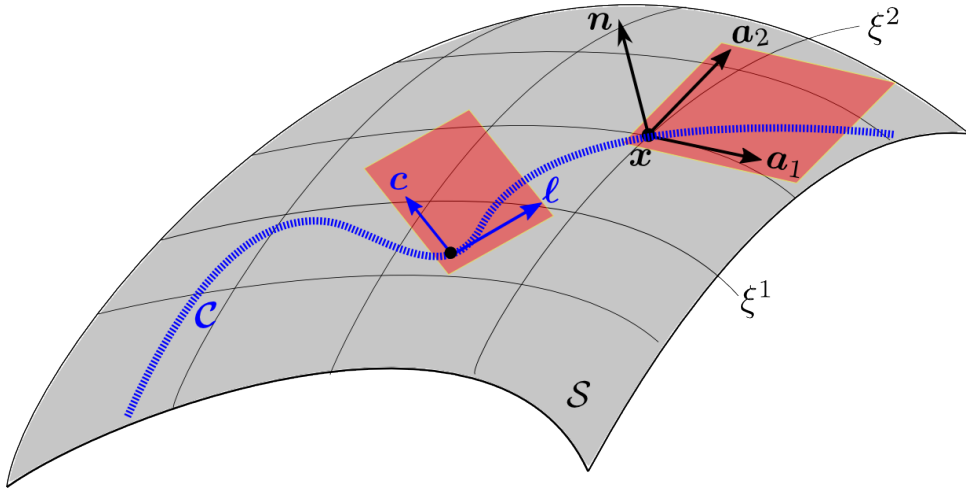


Figure 1: A fiber bundle represented by curve \mathcal{C} is embedded in shell surface \mathcal{S} . The red planes illustrate tangent planes

³In this paper, the summation convention is applied for repeated Greek indices taking values from 1 to 2.

Further, in order to model fibrous thin shells, a fiber (or a bundle of fibers) is geometrically represented by a curve \mathcal{C} defined by the points $\mathbf{x} = \mathbf{x}_c(s, t)$, with $ds = \|\mathrm{d}\mathbf{x}\|$, embedded in surface \mathcal{S} (see Fig. 1). The distribution of fibers is considered continuous such that a homogenized shell theory is obtained. The normalized tangent vector of \mathcal{C} , defined by

$$\boldsymbol{\ell} := \frac{\partial \mathbf{x}_c}{\partial s} = \ell_\alpha \mathbf{a}^\alpha = \ell^\alpha \mathbf{a}_\alpha, \quad (6)$$

represents the fiber direction at location s . Here, $\ell_\alpha := \boldsymbol{\ell} \cdot \mathbf{a}_\alpha$ and $\ell^\alpha := \boldsymbol{\ell} \cdot \mathbf{a}^\alpha$ denote the covariant and contravariant components of vector $\boldsymbol{\ell}$ in the convective coordinate system, respectively. Assuming that the deformation of fibers satisfies Euler-Bernoulli kinematics, the in-plane director for the fiber \mathcal{C} can be defined by

$$\mathbf{c} := \mathbf{n} \times \boldsymbol{\ell} = c_\alpha \mathbf{a}^\alpha = c^\alpha \mathbf{a}_\alpha, \quad (7)$$

where, $c_\alpha := \mathbf{c} \cdot \mathbf{a}_\alpha$ and $c^\alpha := \mathbf{c} \cdot \mathbf{a}^\alpha$ are the covariant and contravariant components of vector \mathbf{c} , respectively. With Eqs. (6) and (7), bases $\{\mathbf{a}_1, \mathbf{a}_2, \mathbf{n}\}$ and $\{\mathbf{a}^1, \mathbf{a}^2, \mathbf{n}\}$ can be represented by the local Cartesian basis $\{\boldsymbol{\ell}, \mathbf{c}, \mathbf{n}\}$ as

$$\mathbf{a}_\alpha = \ell_\alpha \boldsymbol{\ell} + c_\alpha \mathbf{c}, \quad \text{and} \quad \mathbf{a}^\alpha = \ell^\alpha \boldsymbol{\ell} + c^\alpha \mathbf{c}. \quad (8)$$

The surface identity tensor \mathbf{i} and the full identity $\mathbf{1}$ in \mathbb{R}^3 can then be written as

$$\mathbf{i} := \mathbf{a}_\alpha \otimes \mathbf{a}^\alpha = \mathbf{a}^\alpha \otimes \mathbf{a}_\alpha = \mathbf{c} \otimes \mathbf{c} + \boldsymbol{\ell} \otimes \boldsymbol{\ell}, \quad (9)$$

and

$$\mathbf{1} = \mathbf{i} + \mathbf{n} \otimes \mathbf{n}. \quad (10)$$

2.2 Surface curvature

The curvature of surface \mathcal{S} can be described by the symmetric second order tensor

$$\mathbf{b} := b_{\alpha\beta} \mathbf{a}^\alpha \otimes \mathbf{a}^\beta = b_{\alpha\beta}^\beta \mathbf{a}^\alpha \otimes \mathbf{a}_\beta = b^{\alpha\beta} \mathbf{a}_\alpha \otimes \mathbf{a}_\beta. \quad (11)$$

The components $b_{\alpha\beta}$ can be computed from the derivative of surface normal \mathbf{n} as

$$b_{\alpha\beta} := -\mathbf{n}_{,\alpha} \cdot \mathbf{a}_\beta, \quad (12)$$

which leads to Weingarten's formula

$$\mathbf{n}_{,\alpha} = -b_{\alpha\beta} \mathbf{a}^\beta. \quad (13)$$

Alternatively, components $b_{\alpha\beta}$ can be extracted from the derivatives of tangent vectors \mathbf{a}_α as

$$b_{\alpha\beta} := \mathbf{n} \cdot \mathbf{a}_{\alpha,\beta} = \mathbf{n} \cdot \mathbf{a}_{\alpha;\beta}, \quad (14)$$

where

$$\mathbf{a}_{\alpha,\beta} := \frac{\partial \mathbf{a}_\alpha}{\partial \xi^\beta} = \mathbf{x}_{,\alpha\beta}, \quad \text{and} \quad \mathbf{a}_{\alpha;\beta} := (\mathbf{n} \otimes \mathbf{n}) \mathbf{a}_{\alpha,\beta} = b_{\alpha\beta} \mathbf{n} \quad (15)$$

are the parametric and covariant derivative of \mathbf{a}_α , respectively.⁴

Unlike $\mathbf{n}_{,\alpha}$, which always lies in the tangent plane, $\mathbf{a}_{\alpha,\beta}$ can have both tangential and normal components. With respect to basis $\{\mathbf{a}_1, \mathbf{a}_2, \mathbf{n}\}$ the vectors $\mathbf{a}_{\alpha,\beta}$ can be expressed as

$$\mathbf{a}_{\alpha,\beta} = \Gamma_{\alpha\beta}^\gamma \mathbf{a}_\gamma + b_{\alpha\beta} \mathbf{n}, \quad (16)$$

⁴They only differ for quantities with free indices. Index-free quantities, such as \mathbf{n} , satisfy $\mathbf{n}_{,\alpha} = \mathbf{n}_{,\alpha}$.

where the tangential components

$$\Gamma_{\alpha\beta}^\gamma := \mathbf{a}_{\alpha,\beta} \cdot \mathbf{a}^\gamma \quad (17)$$

are known as the surface Christoffel symbols. They are symmetric in indices α and β . Using transformation (8.2), they can be expressed as

$$\Gamma_{\alpha\beta}^\gamma = c^\gamma \Gamma_{\alpha\beta}^c + \ell^\gamma \Gamma_{\alpha\beta}^\ell, \quad (18)$$

where we have defined

$$\begin{aligned} \Gamma_{\alpha\beta}^c &:= \mathbf{c} \cdot \mathbf{a}_{\alpha,\beta} = c_\gamma \Gamma_{\alpha\beta}^\gamma, \\ \Gamma_{\alpha\beta}^\ell &:= \mathbf{\ell} \cdot \mathbf{a}_{\alpha,\beta} = \ell_\gamma \Gamma_{\alpha\beta}^\gamma. \end{aligned} \quad (19)$$

The curvature tensor \mathbf{b} defined in Eq. (11) has the two invariants

$$H := \frac{1}{2} \text{tr}_s \mathbf{b} = \frac{1}{2} b_\alpha^\alpha, \quad \text{and} \quad \kappa = \det_s \mathbf{b} := \det[b_\alpha^\beta]. \quad (20)$$

They correspond to the mean and Gaussian curvatures, respectively. The curvature tensor \mathbf{b} fully describes the out-of-plane curvature of surface \mathcal{S} . Thus, we can extract from it the curvature of \mathcal{S} along any direction. For example,

$$\kappa_n := \mathbf{b} : \boldsymbol{\ell} \otimes \boldsymbol{\ell} = b_{\alpha\beta} \ell^{\alpha\beta}, \quad \text{with} \quad \ell^{\alpha\beta} := \ell^\alpha \ell^\beta, \quad (21)$$

represents the curvature of \mathcal{S} in direction $\boldsymbol{\ell}$. Hence, κ_n also expresses the so-called normal curvature of the curve \mathcal{C} embedded in \mathcal{S} . Further,

$$\tau_g := \mathbf{b} : \boldsymbol{\ell} \otimes \mathbf{c} = \mathbf{b} : \mathbf{c} \otimes \boldsymbol{\ell} = b_{\alpha\beta} \ell^\alpha c^\beta, \quad (22)$$

denotes the so-called geodesic torsion of \mathcal{C} .

The mentioned invariants H , κ , κ_n , and τ_g are included in Tab. 1. They are useful in constructing material models for (both isotropic and anisotropic) out-of-plane bending.

2.3 Curvature of embedded curves

We aim at capturing any geodesic torsion, normal and in-plane curvature of an embedded curve $\mathcal{C} \in \mathcal{S}$. As seen in Eqs. (21) and (22), the normal curvature and geodesic torsion of \mathcal{C} can already be described via the out-of-plane curvature tensor (11). The in-plane curvature, on the other hand, does not follow from tensor \mathbf{b} . Instead, it can be extracted from the so-called curvature vector of \mathcal{C} that is defined by the directional derivative of $\boldsymbol{\ell}$ in direction $\boldsymbol{\ell}$, i.e.

$$\boldsymbol{\ell}_{,s} := \frac{\partial \boldsymbol{\ell}}{\partial s} = (\nabla_s \boldsymbol{\ell}) \boldsymbol{\ell} = \ell^\alpha \boldsymbol{\ell}_{,\alpha}. \quad (23)$$

Here and henceforth, $\nabla_s \bullet := \bullet_{,\alpha} \otimes \mathbf{a}^\alpha$ denotes the surface gradient operator.⁵ Following Eq. (6) and considering Eqs. (4) and (16), derivative $\boldsymbol{\ell}_{,\alpha}$ can be expressed as

$$\boldsymbol{\ell}_{,\alpha} = \ell_{;\alpha}^\beta \mathbf{a}_\beta + \ell^\beta b_{\beta\alpha} \mathbf{n} = \ell_{\beta;\alpha} \mathbf{a}^\beta + \ell^\beta b_{\beta\alpha} \mathbf{n}, \quad (24)$$

where the semicolon denotes the covariant derivatives

$$\begin{aligned} \ell_{;\alpha}^\beta &:= \boldsymbol{\ell}_{,\alpha} \cdot \mathbf{a}^\beta = \ell_{,\alpha}^\beta + \ell^\gamma \Gamma_{\gamma\alpha}^\beta, \\ \ell_{\beta;\alpha} &:= \boldsymbol{\ell}_{,\alpha} \cdot \mathbf{a}_\beta = \ell_{\beta,\alpha} - \ell^\gamma \Gamma_{\beta\alpha}^\gamma. \end{aligned} \quad (25)$$

⁵Note, that $\nabla_s \bullet$ can have both in-plane and out-of-plane components.

Invariant	tensor notation	index notation	geometrical meaning
out-of-plane and in-plane curvature tensors: $\mathbf{b} = b_{\alpha\beta} \mathbf{a}^\alpha \otimes \mathbf{a}^\beta$ and $\bar{\mathbf{b}} = \bar{b}_{\alpha\beta} \mathbf{a}^\alpha \otimes \mathbf{a}^\beta$			
$H :=$	$\frac{1}{2} \text{tr}_s \mathbf{b}$	$\frac{1}{2} b_\alpha^\alpha$	mean curvature of \mathcal{S}
$\kappa :=$	$\det_s \mathbf{b}$	$\det[b_\alpha^\beta]$	Gaussian curvature of \mathcal{S}
$\kappa_n :=$	$\mathbf{b} : \boldsymbol{\ell} \otimes \boldsymbol{\ell} = \boldsymbol{\ell}_{,s} \cdot \mathbf{n}$	$b_{\alpha\beta} \ell^{\alpha\beta}$	normal curvature of $\mathcal{C} \in \mathcal{S}$
$\tau_g :=$	$\mathbf{b} : \boldsymbol{\ell} \otimes \mathbf{c} = \mathbf{b} : \mathbf{c} \otimes \boldsymbol{\ell}$	$b_{\alpha\beta} \ell^\alpha c^\beta$	geodesic torsion of $\mathcal{C} \in \mathcal{S}$
$\kappa_g :=$	$\bar{\mathbf{b}} : \boldsymbol{\ell} \otimes \boldsymbol{\ell}$	$\bar{b}_{\alpha\beta} \ell^{\alpha\beta}$	geodesic curvature of $\mathcal{C} \in \mathcal{S}$
$\kappa_p :=$	$\ \boldsymbol{\ell}_{,s}\ $	$\sqrt{\kappa_g^2 + \kappa_n^2}$	principal curvature of $\mathcal{C} \in \mathcal{S}$
measures for the change in normal curvature κ_n of $\mathcal{C} \in \mathcal{S}$			
$k_n :=$	$\mathbf{b} : \boldsymbol{\ell} \otimes \boldsymbol{\ell} - \mathbf{b}_0 : \mathbf{L} \otimes \mathbf{L}$	$\kappa_n - \kappa_n^0$	absolute change
$k_n :=$	$\mathbf{b} : \lambda \boldsymbol{\ell} \otimes \boldsymbol{\ell} - \mathbf{b}_0 : \mathbf{L} \otimes \mathbf{L}$	$\kappa_n \lambda - \kappa_n^0$	stretch-excluded change
$K_n :=$	$\mathbf{K} : \mathbf{L} \otimes \mathbf{L}$	$\kappa_n \lambda^2 - \kappa_n^0$	nominal change
measures for the change in geodesic torsion τ_g of $\mathcal{C} \in \mathcal{S}$			
$t_g :=$	$\mathbf{b} : \boldsymbol{\ell} \otimes \mathbf{c} - \mathbf{b}_0 : \mathbf{L} \otimes \mathbf{c}_0$	$\tau_g - \tau_g^0$	absolute change
$t_g :=$	$\mathbf{b} : \lambda \boldsymbol{\ell} \otimes \mathbf{c} - \mathbf{b}_0 : \mathbf{L} \otimes \mathbf{c}_0$	$\tau_g \lambda - \tau_g^0$	stretch-excluded change
$T_g :=$	$\mathbf{K} : \mathbf{L} \otimes \mathbf{c}_0$	$b_{\alpha\beta} c_0^\alpha L^\beta - \tau_g^0$	nominal change
measures for the change in geodesic curvature κ_g of $\mathcal{C} \in \mathcal{S}$			
$k_g :=$	$\bar{\mathbf{b}} : \boldsymbol{\ell} \otimes \boldsymbol{\ell} - \bar{\mathbf{b}}_0 : \mathbf{L} \otimes \mathbf{L}$	$\kappa_g - \kappa_g^0$	absolute change
$k_g :=$	$\bar{\mathbf{b}} : \lambda \boldsymbol{\ell} \otimes \boldsymbol{\ell} - \bar{\mathbf{b}}_0 : \mathbf{L} \otimes \mathbf{L}$	$\kappa_g \lambda - \kappa_g^0$	stretch-excluded change
$K_g :=$	$\bar{\mathbf{K}} : \mathbf{L} \otimes \mathbf{L}$	$\kappa_g \lambda^2 - \kappa_g^0$	nominal change

Table 1: Various curvature measures of the surface \mathcal{S} and of a fiber family \mathcal{C} embedded in \mathcal{S} . Note, that the magnitude of these measures is invariant, but their sign (except for κ and κ_p) depends on the direction of directors \mathbf{n} and/or \mathbf{c} . All these measures can be shown to be frame invariant under superimposed rigid body motions of \mathcal{S} , see Appendix B.

The magnitude $\|\boldsymbol{\ell}_{,s}\| =: \kappa_p$ is called the principal curvature of \mathcal{C} ,⁶ and the direction $\boldsymbol{\ell}_{,s}/\kappa_p =: \mathbf{n}_p$ is referred to as the principal normal to \mathcal{C} . Note that \mathbf{n}_p is normal to the curve but not necessarily normal to the surface \mathcal{S} .

In principle, vector $\boldsymbol{\ell}_{,s}$ can be expressed in any basis, which then induces different curvatures from the corresponding components. Here, we express $\boldsymbol{\ell}_{,s}$ in the basis $\{\boldsymbol{\ell}, \mathbf{c}, \mathbf{n}\}$, i.e.

$$\boldsymbol{\ell}_{,s} = \kappa_p \mathbf{n}_p = \kappa_g \mathbf{c} + \kappa_n \mathbf{n}, \quad (26)$$

where

$$\kappa_n := \mathbf{n} \cdot \boldsymbol{\ell}_{,s}, \quad (27)$$

denotes the normal curvature of \mathcal{C} . By inserting (23) and (24), κ_n can be shown to be identical to Eq. (21). On the other hand,

$$\kappa_g := \mathbf{c} \cdot \boldsymbol{\ell}_{,s} \quad (28)$$

⁶since it is the sole principal invariant of the first order tensor $\boldsymbol{\ell}_{,s}$.

is the in-plane (i.e. geodesic) curvature of \mathcal{C} . It can be computed by inserting (23) and (24) into Eq. (28), giving

$$\kappa_g = \ell_{\alpha;\beta} c^\alpha \ell^\beta = \ell_{;\beta}^\alpha c_\alpha \ell^\beta = (\bar{\nabla}_s \boldsymbol{\ell}) : \mathbf{c} \otimes \boldsymbol{\ell} , \quad (29)$$

where

$$\bar{\nabla}_s \boldsymbol{\ell} := \mathbf{i} \nabla_s \boldsymbol{\ell} = \ell_{\alpha;\beta} \mathbf{a}^\alpha \otimes \mathbf{a}^\beta = \ell_{;\beta}^\alpha \mathbf{a}_\alpha \otimes \mathbf{a}^\beta \quad (30)$$

denotes the projected surface gradient of $\boldsymbol{\ell}$.⁷

Remark 2.1: From Eq. (26) follows

$$\kappa_p^2 = \kappa_g^2 + \kappa_n^2 . \quad (31)$$

Remark 2.2: The three scalars κ_n , κ_g , and τ_g are associated with the three bending modes of $\mathcal{C} \in \mathcal{S}$: normal (i.e. out-of-plane) bending, geodesic (i.e. in-plane) bending, and geodesic torsion, respectively.

2.4 Definition of the in-plane curvature tensor

In principle, we can use the second order tensor $\bar{\nabla}_s \boldsymbol{\ell}$ to characterize the in-plane curvature as the counterpart to tensor \mathbf{b} from Eq. (11), which characterizes the out-of-plane curvature. Tensor $\bar{\nabla}_s \boldsymbol{\ell}$ is, however, unsymmetric. We thus construct an alternative tensor by rewriting Eq. (29) and using identity $\mathbf{c}_{,s} \cdot \boldsymbol{\ell} = -\mathbf{c} \cdot \boldsymbol{\ell}_{,s}$ that follows from $\mathbf{c} \cdot \boldsymbol{\ell} = 0$, so that

$$\kappa_g := -\ell_\alpha^\beta c_{;\beta}^\alpha = -\ell^{\alpha\beta} c_{\alpha;\beta} = \bar{\mathbf{b}} : \boldsymbol{\ell} \otimes \boldsymbol{\ell} , \quad (32)$$

where

$$c_{;\alpha}^\beta := c_{,\alpha}^\beta + c^\gamma \Gamma_{\gamma\alpha}^\beta , \quad \text{and} \quad c_{\beta;\alpha} := c_{\beta,\alpha} - c_\gamma \Gamma_{\beta\alpha}^\gamma , \quad (33)$$

similar to Eq. (25). Here, we have defined the so-called in-plane curvature tensor of \mathcal{C} as

$$\bar{\mathbf{b}} := -\frac{1}{2} [\bar{\nabla}_s \mathbf{c} + (\bar{\nabla}_s \mathbf{c})^T] = -\frac{1}{2} (c_{\alpha;\beta} + c_{\beta;\alpha}) \mathbf{a}^\alpha \otimes \mathbf{a}^\beta = \bar{b}_{\alpha\beta} \mathbf{a}^\alpha \otimes \mathbf{a}^\beta . \quad (34)$$

Components $\bar{b}_{\alpha\beta}$ thus can be computed from

$$\bar{b}_{\alpha\beta} = \bar{\mathbf{b}} : \mathbf{a}_\alpha \otimes \mathbf{a}_\beta = -\frac{1}{2} (c_{\alpha;\beta} + c_{\beta;\alpha}) = -\frac{1}{2} (\mathbf{c}_{,\alpha} \cdot \mathbf{a}_\beta + \mathbf{c}_{,\beta} \cdot \mathbf{a}_\alpha) , \quad (35)$$

where

$$\begin{aligned} \mathbf{c}_{,\alpha} = \mathbf{c}_{;\alpha} &= c^\beta \mathbf{a}_{\beta;\alpha} + c_{;\alpha}^\beta \mathbf{a}_\beta \\ &= c_\beta \mathbf{a}_{;\alpha}^\beta + c_{\beta;\alpha} \mathbf{a}^\beta \\ &= b_{\alpha\beta} c^\beta \mathbf{n} - c^\beta \ell_{\beta;\alpha} \boldsymbol{\ell} . \end{aligned} \quad (36)$$

The last equation is obtained from identities $\mathbf{c} \cdot \mathbf{n} = 0$, $\boldsymbol{\ell} \cdot \mathbf{n} = 0$, Eqs. (24) and (13). The quantities $\bar{b}_{\alpha\beta}$, κ_g , $c_{\beta;\alpha}$, and $\ell_{\beta;\alpha}$ can be shown to be frame invariant under superimposed rigid body motions of \mathcal{S} , see Appendix B.

Remark 2.3: Since vector $\boldsymbol{\ell}$ is normalized, we have the identity

$$\boldsymbol{\ell} \cdot \boldsymbol{\ell}_{,\alpha} = \ell_\beta \ell_{;\alpha}^\beta = \ell^\beta \ell_{\beta;\alpha} = 0 , \quad (37)$$

due to Eq. (24). Further, equating Eqs. (29) and (32) gives the relation

$$\ell^\beta c_{\beta;\alpha} = -c^\beta \ell_{\beta;\alpha} , \quad (38)$$

and from Eq. (36), we find

$$\begin{aligned} c_{\beta;\alpha} &= \mathbf{a}_\beta \cdot \mathbf{c}_{,\alpha} = -c^\gamma \ell_\beta \ell_{\gamma;\alpha} \\ c_{;\alpha}^\beta &= \mathbf{a}^\beta \cdot \mathbf{c}_{,\alpha} = -c^\gamma \ell^\beta \ell_{\gamma;\alpha} . \end{aligned} \quad (39)$$

⁷Unlike $\nabla_s \bullet$, $\bar{\nabla}_s \bullet$ has only in-plane components.

2.5 Shell deformation

To characterize the shell deformation, a reference configuration \mathcal{S}_0 is chosen. The tangent vectors \mathbf{A}_α , the normal vector \mathbf{N} , the surface metric $A_{\alpha\beta}$, the out-of-plane curvature tensor $\mathbf{b}_0 := B_{\alpha\beta} \mathbf{A}^\alpha \otimes \mathbf{A}^\beta$ are defined on \mathcal{S}_0 similarly to Eqs (2), (3), (5), and (11), respectively. The fiber embedded within the shell surface is denoted by \mathcal{C}_0 in the reference configuration. Also, the normalized fiber direction $\mathbf{L} = L^\alpha \mathbf{A}_\alpha = L_\alpha \mathbf{A}^\alpha$, the in-plane fiber director $\mathbf{c}_0 = c_\alpha^0 \mathbf{A}^\alpha$, and the in-plane curvature tensor $\bar{\mathbf{b}}_0 := \bar{B}_{\alpha\beta} \mathbf{A}^\alpha \otimes \mathbf{A}^\beta = -\frac{1}{2} (c_{\alpha;\beta}^0 + c_{\beta;\alpha}^0) \mathbf{A}^\alpha \otimes \mathbf{A}^\beta$ are defined similarly to Eqs. (6), (7), and (34), respectively.

Having $a_{\alpha\beta}$, $b_{\alpha\beta}$, and $\bar{b}_{\alpha\beta}$ the deformation of a shell can now be characterized by the following three tensors:

1. The surface deformation gradient:

$$\mathbf{F} := \mathbf{a}_\alpha \otimes \mathbf{A}^\alpha . \quad (40)$$

This tensor can be used to map the reference fiber direction \mathbf{L} to $\boldsymbol{\ell}$ as

$$\lambda \boldsymbol{\ell} = \mathbf{F} \mathbf{L} = L^\alpha \mathbf{a}_\alpha , \quad (41)$$

where λ is the fiber stretch. Comparing (6) and (41) gives

$$\boldsymbol{\ell}^\alpha = L^\alpha \lambda^{-1} . \quad (42)$$

From (25) and (42) follows that

$$\ell_{\alpha;\beta} = \hat{L}_{\alpha,\beta} - \ell_{\alpha\gamma} (\hat{L}_{,\beta}^\gamma + \ell^\delta \Gamma_{\delta\beta}^\gamma) + \ell^\gamma \mathbf{a}_\alpha \cdot \mathbf{a}_{\gamma,\beta} , \quad (43)$$

where

$$\hat{L}_{,\beta}^\alpha := \lambda^{-1} L_{,\beta}^\alpha , \quad \text{and} \quad \hat{L}_{\alpha,\beta} := a_{\alpha\gamma} \hat{L}_{,\beta}^\gamma . \quad (44)$$

Inserting (43) into Eq. (39) gives

$$\begin{aligned} c_{\beta;\alpha} &= -\ell_\beta (c^\gamma \hat{L}_{\gamma,\alpha} + \ell^\gamma \Gamma_{\gamma\alpha}^c) , \\ c_{;\alpha}^\beta &= -\ell^\beta (c^\gamma \hat{L}_{\gamma,\alpha} + \ell^\gamma \Gamma_{\gamma\alpha}^c) . \end{aligned} \quad (45)$$

With the surface deformation gradient, the right Cauchy-Green surface tensor is defined by $\mathbf{C} := \mathbf{F}^T \mathbf{F} = a_{\alpha\beta} \mathbf{A}^\alpha \otimes \mathbf{A}^\beta$. Tab. 2 lists some invariants induced by \mathbf{C} that can be useful for constructing material models. The Green-Lagrange surface strain tensor, which represents the change of the surface metric, is then defined by

$$\mathbf{E} := \frac{1}{2} (\mathbf{C} - \mathbf{I}) = \frac{1}{2} (a_{\alpha\beta} - A_{\alpha\beta}) \mathbf{A}^\alpha \otimes \mathbf{A}^\beta = E_{\alpha\beta} \mathbf{A}^\alpha \otimes \mathbf{A}^\beta . \quad (46)$$

2. The change of the out-of-plane curvature tensor:

$$\mathbf{K} := \mathbf{F}^T \mathbf{b} \mathbf{F} - \mathbf{b}_0 = (b_{\alpha\beta} - B_{\alpha\beta}) \mathbf{A}^\alpha \otimes \mathbf{A}^\beta = K_{\alpha\beta} \mathbf{A}^\alpha \otimes \mathbf{A}^\beta . \quad (47)$$

3. The change of the in-plane curvature tensor:

$$\bar{\mathbf{K}} := \mathbf{F}^T \bar{\mathbf{b}} \mathbf{F} - \bar{\mathbf{b}}_0 = (\bar{b}_{\alpha\beta} - \bar{B}_{\alpha\beta}) \mathbf{A}^\alpha \otimes \mathbf{A}^\beta = \bar{K}_{\alpha\beta} \mathbf{A}^\alpha \otimes \mathbf{A}^\beta . \quad (48)$$

Here, $\bar{b}_{\alpha\beta}$ can be computed from Eq. (35) taking into account Eq. (45). This gives

$$\bar{b}_{\alpha\beta} = \frac{1}{2} \ell^\gamma (\ell_\alpha \Gamma_{\gamma\beta}^c + \ell_\beta \Gamma_{\gamma\alpha}^c) + \frac{1}{2} c^\gamma (\ell_\alpha \hat{L}_{\gamma,\beta} + \ell_\beta \hat{L}_{\gamma,\alpha}) . \quad (49)$$

Accordingly, the geodesic curvature follows from Eq. (32) as

$$\kappa_g := \bar{b}_{\alpha\beta} \ell^{\alpha\beta} = \ell^{\alpha\beta} \Gamma_{\alpha\beta}^\gamma c_\gamma + \lambda^{-1} c_\alpha \ell^\beta L_{;\beta}^\alpha . \quad (50)$$

Further, by using relation $L_{;\beta}^\alpha = \mathbf{L}_{;\beta} \cdot \mathbf{A}^\alpha - L^\gamma \bar{\Gamma}_{\gamma\beta}^\alpha$, similar to Eq. (25.1) – where $\bar{\Gamma}_{\alpha\beta}^\gamma := \mathbf{A}^\gamma \cdot \mathbf{A}_{\alpha,\beta}$ denote the Christoffel symbols of the initial configuration – Eq. (50) can be rewritten as

$$\kappa_g = \underbrace{\ell^{\alpha\beta} c_\gamma S_{\alpha\beta}^\gamma}_{=:\kappa_g^\Gamma} + \underbrace{\lambda^{-1} c_\alpha \ell^\beta L_{;\beta}^\alpha}_{=:\kappa_g^L} , \quad (51)$$

where $S_{\alpha\beta}^\gamma := \Gamma_{\alpha\beta}^\gamma - \bar{\Gamma}_{\alpha\beta}^\gamma$ and $L_{;\beta}^\alpha := \mathbf{A}^\alpha \cdot \mathbf{L}_{;\beta}$.

Remark 2.4: As seen in Eq. (51), the geodesic curvature involves not only the change in the Christoffel symbols (term κ_g^Γ), but also the gradient of \mathbf{L} (term κ_g^L). For initially straight fiber, the geodesic curvature becomes

$$\kappa_g := \kappa_g^\Gamma = \ell^{\alpha\beta} c_\gamma S_{\alpha\beta}^\gamma \quad (52)$$

as κ_g^L vanishes. But for initially curved fibers, where $\kappa_g^L \neq 0$, expression (51) should be used. This point will be demonstrated in Sec. 7.1.

Remark 2.5: To measure the change in the curvatures, one can use the invariants

$$\begin{aligned} k_n &:= \mathbf{b} : \boldsymbol{\ell} \otimes \boldsymbol{\ell} - \mathbf{b}_0 : \mathbf{L} \otimes \mathbf{L} = \kappa_n - \kappa_n^0 , \\ k_g &:= \bar{\mathbf{b}} : \boldsymbol{\ell} \otimes \boldsymbol{\ell} - \bar{\mathbf{b}}_0 : \mathbf{L} \otimes \mathbf{L} = \kappa_g - \kappa_g^0 , \\ t_g &:= \mathbf{b} : \boldsymbol{\ell} \otimes \mathbf{c} - \mathbf{b}_0 : \mathbf{L} \otimes \mathbf{c}_0 = \tau_g - \tau_g^0 , \end{aligned} \quad (53)$$

called the *absolute change* in the normal curvature, geodesic curvature, and geodesic torsion, respectively. Here, \bullet^0 denotes the corresponding quantities in the initial configuration.

Remark 2.6: However, the curvature changes (53) are not ideal for constitutive models, as they can lead to unphysical stress couples that respond to fiber stretching even when there is no bending. An example is pure dilatation, e.g. due to thermal expansion or hydrostatic stress states as is discussed in example 7.4. To exclude fiber stretching, we define the invariants

$$\begin{aligned} k_n &:= \mathbf{b} : \lambda \boldsymbol{\ell} \otimes \boldsymbol{\ell} - \mathbf{b}_0 : \mathbf{L} \otimes \mathbf{L} = \kappa_n \lambda - \kappa_n^0 , \\ k_g &:= \bar{\mathbf{b}} : \lambda \boldsymbol{\ell} \otimes \boldsymbol{\ell} - \bar{\mathbf{b}}_0 : \mathbf{L} \otimes \mathbf{L} = \kappa_g \lambda - \kappa_g^0 , \\ t_g &:= \mathbf{b} : \lambda \boldsymbol{\ell} \otimes \mathbf{c} - \mathbf{b}_0 : \mathbf{L} \otimes \mathbf{c}_0 = \tau_g \lambda - \tau_g^0 , \end{aligned} \quad (54)$$

called the *stretch-excluded change* in the normal curvature, geodesic curvature, and geodesic torsion, respectively.

Remark 2.7: Both curvature changes (53) and (54) can cause fiber tension apart from fiber bending. Therefore, one can use the so-called *nominal change* in the normal curvature, geodesic curvature, and geodesic torsion, defined by

$$\begin{aligned} K_n &:= \mathbf{K} : \mathbf{L} \otimes \mathbf{L} = \kappa_n \lambda^2 - \kappa_n^0 , \\ K_g &:= \bar{\mathbf{K}} : \mathbf{L} \otimes \mathbf{L} = \kappa_g \lambda^2 - \kappa_g^0 , \\ T_g &:= \mathbf{K} : \mathbf{L} \otimes \mathbf{c}_0 = b_{\alpha\beta} c_0^\alpha L^\beta - \tau_g^0 , \end{aligned} \quad (55)$$

where \mathbf{K} and $\bar{\mathbf{K}}$ are defined by (47) and (48), respectively. These invariants can also be found e.g. in Steigmann and Dell'Isola (2015) and Schulte et al. (2020). Since the measures (55) do not cause an axial tension in the fibers, their material tangents simplify significantly. Note however that, like (53), they can cause unphysical stress couples responding to fiber stretching.

Remark 2.8: The mentioned curvature measures (53), (54), and (55) are also listed in Tab. 1. It should be noted that all these measures are equivalent for inextensible fibers, i.e. $\lambda = 1$, which is usually assumed for textile composites.

Invariant	tensor notation	index notation	geometrical relevance
(in-plane) right Cauchy-Green surface strain tensor $\mathbf{C} = a_{\alpha\beta} \mathbf{A}^\alpha \otimes \mathbf{A}^\beta$			
$I_1 :=$	$\text{tr}_s \mathbf{C}$	$A^{\alpha\beta} a_{\alpha\beta}$	surface shearing of \mathcal{S}
$I_2 = J^2 :=$	$\det_s \mathbf{C} = (\det_s \mathbf{F})^2$	$\det[a_{\alpha\beta}] / \det[A_{\alpha\beta}]$	surface area change of \mathcal{S}
$\Lambda_i = \lambda_i^2 :=$	$\mathbf{C} : \mathbf{L}_i \otimes \mathbf{L}_i$ (no sum in i)	$a_{\alpha\beta} L_i^{\alpha\beta}$	stretching of \mathcal{C}_i
$\gamma_{ij} :=$	$\mathbf{C} : \mathbf{L}_i \otimes \mathbf{L}_j$	$a_{\alpha\beta} L_i^\alpha L_j^\beta$	nominal angle between \mathcal{C}_i & \mathcal{C}_j , $i \neq j$
$\hat{\gamma}_{ij} :=$	$\boldsymbol{\ell}_1 \cdot \boldsymbol{\ell}_2$	$a_{\alpha\beta} \ell_i^\alpha \ell_j^\beta$	absolute angle between \mathcal{C}_i & \mathcal{C}_j , $i \neq j$

Table 2: Various invariants of the right surface Cauchy-Green tensor \mathbf{C} , induced by multiple fiber families \mathcal{C}_i ($i = 1, \dots, n_f$). Here, $L_i^{\alpha\beta} := L_i^\alpha L_i^\beta$ (no sum in i).

3 Balance laws

In this section, we discuss the balance laws for fibrous thin shells taking into account not only in-plane stretching and out-of-plane bending, but also in-plane bending. Like in classical Kirchhoff-Love shell theory, we directly postulate linear and angular momentum balance for our generalized Kirchhoff-Love shell with in-plane bending. Although the presented theory is not derived from general Cosserat theory, we show in Appendix C that our set of balance equations is consistent with that of Cosserat shell theory.

We consider that the out-of-plane shear energy and the out-of-plane thickness strain energy are negligible. The first condition amounts to the Kirchhoff-Love kinematical assumption of zero out-of-plane shear strains. The second condition is satisfied here by the plane stress assumption (i.e. zero thickness stress), which is commonly used for thin shells. It still allows for thickness changes, e.g. due to large membrane stretching. Note, however, that these assumptions on the shear strains and thickness stress are mathematically independent of the thickness, so that the governing equations can be written directly in surface form without the need of a thickness variable. Instead, the influence of the thickness appears in the constitutive equations, see e.g. Naghdi (1982); Steigmann (1999a); Sauer and Duong (2017); Duong et al. (2017).

In the following, we first discuss in detail the theory with one embedded fiber family \mathcal{C} . The extension to multiple fiber families is straightforward and will be discussed subsequently.

In order to define internal stresses and internal moment tensors, the shell \mathcal{S} is virtually cut into two parts at position \mathbf{x} as depicted in Fig. 2. On the parametrized cut, denoted by $\mathcal{I}(s)$, we define the unit tangent vector $\boldsymbol{\tau} := \partial \mathbf{x} / \partial s$ and the unit normal $\boldsymbol{\nu} := \boldsymbol{\tau} \times \mathbf{n} = \nu_\alpha \mathbf{a}^\alpha$ at \mathbf{x} .

3.1 Stress tensor

This section discusses Cauchy stress tensor $\boldsymbol{\sigma}$ for thin shells under plane-stress conditions. The influence of angular momentum balance on the stress tensor is then discussed in Sec. 3.4.

The traction vector \mathbf{T} appearing on the cut can have arbitrary direction (see Fig. 2b), but we can generally express it with respect to the basis $\{\mathbf{a}_1, \mathbf{a}_2, \mathbf{n}\}$ as

$$\mathbf{T} = T^\alpha \mathbf{a}_\alpha + T^3 \mathbf{n}, \quad (56)$$

where T^α and T^3 are the contravariant components of \mathbf{T} . This traction induces the Cauchy stress tensor $\boldsymbol{\sigma}$. Following Cauchy's theorem, the components of $\boldsymbol{\sigma}$ are balanced by the traction

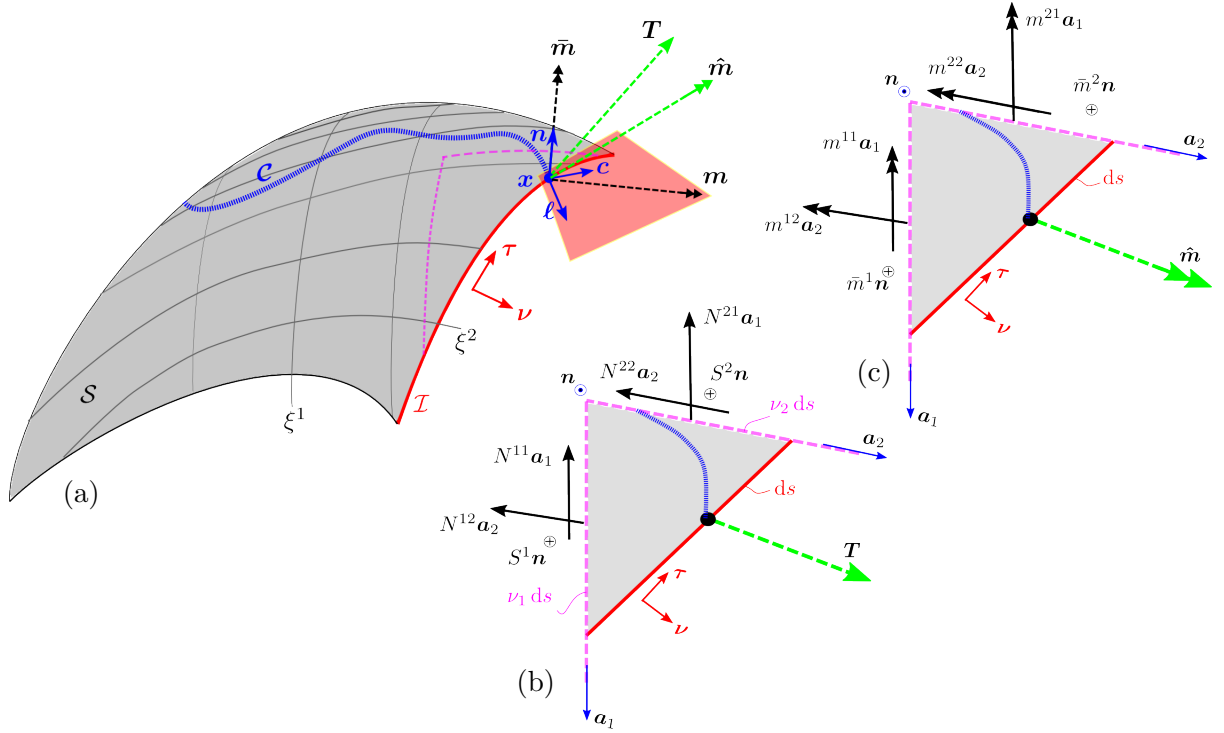


Figure 2: Internal stresses and moments: (a) illustration of physical traction vector \mathbf{T} and moment vector $\hat{\mathbf{m}}$ acting on the cut \mathcal{I} (red curve) through surface \mathcal{S} with its embedded fiber \mathcal{C} (blue curve). Both \mathbf{T} and $\hat{\mathbf{m}}$ are general vectors in 3D space. The moment vector $\hat{\mathbf{m}}$ can be decomposed into the component $\bar{\mathbf{m}}$, causing in-plane bending, and the component \mathbf{m} , causing out-of-plane bending and twisting. Vectors $\ell, \mathbf{c}, \boldsymbol{\nu}, \boldsymbol{\tau}$, and \mathbf{m} lie in the tangent plane of \mathcal{S} . (b) Stress and (c) moment components appearing on a triangular element – which is in force and moment equilibrium – under the action of the traction \mathbf{T} and moment $\hat{\mathbf{m}}$, respectively. These stress and moment components appear on the cuts that intersect with the tangent plane (pink dash lines). Assuming plane stress conditions, the stress and moment on any cut perpendicular to the surface normal \mathbf{n} (grey area) are neglected for the equilibrium of the triangular element.

\mathbf{T} on an infinitesimal triangular element, as shown in Fig. 2b. Under plane-stress conditions, all stresses on any cut perpendicular to surface normal \mathbf{n} are neglected for the (force) equilibrium of the triangular element. That is, the components of tensor $\boldsymbol{\sigma}$ associated with bases $\mathbf{n} \otimes \mathbf{a}_\alpha$ and $\mathbf{n} \otimes \mathbf{n}$ are considered to be zero. This results in the asymmetry of tensor $\boldsymbol{\sigma}$ in the form,

$$\boldsymbol{\sigma} = N^{\alpha\beta} \mathbf{a}_\alpha \otimes \mathbf{a}_\beta + S^\alpha \mathbf{a}_\alpha \otimes \mathbf{n} , \quad (57)$$

where $N^{\alpha\beta}$ and S^α are the membrane stress and out-of-plane shear stress components of $\boldsymbol{\sigma}$. Accordingly, the components of $\boldsymbol{\sigma}^\mathbf{T}$ on the cross-section perpendicular to \mathbf{a}^α are defined by

$$\mathbf{T}^\alpha := \boldsymbol{\sigma}^\mathbf{T} \mathbf{a}^\alpha = N^{\alpha\beta} \mathbf{a}_\beta + S^\alpha \mathbf{n} , \quad (58)$$

which is illustrated in Fig. 2b for an infinitesimal triangular element on \mathcal{S} . With this, we can write

$$\boldsymbol{\sigma} = \mathbf{a}_\alpha \otimes \mathbf{T}^\alpha . \quad (59)$$

Further, the force equilibrium of the triangle (see Fig. 2b) gives

$$\mathbf{T} ds = (\nu_\alpha N^{\alpha\beta}) \mathbf{a}_\beta ds + (\nu_\alpha S^\alpha) \mathbf{n} ds = \mathbf{T}^\alpha \nu_\alpha ds , \quad (60)$$

which implies Cauchy's formula

$$\mathbf{T} = (\mathbf{T}^\alpha \otimes \mathbf{a}_\alpha) \boldsymbol{\nu} = \boldsymbol{\sigma}^\mathbf{T} \boldsymbol{\nu} , \quad (61)$$

since $\nu_\alpha = \boldsymbol{\nu} \cdot \mathbf{a}_\alpha$. By comparing Eq. (61) with Eq. (56), we can further write

$$T^\alpha = \nu_\beta N^{\beta\alpha} , \quad T^3 = \nu_\alpha S^\alpha . \quad (62)$$

Remark 3.1: Due to the presence of transverse shear components S^α , the traction vector \mathbf{T} has both in-plane and out-of-plane components as is seen from Eq. (56) and (62). As shown in Sec. 3.4, in general $N^{\alpha\beta}$ in Eq. (57) is not symmetric according to angular momentum balance. Instead, the so-called effective stress – denoted by $\bar{\sigma}^{\alpha\beta}$ and defined in Eq. (93) – is symmetric according to angular momentum balance.

Remark 3.2: The format of the Cauchy stress (57) also contains all the stresses within a cut fiber. Indeed, consider a fiber \mathcal{C} described by beam theory. According to beam theory, all stresses are neglected on a cut parallel to the fiber. Accordingly, the stress tensor in the fiber \mathcal{C} – denoted by $\boldsymbol{\sigma}_{\text{fib}}$ – can be written as

$$\boldsymbol{\sigma}_{\text{fib}} = \sigma \boldsymbol{\ell} \otimes \boldsymbol{\ell} + s_c \boldsymbol{\ell} \otimes \mathbf{c} + s_n \boldsymbol{\ell} \otimes \mathbf{n} , \quad (63)$$

where σ , s_c , and s_n denote the axial stress and the two shear stresses. By inserting the basis vectors $\boldsymbol{\ell} = \ell^\alpha \mathbf{a}_\alpha$, and $\mathbf{c} = c^\alpha \mathbf{a}_\alpha$, Eq. (63) becomes

$$\boldsymbol{\sigma}_{\text{fib}} = N^{\alpha\beta} \mathbf{a}_\alpha \otimes \mathbf{a}_\beta + S^\alpha \mathbf{a}_\alpha \otimes \mathbf{n} , \quad (64)$$

with

$$\begin{aligned} N^{\alpha\beta} &= \sigma \ell^{\alpha\beta} + s_c \ell^\alpha c^\beta , \\ S^\alpha &= s_n \ell^\alpha . \end{aligned} \quad (65)$$

3.2 Generalized moment tensor

This section discusses the moment tensor $\hat{\boldsymbol{\mu}}$ for Kirchhoff-Love shells with in-plane bending. Also, equivalent stress couple tensors $\boldsymbol{\mu}$ and $\bar{\boldsymbol{\mu}}$ are defined by introducing stress couple vectors that are equivalent to the in-plane and out-of-plane bending moments.

At position \mathbf{x} on cut $\mathcal{I}(s)$ (see Fig. 2c), the bending moment vector, denoted by $\hat{\mathbf{m}}$ (with unit moment per unit length), is allowed to have both in-plane and out-of-plane components. It can be expressed with respect to basis $\{\boldsymbol{\tau}, \boldsymbol{\nu}, \mathbf{n}\}$ as

$$\hat{\mathbf{m}} := m_\tau \boldsymbol{\tau} + m_\nu \boldsymbol{\nu} + \bar{m} \mathbf{n} , \quad (66)$$

where⁸ $\bar{m} \mathbf{n} := \bar{\mathbf{m}}$ is the moment causing in-plane bending and

$$m_\tau \boldsymbol{\tau} + m_\nu \boldsymbol{\nu} := \mathbf{m} , \quad (67)$$

denotes the combined moment causing out-of-plane bending and twisting.

Similar to the Cauchy stress tensor (57), all moments on a cut perpendicular to surface normal \mathbf{n} are zero under Kirchhoff-Love assumptions. The total moment tensor $\hat{\boldsymbol{\mu}}$ induced by $\hat{\mathbf{m}}$ can thus be expressed in the form

$$\hat{\boldsymbol{\mu}} := m^{\alpha\beta} \mathbf{a}_\alpha \otimes \mathbf{a}_\beta + \bar{m}^\alpha \mathbf{a}_\alpha \otimes \mathbf{n} . \quad (68)$$

In this form, the first term $m^{\alpha\beta} \mathbf{a}_\alpha \otimes \mathbf{a}_\beta$ combines both out-of-plane bending and twisting in response to a change in the out-of-plane curvature of \mathcal{S} , while the second term $\bar{m}^\alpha \mathbf{a}_\alpha \otimes \mathbf{n}$ is the response to a change in the in-plane curvature of fiber \mathcal{C} .

⁸Here and henceforth, the new terms for in-plane bending that are added to classical Kirchhoff-Love shell theory, see e.g. Sauer and Duong (2017), are denoted by a bar.

The components of $\hat{\boldsymbol{\mu}}^T$, on the cross-section perpendicular to \mathbf{a}^α , thus read as (see Fig. 2c)

$$\hat{\mathbf{m}}^\alpha := \hat{\boldsymbol{\mu}}^T \mathbf{a}^\alpha = m^{\alpha\beta} \mathbf{a}_\beta + \bar{m}^\alpha \mathbf{n} . \quad (69)$$

Here, moment vectors $m^{\alpha\beta} \mathbf{a}_\beta$ and $\bar{m}^\alpha \mathbf{n}$ are associated with the angular velocity vector around the in-plane axis

$$\mathbf{n} \times \dot{\mathbf{n}} = (\mathbf{n} \cdot \dot{\mathbf{a}}^\alpha) \mathbf{a}_\alpha \times \mathbf{n} , \quad (70)$$

and the out-of-plane axis $\mathbf{n} = \boldsymbol{\ell} \times \mathbf{c} = \ell^\alpha \mathbf{a}_\alpha \times \mathbf{c}$, respectively. Therefore, it is mathematically convenient to express $\hat{\mathbf{m}}^\alpha$ with respect to the basis $\{\mathbf{a}_1 \times \mathbf{n}, \mathbf{a}_2 \times \mathbf{n}, \mathbf{n}\}$, i.e.

$$\begin{aligned} \hat{\mathbf{m}}^\alpha &= M^{\alpha\beta} (\mathbf{a}_\beta \times \mathbf{n}) + \bar{M}^{\alpha\beta} (\mathbf{a}_\beta \times \mathbf{c}) \\ &= \mathbf{n} \times \mathbf{M}^\alpha + \mathbf{c} \times \bar{\mathbf{M}}^\alpha , \end{aligned} \quad (71)$$

where $M^{\alpha\beta}$ and $\bar{M}^{\alpha\beta}$ denote the components of vectors $\hat{\mathbf{m}}^\alpha$ in directions $\mathbf{a}_\beta \times \mathbf{n}$ and $\mathbf{a}_\beta \times \mathbf{c}$, respectively. Here, we have defined the so-called stress couple vectors for out-of-plane and in-plane bending⁹

$$\mathbf{M}^\alpha := -M^{\alpha\beta} \mathbf{a}_\beta , \quad \text{and} \quad \bar{\mathbf{M}}^\alpha := -\bar{M}^{\alpha\beta} \mathbf{a}_\beta , \quad \text{with} \quad \bar{M}^{\alpha\beta} := \bar{m}^\alpha \ell^\beta . \quad (72)$$

Eq. (68) thus becomes

$$\hat{\boldsymbol{\mu}} := M^{\alpha\beta} \mathbf{a}_\alpha \otimes (\mathbf{a}_\beta \times \mathbf{n}) + \bar{M}^{\alpha\beta} \mathbf{a}_\alpha \otimes (\mathbf{a}_\beta \times \mathbf{c}) . \quad (73)$$

Similar to Eq. (61), moment equilibrium of the triangle (see Fig. 2c) results in Cauchy's formula

$$\hat{\mathbf{m}} = \hat{\mathbf{m}}^\alpha \nu_\alpha = \mathbf{n} \times \mathbf{M} + \mathbf{c} \times \bar{\mathbf{M}} = \hat{\boldsymbol{\mu}}^T \boldsymbol{\nu} , \quad (74)$$

where

$$\mathbf{M} := M^\alpha \nu_\alpha , \quad \text{and} \quad \bar{\mathbf{M}} := \bar{M}^\alpha \nu_\alpha \quad (75)$$

are referred to as the stress couple vectors associated with out-of-plane and in-plane bending, respectively. By comparing Eq. (74) and (66), the stress couple vectors \mathbf{M} and $\bar{\mathbf{M}}$ can be related to their moment vector counterparts by

$$\mathbf{m} = \mathbf{n} \times \mathbf{M} , \quad \text{and} \quad \bar{\mathbf{m}} = \mathbf{c} \times \bar{\mathbf{M}} , \quad \text{with} \quad \bar{\mathbf{M}} = -\bar{m} \boldsymbol{\ell} . \quad (76)$$

In line with previous works, see e.g. Sauer and Duong (2017), we can also define the stress couple tensors,⁹

$$\boldsymbol{\mu} := -M^{\alpha\beta} \mathbf{a}_\alpha \otimes \mathbf{a}_\beta , \quad \text{and} \quad \bar{\boldsymbol{\mu}} := -\bar{M}^{\alpha\beta} \mathbf{a}_\alpha \otimes \mathbf{a}_\beta , \quad (77)$$

associated with out-of-plane and in-plane bending, respectively. In view of (74), we obtain the mapping

$$\mathbf{M} = \boldsymbol{\mu}^T \boldsymbol{\nu} , \quad \text{and} \quad \bar{\mathbf{M}} = \bar{\boldsymbol{\mu}}^T \boldsymbol{\nu} . \quad (78)$$

In order to relate the components of the moment vector (66) to the components of the stress couple tensors, we can equate equations (66) and (74). This results in

$$\begin{aligned} m_\nu &:= \hat{\mathbf{m}} \cdot \boldsymbol{\nu} = \mathbf{m} \cdot \boldsymbol{\nu} = M^{\alpha\beta} \nu_\alpha \tau_\beta , \\ m_\tau &:= \hat{\mathbf{m}} \cdot \boldsymbol{\tau} = \mathbf{m} \cdot \boldsymbol{\tau} = -M^{\alpha\beta} \nu_\alpha \nu_\beta , \\ \bar{m} &:= \hat{\mathbf{m}} \cdot \mathbf{n} = \bar{\mathbf{m}} \cdot \mathbf{n} = \bar{M}^{\alpha\beta} \nu_\alpha \ell_\beta = \bar{m}^\alpha \nu_\alpha , \end{aligned} \quad (79)$$

where we have used the relations $\mathbf{a}_\beta \times \mathbf{n} = \tau_\beta \boldsymbol{\nu} - \nu_\beta \boldsymbol{\tau}$ due to $\mathbf{a}_\alpha = \tau_\alpha \boldsymbol{\tau} + \nu_\alpha \boldsymbol{\nu}$.

⁹The sign convention for the moment components follows Steigmann (1999b) and Sauer and Duong (2017).

Remark 3.3: Similar to Eq. (63), the moment tensor for a fiber described by beam theory – denoted by $\hat{\boldsymbol{\mu}}_{\text{fib}}$ – can also be written in the form of Eq. (68), i.e.

$$\hat{\boldsymbol{\mu}}_{\text{fib}} := \mu_\ell \boldsymbol{\ell} \otimes \boldsymbol{\ell} + \mu_c \boldsymbol{\ell} \otimes \boldsymbol{c} + \bar{\mu} \boldsymbol{\ell} \otimes \boldsymbol{n} = m^{\alpha\beta} \boldsymbol{a}_\alpha \otimes \boldsymbol{a}_\beta + \bar{m}^\alpha \boldsymbol{a}_\alpha \otimes \boldsymbol{n}. \quad (80)$$

Here, μ_ℓ , μ_c , and $\bar{\mu}$ denote twisting, out-of-plane bending, and in-plane bending moments in fiber \mathcal{C} , respectively, and we have identified

$$\begin{aligned} m^{\alpha\beta} &= \mu_\ell \ell^{\alpha\beta} + \mu_c \ell^\alpha c^\beta, \\ \bar{m}^\alpha &= \bar{\mu} \ell^\alpha. \end{aligned} \quad (81)$$

Remark 3.4: Further, inserting \bar{m}^α from Eq. (81) into (72.3) and (79.3) gives

$$\begin{aligned} \bar{M}^{\alpha\beta} &= \bar{\mu} \ell^{\alpha\beta} \\ \bar{\boldsymbol{m}} &= \bar{\mu} \boldsymbol{\ell} \cdot \boldsymbol{\nu}. \end{aligned} \quad (82)$$

Therefore, we can conclude that $\bar{M}^{\alpha\beta}$ is symmetric. Note that $\bar{\mu}$ does not depend on the cut \mathcal{I} since it is a component of the internal moment tensor, but $\bar{\boldsymbol{m}}$ does depend on \mathcal{I} as seen in Eq. (82.2). For example, $\bar{\boldsymbol{m}} = 0$ when the cut is parallel to the fiber, i.e. when $\boldsymbol{\ell} \cdot \boldsymbol{\nu} = 0$.

3.3 Balance of linear momentum

Consider body forces \boldsymbol{f} acting on an arbitrary simply-connected region $\mathcal{R} \subset \mathcal{S}$. The balance of linear momentum implies that the temporal change of the linear momentum is equal to the resultant of all acting external forces. That is,

$$\frac{D}{Dt} \int_{\mathcal{R}} \rho \boldsymbol{v} \, da = \int_{\mathcal{R}} \boldsymbol{f} \, da + \int_{\partial\mathcal{R}} \boldsymbol{T} \, ds, \quad \forall \mathcal{R} \in \mathcal{S}, \quad (83)$$

where \boldsymbol{v} denotes the material velocity of the surface. Inserting \boldsymbol{T} from Eq. (61), and applying the surface divergence theorem and conservation of mass, one obtains the local form of linear momentum balance

$$\text{div}_s \boldsymbol{\sigma}^T + \boldsymbol{f} = \rho \dot{\boldsymbol{v}}, \quad (84)$$

where div_s denotes the surface divergence operator, defined by $\text{div}_s \bullet := \bullet_{,\alpha} \cdot \boldsymbol{a}^\alpha$. Note that Eq. (84) can also be written in the form (see Sauer and Duong (2017))

$$\boldsymbol{T}_{;\alpha}^\alpha + \boldsymbol{f} = \rho \dot{\boldsymbol{v}}, \quad (85)$$

since

$$\text{div}_s \boldsymbol{\sigma}^T = \boldsymbol{\sigma}_{,\beta}^T \cdot \boldsymbol{a}^\beta = \boldsymbol{T}_{,\alpha}^\alpha + \Gamma_{\alpha\beta}^\beta \boldsymbol{T}^\alpha = \boldsymbol{T}_{;\alpha}^\alpha, \quad (86)$$

follows from Eq. (59).

3.4 Balance of angular momentum

The balance of angular momentum implies that the temporal change of angular momentum is equal to the resultant of all external moments. That is,

$$\frac{D}{Dt} \int_{\mathcal{R}} \rho \boldsymbol{x} \times \boldsymbol{v} \, da = \int_{\mathcal{R}} \boldsymbol{x} \times \boldsymbol{f} \, da + \int_{\partial\mathcal{R}} \boldsymbol{x} \times \boldsymbol{T} \, ds + \int_{\partial\mathcal{R}} \hat{\boldsymbol{m}} \, ds, \quad (87)$$

where $\hat{\boldsymbol{m}}$ includes both in-plane and out-of-plane bending moments acting on $\partial\mathcal{R}$. From Eqs. (61) and (74), the surface divergence theorem gives

$$\int_{\partial\mathcal{R}} \boldsymbol{x} \times \boldsymbol{T} \, ds = \int_{\mathcal{R}} (\boldsymbol{a}_\alpha \times \boldsymbol{T}^\alpha + \boldsymbol{x} \times \text{div}_s \boldsymbol{\sigma}^T) \, da \quad (88)$$

and

$$\int_{\partial\mathcal{R}} \hat{\mathbf{m}} \, ds = \int_{\mathcal{R}} \operatorname{div}_s \hat{\boldsymbol{\mu}}^T \, da . \quad (89)$$

Inserting these equations into (87) and applying local mass conservation gives

$$\int_{\mathcal{R}} (\mathbf{a}_\alpha \times \mathbf{T}^\alpha + \operatorname{div}_s \hat{\boldsymbol{\mu}}^T) \, da + \int_{\mathcal{R}} \mathbf{x} \times (\operatorname{div}_s \boldsymbol{\sigma}^T + \mathbf{f} - \rho \dot{\mathbf{v}}) \, da = \mathbf{0} . \quad (90)$$

The second integral in Eq. (90) vanishes due to (84). This leads to the local form of the angular momentum balance,

$$\mathbf{a}_\alpha \times \mathbf{T}^\alpha + \operatorname{div}_s \hat{\boldsymbol{\mu}}^T = \mathbf{0} . \quad (91)$$

Keeping Eq. (82.1) in mind, the surface divergence of tensor $\hat{\boldsymbol{\mu}}^T$ follows from Eq. (73) as

$$\operatorname{div}_s \hat{\boldsymbol{\mu}}^T = \left(-M^{\alpha\beta} b_\alpha^\gamma + \bar{m}_{;\alpha}^\gamma \ell^\beta c^\gamma \right) \mathbf{a}_\beta \times \mathbf{a}_\gamma + \left(M_{;\beta}^{\beta\alpha} + \bar{\mu} \tau_g \ell^\alpha - \bar{\mu} \kappa_n c^\alpha \right) \mathbf{a}_\alpha \times \mathbf{n} , \quad (92)$$

where we have used $\mathbf{a}_\alpha = \ell_\alpha \boldsymbol{\ell} + c_\alpha \mathbf{c} = (\ell_\alpha c^\gamma - c_\alpha \ell^\gamma) \mathbf{a}_\gamma \times \mathbf{n}$. Inserting Eqs. (92) and (58) into Eq. (91) then implies that the so-called effective membrane stress¹⁰

$$\tilde{\sigma}^{\alpha\beta} := N^{\alpha\beta} - M^{\gamma\alpha} b_\gamma^\beta + \bar{m}_{;\gamma}^\alpha \ell^\gamma c^\beta \quad (93)$$

is symmetric, and that the shear stress is given by

$$S^\alpha = -M_{;\beta}^{\beta\alpha} + \bar{\mu} (\kappa_n c^\alpha - \tau_g \ell^\alpha) . \quad (94)$$

Thus, angular momentum balance implies the symmetry of the effective stress $\tilde{\sigma}^{\alpha\beta}$ instead of the Cauchy stress $N^{\alpha\beta}$. The latter is only symmetric when there is no in-plane and out-of-plane bending resistance.

Remark 3.5: The last term in stress expression (93) relates to the in-plane shear force in the fiber, which, in accordance with the assumed Euler-Bernoulli kinematics, follows as the derivative of the in-plane bending moment.

3.5 Mechanical power balance

The mechanical power balance can be obtained from local momentum balance (84). To this end, we can write

$$\int_{\mathcal{R}} \mathbf{v} \cdot (\operatorname{div}_s \boldsymbol{\sigma}^T + \mathbf{f} - \rho \dot{\mathbf{v}}) \, da = 0 . \quad (95)$$

Here, the divergence term can be transformed by the identity

$$\mathbf{v} \cdot \operatorname{div}_s \boldsymbol{\sigma}^T = \operatorname{div}_s (\mathbf{v} \boldsymbol{\sigma}^T) - \boldsymbol{\sigma}^T : \nabla_s \mathbf{v} , \quad (96)$$

by the divergence theorem

$$\int_{\mathcal{R}} \operatorname{div}_s (\mathbf{v} \boldsymbol{\sigma}^T) \, da = \int_{\partial\mathcal{R}} \mathbf{v} \cdot \boldsymbol{\sigma}^T \boldsymbol{\nu} \, ds = \int_{\partial\mathcal{R}} \mathbf{v} \cdot \mathbf{T} \, ds , \quad (97)$$

and by using the relation

$$\boldsymbol{\sigma}^T : \nabla_s \mathbf{v} = N^{\alpha\beta} \mathbf{a}_\beta \cdot \dot{\mathbf{a}}_\alpha + S^\alpha \mathbf{n} \cdot \dot{\mathbf{a}}_\alpha . \quad (98)$$

¹⁰Note that we will redefine $\tilde{\sigma}^{\alpha\beta}$ later in Eq. (106.2) and (112) for various choices of the strain measure for in-plane bending.

Inserting Eq. (93) and (94) into Eq. (98) gives

$$\boldsymbol{\sigma}^T : \nabla_s \mathbf{v} = \frac{1}{2} \tilde{\sigma}^{\alpha\beta} \dot{a}_{\alpha\beta} - M^{\alpha\beta} \mathbf{n}_{;\alpha} \cdot \dot{\mathbf{a}}_\beta - \bar{\mu} (\kappa_n \mathbf{c} \cdot \dot{\mathbf{n}} - \tau_g \boldsymbol{\ell} \cdot \dot{\mathbf{n}}) - M_{;\beta}^{\beta\alpha} \mathbf{n} \cdot \dot{\mathbf{a}}_\alpha + \bar{m}_{;\alpha}^\alpha \boldsymbol{\ell} \cdot \dot{\mathbf{c}}. \quad (99)$$

Considering Eq. (15.2), (36), and (81.2), the last two terms can be written as

$$\begin{aligned} M_{;\beta}^{\beta\alpha} \mathbf{n} \cdot \dot{\mathbf{a}}_\alpha &= (\dot{\mathbf{n}} \cdot \mathbf{M}^\alpha)_{;\alpha} + M^{\alpha\beta} \dot{\mathbf{n}}_{;\alpha} \cdot \mathbf{a}_\beta, \\ \bar{m}_{;\alpha}^\alpha \boldsymbol{\ell} \cdot \dot{\mathbf{c}} &= (\bar{m}^\alpha \boldsymbol{\ell} \cdot \dot{\mathbf{c}})_{;\alpha} + \bar{m}^\alpha \overline{(c^\beta \ell_{\beta;\alpha})^\cdot} + \bar{\mu} (\kappa_n \mathbf{c} \cdot \dot{\mathbf{n}} - \tau_g \boldsymbol{\ell} \cdot \dot{\mathbf{n}}). \end{aligned} \quad (100)$$

By taking Eqs. (96), (97), (99), (100), and local mass conservation into account, Eq. (95) becomes

$$\dot{K} + P_{\text{int}} = P_{\text{ext}}, \quad (101)$$

where

$$\dot{K} = \int_{\mathcal{R}} \rho \mathbf{v} \cdot \dot{\mathbf{v}} \, da \quad (102)$$

is the rate of kinetic energy,

$$P_{\text{int}} = \frac{1}{2} \int_{\mathcal{R}} \tilde{\sigma}^{\alpha\beta} \dot{a}_{\alpha\beta} \, da + \int_{\mathcal{R}} M^{\alpha\beta} \dot{b}_{\alpha\beta} \, da + \int_{\mathcal{R}} \bar{m}^\alpha \overline{(c^\beta \ell_{\beta;\alpha})^\cdot} \, da, \quad (103)$$

is the internal power, and

$$P_{\text{ext}} = \int_{\mathcal{R}} \mathbf{v} \cdot \mathbf{f} \, da + \int_{\partial\mathcal{R}} \mathbf{v} \cdot \mathbf{T} \, ds + \int_{\partial\mathcal{R}} \dot{\mathbf{n}} \cdot \mathbf{M} \, ds + \int_{\partial\mathcal{R}} \dot{\mathbf{c}} \cdot \bar{\mathbf{M}} \, ds \quad (104)$$

denotes the external power. The last term in P_{int} can be written in alternative forms, as is discussed in the following section. The mechanical power balance (101) simplifies to the expression in Sauer and Duong (2017), for $\bar{m}^\alpha \equiv 0$ and $\bar{\mathbf{M}} = \mathbf{0}$.

4 Work-conjugate variables and constitutive equations

As seen from the expression (103), the internal stress power per current area reads

$$\dot{w}_{\text{int}} := \frac{1}{2} \tilde{\sigma}^{\alpha\beta} \dot{a}_{\alpha\beta} + M^{\alpha\beta} \dot{b}_{\alpha\beta} + \bar{m}^\alpha \overline{(c^\beta \ell_{\beta;\alpha})^\cdot}, \quad (105)$$

which directly shows work-conjugate pairs. Accordingly, $c^\beta \ell_{\beta;\alpha} \mathbf{A}^\alpha = \mathbf{c} \bar{\nabla}_s \boldsymbol{\ell} \mathbf{F}^{-1}$ is a strain measure for the change in the in-plane curvatures. As shown in Appendix B, the strain measure $c^\beta \ell_{\beta;\alpha}$ is frame invariant under superimposed rigid body motion of the shell. However, it is somewhat unintuitive and thus inconvenient for the construction of material models. In the following, we will present two approaches with alternative definitions of this strain measure.

4.1 Geodesic curvature-based approach

This approach uses the geodesic curvature κ_g instead of $c^\beta \ell_{\beta;\alpha}$ within the in-plane bending power. Namely, inserting \bar{m}^α from (81.2) into Eq. (105) and rearranging terms gives

$$\begin{aligned} \dot{w}_{\text{int}} &:= \frac{1}{2} \sigma^{\alpha\beta} \dot{a}_{\alpha\beta} + M^{\alpha\beta} \dot{b}_{\alpha\beta} + \bar{\mu} \dot{\kappa}_g, \\ \text{with } \sigma^{\alpha\beta} &:= \tilde{\sigma}^{\alpha\beta} + \bar{\mu} \kappa_g \ell^{\alpha\beta}. \end{aligned} \quad (106)$$

Here, $\sigma^{\alpha\beta}$ represents the components of an effective membrane stress tensor¹¹. It is symmetric as both $\tilde{\sigma}^{\alpha\beta}$ and $\ell^{\alpha\beta}$ are symmetric. The internal power (103) then becomes

$$P_{\text{int}} = \frac{1}{2} \int_{\mathcal{R}_0} \tau^{\alpha\beta} \dot{a}_{\alpha\beta} \, dA + \int_{\mathcal{R}_0} M_0^{\alpha\beta} \dot{b}_{\alpha\beta} \, dA + \int_{\mathcal{R}_0} \bar{\mu}_0 \dot{\kappa}_g \, dA, \quad (107)$$

where $\mathcal{R}_0 \in \mathcal{S}_0$ and

$$\tau^{\alpha\beta} := J \sigma^{\alpha\beta}, \quad M_0^{\alpha\beta} := J M^{\alpha\beta}, \quad \bar{\mu}_0 := J \bar{\mu}. \quad (108)$$

These are the nominal quantities corresponding to the physical quantities $\sigma^{\alpha\beta}$, $M^{\alpha\beta}$, and $\bar{\mu}$, respectively. Accordingly, we can assume a stored energy function of an hyperelastic shell in the form

$$W = \check{W}(a_{\alpha\beta}, b_{\alpha\beta}, \kappa_g; h^{\alpha\beta}), \quad (109)$$

where $h^{\alpha\beta}$ collectively represents the components of the structural tensor(s), e.g. $\ell^{\alpha\beta}$, $c^{\alpha\beta}$, or, $c^\alpha \ell^\beta$, that characterize material anisotropy due to embedded fibers. Eq. (109) can equivalently be expressed in terms of invariants. All the strain measures $a_{\alpha\beta}$, $b_{\alpha\beta}$, κ_g , and $h^{\alpha\beta}$ used in Eq. (109) are frame invariant under superimposed rigid body motions as shown in Appendix B. Using the usual arguments of Coleman and Noll (1964), the constitutive equations can be written as

$$\tau^{\alpha\beta} = 2 \frac{\partial \check{W}}{\partial a_{\alpha\beta}}, \quad M_0^{\alpha\beta} = \frac{\partial \check{W}}{\partial b_{\alpha\beta}}, \quad \bar{\mu}_0 = \frac{\partial \check{W}}{\partial \kappa_g}. \quad (110)$$

Remark 4.1: Compared to classical Kirchhoff-Love shell theory (see e.g. Naghdi (1982); Sauer and Duong (2017)), the effective membrane stress $\sigma^{\alpha\beta}$ in (106.2) additionally contains the high order bending term $\bar{\mu}$ and the in-plane fiber shear term $m_{,\gamma}^\gamma$ (see Eq. (93)). For slender fibers, they are negligible since the in-plane bending stiffness is usually much smaller than the membrane stiffness. However, these terms may become significant when there is a large (usually local) change in curvature (e.g. at shear bands).

Remark 4.2: Although a constitutive formulation following from (107) appears elegant, expression (110.3) is restricted to a material response expressible in terms of the geodesic curvature κ_g . Therefore, this setup might be unsuited for complex material behavior, e.g. due to fiber dispersion (Gasser et al., 2006). In such cases, a more sophisticated structural tensor is usually desired for the in-plane bending response, and it thus may not always be possible to express W in terms of κ_g . This motivates the following director gradient-based approach.

Remark 4.3: In Eq. (110), the stress components $\tau^{\alpha\beta}$ and $M_0^{\alpha\beta}$, together with the strain components $a_{\alpha\beta}$ and $b_{\alpha\beta}$ in Eq. (109), are defined in the parameter space \mathcal{P} , where they can be treated as independent variables without forming them into tensors. It is possible, though, to construct different stress and strain tensors from these components, such that their scalar product results in the same power as in Eq. (107). For example, $\tau^{\alpha\beta}$ can be the components of the Kirchhoff surface stress tensor $\hat{\boldsymbol{\tau}} := \tau^{\alpha\beta} \mathbf{a}_\alpha \otimes \mathbf{a}_\beta$, the second Piola-Kirchhoff stress tensor \mathbf{S} , or the first Piola-Kirchhoff stress tensor \mathbf{P} but with different bases. Indeed, $\mathbf{S} = \mathbf{F}^T \hat{\boldsymbol{\tau}} \mathbf{F} = \tau^{\alpha\beta} \mathbf{A}_\alpha \otimes \mathbf{A}_\beta$, and $\mathbf{P} = \mathbf{F} \mathbf{S} = \tau^{\alpha\beta} \mathbf{a}_\alpha \otimes \mathbf{A}_\beta$. The strain variables work-conjugate to $\hat{\boldsymbol{\tau}}$, \mathbf{S} , and \mathbf{P} are the rate of surface deformation tensor \mathbf{D} , the Green-Lagrange surface strain tensor \mathbf{E} (or $\frac{1}{2} \mathbf{C}$), and the surface deformation gradient tensor \mathbf{F} , respectively, since $\hat{\boldsymbol{\tau}} : \mathbf{D} = \mathbf{S} : \dot{\mathbf{E}} = \mathbf{S} : \frac{1}{2} \dot{\mathbf{C}} = \mathbf{P} : \dot{\mathbf{F}} = \frac{1}{2} \tau^{\alpha\beta} \dot{a}_{\alpha\beta}$. See also Remark 4 in Sauer et al. (2019).

4.2 Director gradient-based approach

In this approach, the power expression (105) is rewritten by employing relation (38) and definitions (72.3) and (34) as

$$\dot{w}_{\text{int}} := \frac{1}{2} \sigma^{\alpha\beta} \dot{a}_{\alpha\beta} + M^{\alpha\beta} \dot{b}_{\alpha\beta} + \bar{M}^{\alpha\beta} \dot{b}_{\beta\alpha}, \quad (111)$$

¹¹ Note that, generally $\sigma^{\alpha\beta} \neq N^{\alpha\beta} = \mathbf{a}^\alpha \boldsymbol{\sigma} \mathbf{a}^\beta$. $\sigma^{\alpha\beta} = N^{\alpha\beta}$ only in special cases, i.e. when both in-plane and out-of-plane bending are negligible.

where $\sigma^{\alpha\beta}$ is now defined by¹¹

$$\sigma^{\alpha\beta} := \tilde{\sigma}^{\alpha\beta} + (\bar{M}^{\gamma\delta} c_{\delta;\gamma}) \ell^{\alpha\beta} . \quad (112)$$

Thus, the internal power can be written as

$$P_{\text{int}} = \frac{1}{2} \int_{\mathcal{R}_0} \tau^{\alpha\beta} \dot{a}_{\alpha\beta} \, dA + \int_{\mathcal{R}_0} M_0^{\alpha\beta} \dot{b}_{\alpha\beta} \, dA + \int_{\mathcal{R}_0} \bar{M}_0^{\alpha\beta} \dot{\bar{b}}_{\alpha\beta} \, dA , \quad (113)$$

where we have again used (108) and defined

$$\bar{M}_0^{\alpha\beta} := J \bar{M}^{\alpha\beta} . \quad (114)$$

Accordingly, the stored energy function can now be given in the form

$$W = \hat{W}(a_{\alpha\beta}, b_{\alpha\beta}, \bar{b}_{\alpha\beta}; h^{\alpha\beta}) . \quad (115)$$

This function can also be expressed equivalently in terms of invariants, and $\bar{b}_{\alpha\beta}$ can be shown to be frame invariant, see Appendix B. The corresponding constitutive equations now read

$$\tau^{\alpha\beta} = 2 \frac{\partial \hat{W}}{\partial a_{\alpha\beta}} , \quad M_0^{\alpha\beta} = \frac{\partial \hat{W}}{\partial b_{\alpha\beta}} , \quad \bar{M}_0^{\alpha\beta} = \frac{\partial \hat{W}}{\partial \bar{b}_{\alpha\beta}} . \quad (116)$$

Remark 4.4: Compared to (109), expression (115) allows to model more complex in-plane bending behavior using a generalized structural tensor applied to $\bar{b}_{\alpha\beta}$. We therefore consider this setup in the following sections.

Remark 4.5: Eq. (113) can also be written in tensor notation as

$$P_{\text{int}} = \int_{\mathcal{R}_0} \mathbf{S} : \dot{\mathbf{E}} \, dA - \int_{\mathcal{R}_0} \boldsymbol{\mu}_0 : \dot{\mathbf{K}} \, dA - \int_{\mathcal{R}_0} \bar{\boldsymbol{\mu}}_0 : \dot{\bar{\mathbf{K}}} \, dA , \quad (117)$$

where \mathbf{E} , \mathbf{K} , and $\bar{\mathbf{K}}$ are the strain tensors defined by (46), (47), and (48), respectively, and

$$\mathbf{S} := \tau^{\alpha\beta} \mathbf{A}_\alpha \otimes \mathbf{A}_\beta , \quad \boldsymbol{\mu}_0 := -M_0^{\alpha\beta} \mathbf{A}_\alpha \otimes \mathbf{A}_\beta , \quad \bar{\boldsymbol{\mu}}_0 := -\bar{M}_0^{\alpha\beta} \mathbf{A}_\alpha \otimes \mathbf{A}_\beta , \quad (118)$$

are the effective second Piola-Kirchhoff surface stress tensor, and the nominal stress couple tensors associated with out-of-plane and in-plane bending, respectively. They are symmetric and follow from the pull-back of tensors $J \sigma^{\alpha\beta} \mathbf{a}_\alpha \otimes \mathbf{a}_\beta$, $J \boldsymbol{\mu}$ and $J \bar{\boldsymbol{\mu}}$ in Eqs. (112) and (77).

Remark 4.6: In view of internal power expression (117), an alternative form of the stored energy function, apart from Eq. (115), is

$$W = \tilde{W}(\mathbf{E}, \mathbf{K}, \bar{\mathbf{K}}; \mathbf{H}) , \quad (119)$$

where \mathbf{H} denotes the structural tensor(s). However, since the temporal change of \mathbf{E} , \mathbf{K} , and $\bar{\mathbf{K}}$ only depends on $a_{\alpha\beta}$, $b_{\alpha\beta}$, and $\bar{b}_{\alpha\beta}$, respectively, the energy form (119) is equivalent to (115), i.e. $\tilde{W}(\mathbf{E}, \mathbf{K}, \bar{\mathbf{K}}) = \hat{W}(a_{\alpha\beta}, b_{\alpha\beta}, \bar{b}_{\alpha\beta})$. Therefore, the stress and moment tensors (118) can be determined either from

$$\mathbf{S} = \frac{\partial \tilde{W}}{\partial \mathbf{E}} , \quad -\boldsymbol{\mu}_0 = \frac{\partial \tilde{W}}{\partial \mathbf{K}} , \quad -\bar{\boldsymbol{\mu}}_0 = \frac{\partial \tilde{W}}{\partial \bar{\mathbf{K}}} , \quad (120)$$

or from their components $\tau^{\alpha\beta}$, $M_0^{\alpha\beta}$, and $\bar{M}_0^{\alpha\beta}$ using Eq. (116).

Remark 4.7: Balance equation (101) and various constitutive equations, such as (120), (116), and (110) have been expressed directly in surface form without introducing a thickness variable. The unit of the strain energy W is thus energy per reference area. However, the influence of the thickness is still present – either in the material parameters of the surface form, or via a through-the-thickness integration of 3D constitutive laws (see e.g. Kiendl et al. (2015); Duong et al. (2017)). In a surface formulation, the thickness strain can be still determined from various approaches: One can enforce incompressibility or the plane stress condition (Duong et al., 2017), or one can introduce an additional degree-of-freedom (Simo et al., 1990).

4.3 Comparison with existing second-gradient theory of Kirchhoff-Love shells

To show the consistency of our proposed theory with the existing second-gradient theory of [Steigmann \(2018\)](#), we insert κ_g obtained from (51) into the power expression (107). This results in the expression (see Appendix D)

$$P_{\text{int}} = \int_{\mathcal{R}_0} \boldsymbol{\tau}^\alpha \cdot \dot{\mathbf{a}}_\alpha \, dA + \int_{\mathcal{R}_0} M_0^{\alpha\beta} \dot{b}_{\alpha\beta} \, dA + \int_{\mathcal{R}_0} \bar{M}_{0\gamma}^{\alpha\beta} \dot{S}_{\alpha\beta}^\gamma \, dA, \quad (121)$$

where $S_{\alpha\beta}^\gamma := \Gamma_{\alpha\beta}^\gamma - \bar{\Gamma}_{\alpha\beta}^\gamma$. The last term in (121) is the power due to in-plane fiber bending. Here, the relative Christoffel symbol $S_{\alpha\beta}^\gamma$ is the chosen strain measure for the in-plane curvature, and $\bar{M}_{0\gamma}^{\alpha\beta} := J \bar{\mu} \ell^{\alpha\beta} c_\gamma$ is the in-plane bending moment corresponding to a change in $S_{\alpha\beta}^\gamma$.

In the first term of (121), $\boldsymbol{\tau}^\alpha := J \sigma^{\alpha\beta} \mathbf{a}_\beta$ denotes the effective stress vectors that are work-conjugate to $\dot{\mathbf{a}}_\alpha$, with $\sigma^{\alpha\beta}$ now being defined by

$$\sigma^{\alpha\beta} := \tilde{\sigma}^{\alpha\beta} - \bar{\mu} \kappa_g \ell^{\alpha\beta} + \bar{\mu} (\lambda^{-1} L_{;\gamma}^\alpha \ell^\gamma + S_{\gamma\delta}^{\alpha\gamma} \ell^{\gamma\delta}) c^\beta - \bar{\mu} (\lambda^{-1} L_{;\delta}^\gamma \ell^\delta + S_{\gamma\delta}^\theta \ell^{\gamma\delta} \ell_\theta) \ell^\alpha c^\beta, \quad (122)$$

which is generally unsymmetric. Therefore, in contrast to expressions (107) and (113), the effective stress $\tau^{\alpha\beta} := \boldsymbol{\tau}^\alpha \cdot \mathbf{a}^\beta$ is generally unsymmetric here. With a possible loss of generality, its symmetrization is adopted in [Steigmann \(2018\)](#), i.e. $\tau^{\alpha\beta} := \frac{1}{2}(\boldsymbol{\tau}^\alpha \cdot \mathbf{a}^\beta + \boldsymbol{\tau}^\beta \cdot \mathbf{a}^\alpha)$, so that the internal power becomes

$$P_{\text{int}} = \frac{1}{2} \int_{\mathcal{R}_0} \tau^{\alpha\beta} \dot{a}_{\alpha\beta} \, dA + \int_{\mathcal{R}_0} M_0^{\alpha\beta} \dot{b}_{\alpha\beta} \, dA + \int_{\mathcal{R}_0} \bar{M}_{0\gamma}^{\alpha\beta} \dot{S}_{\alpha\beta}^\gamma \, dA, \quad (123)$$

which is equivalent to the expression (63) in [Steigmann \(2018\)](#).¹²

Remark 4.8: As shown in Appendix D, the asymmetry of the effective stress (122) is due to the fact that it still contains in-plane bending apart from surface stretching. It is unsymmetric even for initially straight fibers in a general setting. Therefore the symmetrization employed in [Steigmann \(2018\)](#) is valid only for special cases.

Remark 4.9: The power term $\bar{M}_{0\gamma}^{\alpha\beta} \dot{S}_{\alpha\beta}^\gamma$ in the gradient theory of [Steigmann \(2018\)](#) can become ill-defined for initially curved fibers when $\bar{\Gamma}_{\alpha\beta}^\gamma$ approaches zero even though there is a change in geodesic curvature. This can solely result from the choice of parametrization, as seen e.g. in Sec. 7.1. In contrast, the internal power expressions (103), (107) and (113) presented above overcome this limitation.

4.4 Extension to multiple fiber families

In case of n_f fiber families \mathcal{C}_i , $i = 1, \dots, n_f$, we define the tangent $\boldsymbol{\ell}_i$ and director \mathbf{c}_i for each \mathcal{C}_i . The in-plane curvatures (48) and the moment \bar{m} in (66) are then defined for each fiber family \mathcal{C}_i . Then P_{int} in Eq. (113) simply becomes

$$P_{\text{int}} = \frac{1}{2} \int_{\mathcal{R}_0} \tau^{\alpha\beta} \dot{a}_{\alpha\beta} \, dA + \int_{\mathcal{R}_0} M_0^{\alpha\beta} \dot{b}_{\alpha\beta} \, dA + \sum_{i=1}^{n_f} \int_{\mathcal{R}_0} \bar{M}_{0i}^{\alpha\beta} \dot{\bar{b}}_{\alpha\beta}^i \, dA. \quad (124)$$

In accordance with Eq. (124), the form of the stored energy function is extended from (115) to

$$W = \hat{W}(a_{\alpha\beta}, b_{\alpha\beta}, \bar{b}_{\alpha\beta}^i; h_i^{\alpha\beta}). \quad (125)$$

This function can equivalently be expressed in terms of the invariants, e.g. as

$$W = \check{W}(I_1, J, \Lambda_i, \gamma_{ij}, H, \kappa, \kappa_n^i, \tau_g^i, \kappa_g^i), \quad (126)$$

¹²adapted to the notations used in this paper.

since all these invariants are functions of $a_{\alpha\beta}$, $b_{\alpha\beta}$, and $\bar{b}_{\alpha\beta}^i$. The constitutive equations thus read

$$\tau^{\alpha\beta} = 2 \frac{\partial \hat{W}}{\partial a_{\alpha\beta}}, \quad M_0^{\alpha\beta} = \frac{\partial \hat{W}}{\partial b_{\alpha\beta}}, \quad \bar{M}_{0i}^{\alpha\beta} = \frac{\partial \hat{W}}{\partial \bar{b}_{\alpha\beta}^i}, \quad (127)$$

where $\bar{M}_{0i}^{\alpha\beta}$ are the components of the nominal stress couple tensor associated with in-plane bending of fiber i . They correspond to the change in the in-plane curvature $\bar{b}_{\alpha\beta}^i$ of fiber i .

5 Constitutive examples

This section presents constitutive examples for the presented theory considering unconstrained and constrained fibers. We restrict ourselves here to two families of fibers. Note however that our approach allows for any number of fiber families.

5.1 A simple generalized fabric model

A simple generalized shell model for two-fiber-family fabrics that are initially curved and bonded to a matrix is given by

$$W = W_{\text{matrix}} + W_{\text{fib-stretch}} + W_{\text{fib-bending}} + W_{\text{fib-torsion}} + W_{\text{fib-angle}}, \quad (128)$$

where

$$\begin{aligned} W_{\text{matrix}} &= U(J) + \frac{1}{2} \mu (I_1 - 2 - 2 \ln J), \\ W_{\text{fib-stretch}} &= \frac{1}{8} \epsilon_L \sum_{i=1}^2 (\Lambda_i - 1)^2, \\ W_{\text{fib-bending}} &= \frac{1}{2} \sum_{i=1}^2 \left[\beta_n (K_n^i)^2 + \beta_g (K_g^i)^2 \right], \\ W_{\text{fib-torsion}} &= \frac{1}{2} \beta_\tau \sum_{i=1}^2 (T_g^i)^2, \\ W_{\text{fib-angle}} &= \frac{1}{4} \epsilon_a (\gamma_{12} - \gamma_{12}^0)^2 \end{aligned} \quad (129)$$

are the strain energies for matrix deformation, fiber stretching, out-of-plane and in-plane fiber bending, fiber torsion, and the linkage between the two fiber families, respectively. $U(J)$ is the surface dilatation energy. In the above expression, $\sqrt{\Lambda}$, T_g , K_n , K_g , and γ_{12} denote the fiber stretch, the norminal change in geodesic fiber torsion, normal fiber curvature and geodesic fiber curvature, and the relative angle between fiber families, respectively (see Tabs. 1 and 2). Symbols μ , ϵ_\bullet , and β_\bullet are material parameters. ϵ_L can be taken as zero during fiber compression ($\Lambda_i < 1$) to mimic buckling phenomenologically.

From Eq. (116) and (129), we then find the effective stress and moment components for the director gradient-based formulation (Sec. 4.2), (see Appendix A and Sauer and Duong (2017)

for the required derivatives of kinematical quantities) as

$$\begin{aligned}
\tau^{\alpha\beta} &= J \frac{\partial U}{\partial J} a^{\alpha\beta} + \mu (A^{\alpha\beta} - a^{\alpha\beta}) + \frac{1}{2} \epsilon_L \sum_{i=1}^2 (\Lambda_i - 1) L_i^{\alpha\beta} + \epsilon_a (\gamma_{12} - \gamma_{12}^0) (L_1^\alpha L_2^\beta)^{\text{sym}} , \\
M_0^{\alpha\beta} &= \beta_n \sum_{i=1}^2 K_n^i L_i^{\alpha\beta} + \beta_\tau \sum_{i=1}^2 T_g^i (c_{0i}^\alpha L_i^\beta)^{\text{sym}} , \\
\bar{M}_0^{\alpha\beta} &= \beta_g \sum_{i=1}^2 K_g^i L_i^{\alpha\beta} ,
\end{aligned} \tag{130}$$

where $(\bullet^{\alpha\beta})^{\text{sym}} = \frac{1}{2}(\bullet^{\alpha\beta} + \bullet^{\beta\alpha})$ denotes symmetrization.

5.2 Fiber inextensibility constraints

For most textile materials, the deformation is usually characterized by very high tensile stiffness in fiber direction and low in-plane shear and bending stiffness. In this case, one may model the very high tensile stiffness along the fiber direction i by the inextensibility constraint

$$g_i := \Lambda_i - 1 = 0 , \quad \Lambda_i > 1 , \tag{131}$$

where Λ_i is defined in Tab. 2. This constraint then replaces the $W_{\text{fib-stretch}}$ term in (128). To enforce this constraint, we can employ the Lagrange multiplier method in the strain energy function

$$\tilde{W} := W + \sum_{i=1}^{n_f} q_i g_i , \tag{132}$$

where q_i ($i = 1, \dots, n_f$) denote the corresponding Lagrange multipliers. The stress components in this case become

$$\tau^{\alpha\beta} = 2 \frac{\partial \tilde{W}}{\partial a_{\alpha\beta}} = 2 \frac{\partial W}{\partial a_{\alpha\beta}} + \sum_{i=1}^{n_f} 2 q_i L_i^{\alpha\beta} . \tag{133}$$

This leads to the same stress and moment components as in (130.1) with the exception that $\epsilon_L (\Lambda_i - 1)/2$ is now replaced by $2 q_i$.

6 Weak form

This section presents the weak form for the generalized Kirchhoff-Love shell. The weak form is obtained by the same steps as the mechanical power balance in Sec. 3.5, simply by replacing velocity \mathbf{v} by variation $\delta \mathbf{x}$. This gives

$$G_{\text{in}} + G_{\text{int}} - G_{\text{ext}} = 0 \quad \forall \delta \mathbf{x} \in \mathcal{V} , \tag{134}$$

where according to Eq. (101), (102), (104), and (124)

$$\begin{aligned}
G_{\text{in}} &= \int_{S_0} \delta \mathbf{x} \cdot \rho_0 \dot{\mathbf{v}} \, dA , \\
G_{\text{int}} &= \frac{1}{2} \int_{S_0} \tau^{\alpha\beta} \delta a_{\alpha\beta} \, dA + \int_{S_0} M_0^{\alpha\beta} \delta b_{\alpha\beta} \, dA + \sum_{i=1}^{n_f} \int_{S_0} \bar{M}_{0i}^{\alpha\beta} \delta \bar{b}_{\alpha\beta}^i \, dA , \\
G_{\text{ext}} &= \int_S \delta \mathbf{x} \cdot \mathbf{f} \, da + \int_{\partial S} \delta \mathbf{x} \cdot \mathbf{T} \, ds + \int_{\partial S} \delta \mathbf{n} \cdot \mathbf{M} \, ds + \sum_{i=1}^{n_f} \int_{\partial S} \delta \mathbf{c}_i \cdot \bar{\mathbf{M}}_i \, ds .
\end{aligned} \tag{135}$$

Using (127), G_{int} can also be expressed as the variation of potential (125) w.r.t. its arguments,

$$G_{\text{int}} = \int_{\mathcal{S}_0} \delta W \, dA = \int_{\mathcal{S}_0} \frac{\partial W}{\partial a_{\alpha\beta}} \delta a_{\alpha\beta} \, dA + \int_{\mathcal{S}_0} \frac{\partial W}{\partial b_{\alpha\beta}} \delta b_{\alpha\beta} \, dA + \sum_{i=1}^{n_f} \int_{\mathcal{S}_0} \frac{\partial W}{\partial \bar{b}_{\alpha\beta}^i} \delta \bar{b}_{\alpha\beta}^i \, dA. \quad (136)$$

For constrained materials, e.g. (132), G_{int} becomes

$$G_{\text{int}} = \int_{\mathcal{S}_0} \delta \tilde{W} \, dA = \int_{\mathcal{S}_0} \left(\frac{1}{2} \tau^{\alpha\beta} \delta a_{\alpha\beta} + M_0^{\alpha\beta} \delta b_{\alpha\beta} + \sum_{i=1}^{n_f} \bar{M}_{0i}^{\alpha\beta} \delta \bar{b}_{\alpha\beta}^i \right) \, dA + \sum_{i=1}^{n_f} \int_{\mathcal{S}_0} \frac{\partial \tilde{W}}{\partial q_i} \delta q_i \, dA. \quad (137)$$

For the constitutive example in Sec. 5, $\tau^{\alpha\beta}$, $M_0^{\alpha\beta}$ and $\bar{M}_{0i}^{\alpha\beta}$ are given by (133), (130.2) and (130.3), respectively, while $\partial \tilde{W} / \partial q_i = g_i$.

The linearization of weak form (135) and its discretization can be found in Duong et al. (2022).

7 Analytical solutions

This section illustrates the preceding theory by several analytical examples considering simple homogeneous deformation states. They are useful elementary test cases for the verification of computational formulations.

7.1 Geodesic curvature of a circle embedded in an expanding flat surface

The first example presents the computation of geodesic curvature κ_g from Eqs. (51) and (52) and confirms that only Eq. (51) gives the correct value for initially curved fibers. This illustrates the limitation of existing second-gradient Kirchhoff-Love shell theory for cases where $\bar{\Gamma}_{\alpha\beta}^\gamma = 0$ due to the choice of the surface parametrization.

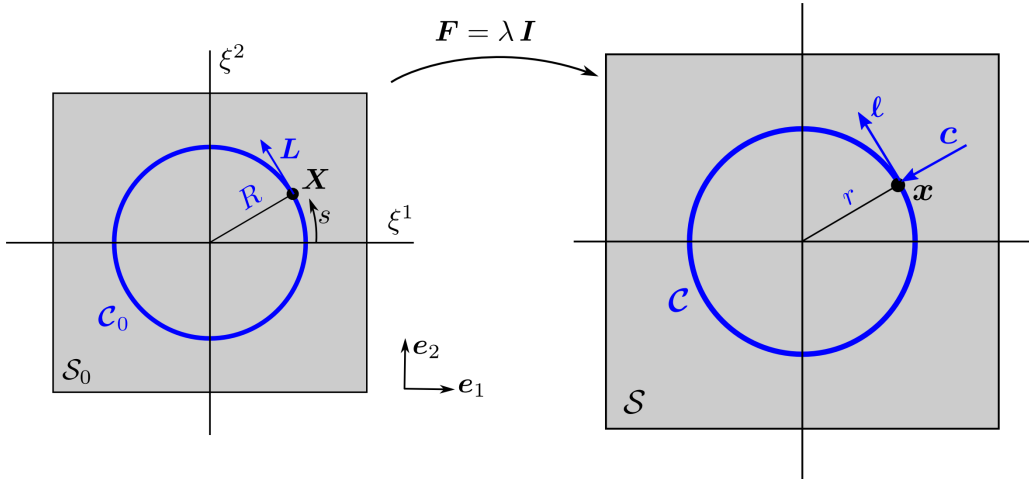


Figure 3: Computation of geodesic curvature κ_g : A circular fiber \mathcal{C} is embedded in the planar surface \mathcal{S} that is expanded by the homogeneous deformation $\mathbf{F} = \lambda \mathbf{I}$.

To this end, we consider a circular fiber $\mathcal{C}_0 \in \mathcal{S}_0$ with initial radius R expanding according to the deformation gradient $\mathbf{F} = \lambda \mathbf{I}$ to $\mathcal{C} \in \mathcal{S}$ with the current radius r as shown in Fig. 3. Therefore, the geodesic curvatures of \mathcal{C}_0 and \mathcal{C} are expected to simply be $\kappa_g^0 = 1/R$ and $\kappa_g = 1/r$, respectively.

With respect to the convective coordinates ($\xi^1 = X$, $\xi^2 = Y$) shown in Fig. (3a), the position vector on any point of \mathcal{S}_0 and \mathcal{S} can be represented by

$$\begin{aligned}\mathbf{X} &= \mathbf{X}_s(\xi^1, \xi^2) := \xi^1 \mathbf{e}_1 + \xi^2 \mathbf{e}_2, \\ \mathbf{x} &= \mathbf{x}_s(\xi^1, \xi^2) := \lambda \xi^1 \mathbf{e}_1 + \lambda \xi^2 \mathbf{e}_2.\end{aligned}\quad (138)$$

The surface tangent and normal vectors follow from Eq. (138) as

$$\begin{aligned}\mathbf{A}_1 &= \mathbf{e}_1, & \mathbf{A}_2 &= \mathbf{e}_2, & \text{and } \mathbf{N} &= \mathbf{e}_3, \\ \mathbf{a}_1 &= \lambda \mathbf{e}_1, & \mathbf{a}_2 &= \lambda \mathbf{e}_2, & \text{and } \mathbf{n} &= \mathbf{e}_3,\end{aligned}\quad (139)$$

so that

$$\begin{aligned}\mathbf{A}^1 &= \mathbf{e}_1, & \mathbf{A}^2 &= \mathbf{e}_2, \\ \mathbf{a}^1 &= \frac{1}{\lambda} \mathbf{e}_1, & \mathbf{a}^2 &= \frac{1}{\lambda} \mathbf{e}_2.\end{aligned}\quad (140)$$

The surface deformation gradient then reads

$$\mathbf{F} = \mathbf{a}_\alpha \otimes \mathbf{A}^\alpha = \lambda (\mathbf{e}_1 \otimes \mathbf{e}_1 + \mathbf{e}_2 \otimes \mathbf{e}_2), \quad (141)$$

and the surface Christoffel symbols take the form

$$\bar{\Gamma}_{\alpha\beta}^\gamma := \mathbf{A}_{\alpha,\beta} \cdot \mathbf{A}^\gamma = 0, \quad \Gamma_{\alpha\beta}^\gamma := \mathbf{a}_{\alpha,\beta} \cdot \mathbf{a}^\gamma = 0. \quad (142)$$

In the reference configuration, the fiber is parametrized by the arc-length coordinate s as

$$\mathbf{X} = \mathbf{X}_c(s) := R \cos \frac{s}{R} \mathbf{e}_1 + R \sin \frac{s}{R} \mathbf{e}_2. \quad (143)$$

From Eq. (143) and (141) follows

$$\begin{aligned}\mathbf{L} &:= \mathbf{X}_{c,s} = -\sin \frac{s}{R} \mathbf{e}_1 + \cos \frac{s}{R} \mathbf{e}_2 = -\frac{Y}{R} \mathbf{A}_1 + \frac{X}{R} \mathbf{A}_2, \\ \lambda \boldsymbol{\ell} &:= \mathbf{F} \mathbf{L} = -\frac{Y}{R} \mathbf{a}_1 + \frac{X}{R} \mathbf{a}_2, \\ \boldsymbol{\ell} &:= \frac{\mathbf{F} \mathbf{L}}{\lambda} = -\frac{Y}{R} \mathbf{e}_1 + \frac{X}{R} \mathbf{e}_2, \\ \mathbf{c} &:= \mathbf{n} \times \boldsymbol{\ell} = -\frac{X}{R} \mathbf{e}_1 - \frac{Y}{R} \mathbf{e}_2.\end{aligned}\quad (144)$$

In this equation $(\xi^1, \xi^2) = (X, Y) \in \mathcal{C}_0$. Thus,

$$[\hat{L}_{,\beta}^\alpha] := \frac{1}{\lambda} [L_{,\beta}^\alpha] = \frac{1}{\lambda R} \begin{bmatrix} 0 & -1 \\ 1 & 0 \end{bmatrix}, \quad (145)$$

and

$$[\ell^\alpha] := [\boldsymbol{\ell} \cdot \mathbf{a}^\alpha] = \frac{1}{\lambda R} \begin{bmatrix} -Y \\ X \end{bmatrix}, \quad [c_\alpha] := [\mathbf{c} \cdot \mathbf{a}_\alpha] = -\frac{\lambda}{R} \begin{bmatrix} X \\ Y \end{bmatrix}. \quad (146)$$

Inserting these expressions into Eq. (51), and using the identity $X^2 + Y^2 = R^2$ gives the geodesic curvature

$$\kappa_g^\Gamma = 0, \quad \kappa_g^L = \frac{1}{\lambda R} = \frac{1}{r}, \quad \kappa_g = \kappa_g^\Gamma + \kappa_g^L = \frac{1}{r}. \quad (147)$$

For \mathcal{C}_0 , setting $\lambda = 1$ directly yields $\kappa_g^0 = 1/R$.

In contrast, Eq. (52) obviously fails to reproduce the correct geodesic curvatures since the Christoffel symbols are zero everywhere solely due to the choice of the surface parametrization. Furthermore, since $\bar{\Gamma}_{\alpha\beta}^\gamma = 0$, the in-plane bending term of the internal power is ill-defined in second-gradient theory (123), whereas we get a well-defined power from (51) with (103), (107) and (113). It correctly captures the change in geodesic curvature.

7.2 Biaxial stretching of a sheet containing diagonal fibers

The second example presents an analytical solution for homogeneous biaxial stretching of a rectangular sheet from dimension $L \times H$ to $\ell \times h$, such that $\ell = \lambda_\ell L$ and $h = \lambda_h H$. The sheet contains matrix material and two fiber families distributed diagonally as shown in Fig. 4. The

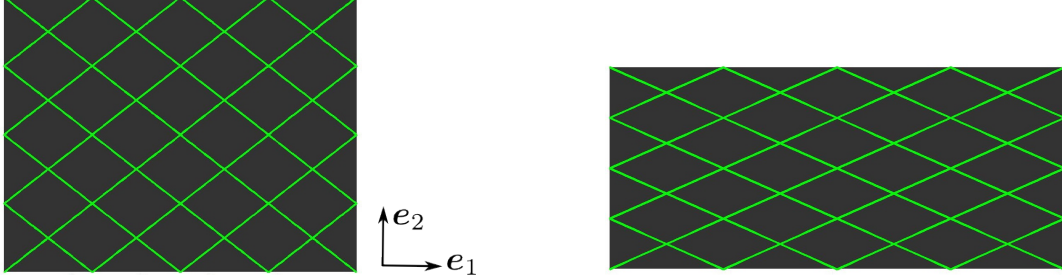


Figure 4: Biaxial stretching of a rectangular sheet from dimension $L \times H$ (left) to $\ell \times h$ (right).

strain energy function in this example is taken from (129) as

$$W = \frac{\mu}{2} (I_1 - 2 - \ln J) + \frac{1}{8} \epsilon_L \sum_{i=1}^2 (\Lambda_i - 1)^2 + \frac{1}{4} \epsilon_a (\gamma_{12} - \gamma_{12}^0)^2. \quad (148)$$

Therefore the stress components follow as

$$\tau^{\alpha\beta} = \mu (A^{\alpha\beta} - a^{\alpha\beta}) + \sum_{i=1}^2 \tau_i L_i^{\alpha\beta} + \epsilon_a (\gamma_{12} - \gamma_{12}^0) (L_1^\alpha L_2^\beta)^{\text{sym}}, \quad (149)$$

where $\tau_i := \frac{1}{2} \epsilon_L (\Lambda_i - 1)$ denotes the nominal fiber tension. The parameterization can be chosen such that the surface tangent vectors are $\mathbf{A}_1 = L \mathbf{e}_1$, $\mathbf{A}_2 = H \mathbf{e}_2$, $\mathbf{a}_1 = \ell \mathbf{e}_1$, and $\mathbf{a}_2 = h \mathbf{e}_2$, where \mathbf{e}_α are the basis vectors shown in Fig. 4. The fiber directions are $\mathbf{L}_1 = (L \mathbf{e}_1 + H \mathbf{e}_2)/D$, $\mathbf{L}_2 = (L \mathbf{e}_1 - H \mathbf{e}_2)/D$, where $D^2 := L^2 + H^2$. We thus find

$$\begin{aligned} [A^{\alpha\beta}] &= \begin{bmatrix} 1/L^2 & 0 \\ 0 & 1/H^2 \end{bmatrix}, & [a^{\alpha\beta}] &= \begin{bmatrix} 1/\ell^2 & 0 \\ 0 & 1/h^2 \end{bmatrix}, & [L_1^{\alpha\beta}] &= \frac{1}{D^2} \begin{bmatrix} 1 & 1 \\ 1 & 1 \end{bmatrix}, \\ [L_2^{\alpha\beta}] &= \frac{1}{D^2} \begin{bmatrix} 1 & -1 \\ -1 & 1 \end{bmatrix}, & \text{and } [L_1^\alpha L_2^\beta]^{\text{sym}} &= \frac{1}{D^2} \begin{bmatrix} 1 & 0 \\ 0 & -1 \end{bmatrix}. \end{aligned} \quad (150)$$

Further, we find the fiber stretch and angles

$$\begin{aligned} \Lambda_f &:= \Lambda_1 = \Lambda_2 = (\ell^2 + h^2)/D^2, \\ \gamma_{12}^0 &= A_{\alpha\beta} L_1^\alpha L_2^\beta = (L^2 - H^2)/D^2, \\ \gamma_{12} &= a_{\alpha\beta} L_1^\alpha L_2^\beta = (\ell^2 - h^2)/D^2. \end{aligned} \quad (151)$$

Inserting Eq. (151) into Eq. (149) gives the stress tensor $\boldsymbol{\sigma} = J^{-1} \tau^{\alpha\beta} \mathbf{a}_\alpha \otimes \mathbf{a}_\beta$, where $J := \lambda_\ell \lambda_h$. The resultant reaction forces at the boundaries then follow as

$$\begin{aligned} F_1 &= h \mathbf{e}_1 \boldsymbol{\sigma} \mathbf{e}_1 = \frac{h}{J} \left[\mu (\lambda_\ell^2 - 1) + \frac{2\ell^2}{D^2} \tau + \epsilon_a \frac{\ell^2}{D^2} (\gamma_{12} - \gamma_{12}^0) \right], \\ F_2 &= \ell \mathbf{e}_2 \boldsymbol{\sigma} \mathbf{e}_2 = \frac{\ell}{J} \left[\mu (\lambda_h^2 - 1) + \frac{2h^2}{D^2} \tau - \epsilon_a \frac{h^2}{D^2} (\gamma_{12} - \gamma_{12}^0) \right], \end{aligned} \quad (152)$$

where $\tau := \tau_1 = \tau_2 = \frac{1}{2} \epsilon_L (\Lambda_f - 1)$.

Remark 7.1: The presented solution (152) includes pure shear by simply setting $\lambda_h = 1/\lambda_\ell$.

Remark 7.2: For uniaxial tension e.g. in the \mathbf{e}_1 direction and with free horizontal boundaries, condition $F_2 = 0$ in Eq. (152.2) gives the solution of λ_h , which in turn can be inserted to Eq. (152.1) for the resultant reaction force $F_1(\lambda_\ell)$ as

$$F_1 = \frac{H}{\lambda_\ell D^4} \left[D^4 \mu (\lambda_\ell^2 - 1) + (\epsilon_L + \epsilon_a) \lambda_\ell^4 L^4 + (\epsilon_L - \epsilon_a) \lambda_\ell^2 \lambda_h^2 H^2 L^2 + (\epsilon_L - \gamma_{12}^0 \epsilon_a) \lambda_\ell^2 L^2 D^2 \right], \quad (153)$$

where

$$\lambda_h^2 = \frac{1}{2a} \left(-b + \sqrt{b^2 + 4a\mu} \right), \quad (154)$$

while $a := \frac{H^2}{D^4} (\epsilon_L + \epsilon_a)$, and $b := \mu + (\epsilon_L - \epsilon_a) \frac{\lambda_\ell^2 L^2 H^2}{D^4} - \epsilon_L \frac{H^2}{D^2} + \gamma_{12}^0 \epsilon_a \frac{H^2}{D^2}$.

Remark 7.3: Solution (152) also captures the inextensibility of fibers. In this case either the vertical, or the horizontal boundaries have to be stress free. In the latter case, $F_2 = 0$ and

$$\lambda_h = \sqrt{\frac{D^2}{H^2} - \lambda_\ell^2 \frac{L^2}{H^2}}, \quad (155)$$

due to $D^2 = \ell^2 + h^2$. In this case the deformation is limited by $\lambda_\ell^{\max} = D/L$. From $F_2 = 0$, the nominal fiber tension now follows as

$$\tau = \frac{1}{2} \epsilon_a (\gamma_{12} - \gamma_{12}^0) - \frac{1}{2} \frac{D^2}{h^2} \mu (\lambda_h^2 - 1). \quad (156)$$

Inserting (156) into (152.1) then gives

$$F_1 = \frac{h}{J} \left[\mu (\lambda_\ell^2 - 1) - \frac{\ell^2}{h^2} \mu (\lambda_h^2 - 1) + 2 \epsilon_a \frac{\ell^2}{D^2} (\gamma_{12} - \gamma_{12}^0) \right]. \quad (157)$$

7.3 Picture frame test

The third example derives an analytical solution for the shear force in the picture frame test of an $L_0 \times L_0$ square sheet with two fiber families as shown in Fig. 5a-b. From the figure, we find the surface tangent vectors

$$\begin{aligned} \mathbf{A}_1 &= L_0 \cos \varphi_0 \mathbf{e}_1 + L_0 \sin \varphi_0 \mathbf{e}_2, & \mathbf{a}_1 &= L_0 \cos \varphi \mathbf{e}_1 + L_0 \sin \varphi \mathbf{e}_2, \\ \mathbf{A}_2 &= -L_0 \cos \varphi_0 \mathbf{e}_1 + L_0 \sin \varphi_0 \mathbf{e}_2, & \mathbf{a}_2 &= -L_0 \cos \varphi \mathbf{e}_1 + L_0 \sin \varphi \mathbf{e}_2, \end{aligned} \quad (158)$$

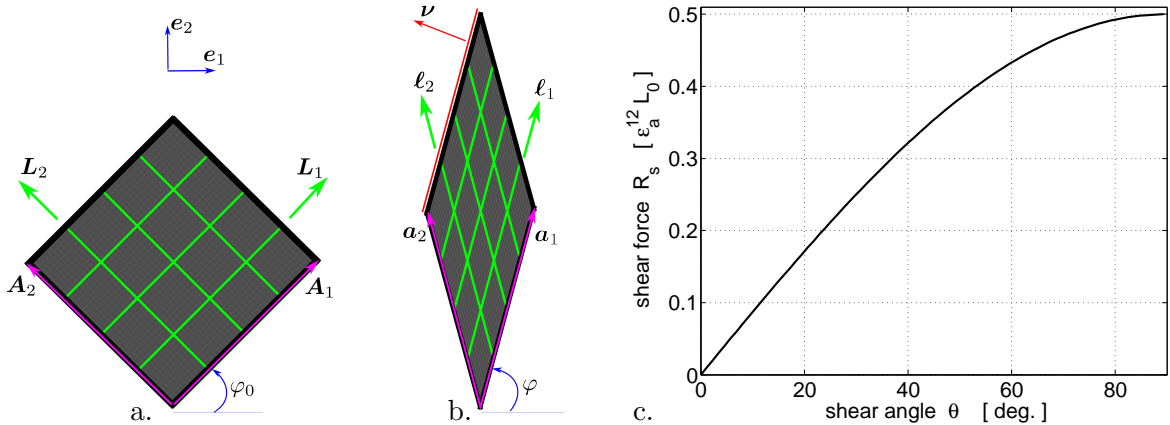


Figure 5: Picture frame test: (a.) Initial and (b.) deformed configurations containing two fiber families. (c.) Exact solution of the shear force vs. shear angle $\theta := 2\varphi - 90^\circ$.

and the fiber directions

$$\begin{aligned} \mathbf{L}_1 &= \cos \varphi_0 \mathbf{e}_1 + \sin \varphi_0 \mathbf{e}_2, & \boldsymbol{\ell}_1 &= \cos \varphi \mathbf{e}_1 + \sin \varphi \mathbf{e}_2, \\ \mathbf{L}_2 &= -\cos \varphi_0 \mathbf{e}_1 + \sin \varphi_0 \mathbf{e}_2, & \boldsymbol{\ell}_2 &= -\cos \varphi \mathbf{e}_1 + \sin \varphi \mathbf{e}_2, \end{aligned} \quad (159)$$

where $\varphi_0 = \pi/4$. Accordingly, the components of tensors \mathbf{C} and $(\mathbf{L}_1 \otimes \mathbf{L}_2)^{\text{sym}}$ read

$$[C_\alpha^\beta] = a_{\alpha\gamma} A^{\gamma\beta} = \begin{bmatrix} 1 & -\cos(2\varphi) \\ -\cos(2\varphi) & 1 \end{bmatrix}, \quad \text{and} \quad [L_1^\alpha L_2^\beta]^{\text{sym}} = \frac{1}{2L_0^2} \begin{bmatrix} 0 & 1 \\ 1 & 0 \end{bmatrix}, \quad (160)$$

respectively. From Eq. (160.1), the surface stretch is found as

$$J = \sqrt{\det[C_\alpha^\beta]} = \sin(2\varphi). \quad (161)$$

Further, the strain energy function in this example is taken from (129) as $W = \frac{1}{4} \epsilon_a (\gamma_{12} - \gamma_{12}^0)^2$, so that the Cauchy stress components are

$$[\sigma^{\alpha\beta}] = \frac{1}{J} \epsilon_a (\gamma_{12} - \gamma_{12}^0) [L_1^\alpha L_2^\beta]^{\text{sym}} = -\frac{1}{2L_0^2} \epsilon_a \cot(2\varphi) \begin{bmatrix} 0 & 1 \\ 1 & 0 \end{bmatrix}. \quad (162)$$

Here, we have used Eq. (160.2), Eq. (161), $\gamma_{12}^0 = \mathbf{L}_1 \cdot \mathbf{L}_2 = 0$, and $\gamma_{12} = \boldsymbol{\ell}_1 \cdot \boldsymbol{\ell}_2 = -\cos(2\varphi)$.

Consider the upper left edge with normal vector $\boldsymbol{\nu} = -\sin \varphi \mathbf{e}_1 + \cos \varphi \mathbf{e}_2 = \nu_\alpha \mathbf{a}^\alpha$, where $\nu_1 = \boldsymbol{\nu} \cdot \mathbf{a}_1 = 0$, and $\nu_2 = \boldsymbol{\nu} \cdot \mathbf{a}_2 = L_0 \sin(2\varphi)$. The traction components on this edge can be computed from

$$[t^\alpha] = [\sigma^{\alpha\beta} \nu_\beta] = -\frac{1}{2L_0} \epsilon_a^{12} \cos(2\varphi) \begin{bmatrix} 1 \\ 0 \end{bmatrix}. \quad (163)$$

Therefore, the traction vector solely contains the shear contribution

$$\mathbf{t} = t^\alpha \mathbf{a}_\alpha = t^1 \mathbf{a}_1 = -\frac{1}{2} \epsilon_a^{12} \cos(2\varphi) (\cos \varphi \mathbf{e}_1 + \sin \varphi \mathbf{e}_2), \quad (164)$$

so that the shear force (i.e. the tangent reaction) at the edge of the sheet is

$$R_s = \mathbf{t} \cdot \frac{\mathbf{a}_1}{\|\mathbf{a}_1\|} L_0 = -\frac{1}{2} \epsilon_a^{12} \cos(2\varphi) L_0 = \frac{1}{2} \epsilon_a^{12} \sin(\theta) L_0, \quad (165)$$

where $\theta := 2\varphi - 90^\circ$ denotes the shear angle. This solution is plotted in Fig. 5c.

7.4 Annulus expansion

The fourth example presents an analytical solution for the expansion of an annulus containing distributed circular fibers and matrix material as depicted in Fig. 6. The inner and the outer rings with radius R_i and R_o , respectively, are expanded to r_i and r_o by the constant stretch $\bar{\lambda} = r_i/R_i = r_o/R_o$. The strain energy density (per reference area) is taken as

$$W = W_{\text{matrix}} + W_{\text{fib-bend}} + W_{\text{fib-stretch}}, \quad (166)$$

where

$$\begin{aligned} W_{\text{matrix}} &= \frac{1}{2} K (J - 1)^2, \\ W_{\text{fib-bend}} &= \frac{1}{2} \beta k_g^2. \\ W_{\text{fib-stretch}} &= \frac{1}{8} \epsilon_L (\Lambda - 1)^2. \end{aligned} \quad (167)$$

Here, $K(R)$, β , and ϵ_L are material parameters for matrix dilatation, fiber bending, and fiber stretching, respectively, and J , Λ , and k_g are invariants induced by tensors \mathbf{C} and $\bar{\mathbf{K}}$ as listed in Tab. 1 and 2.

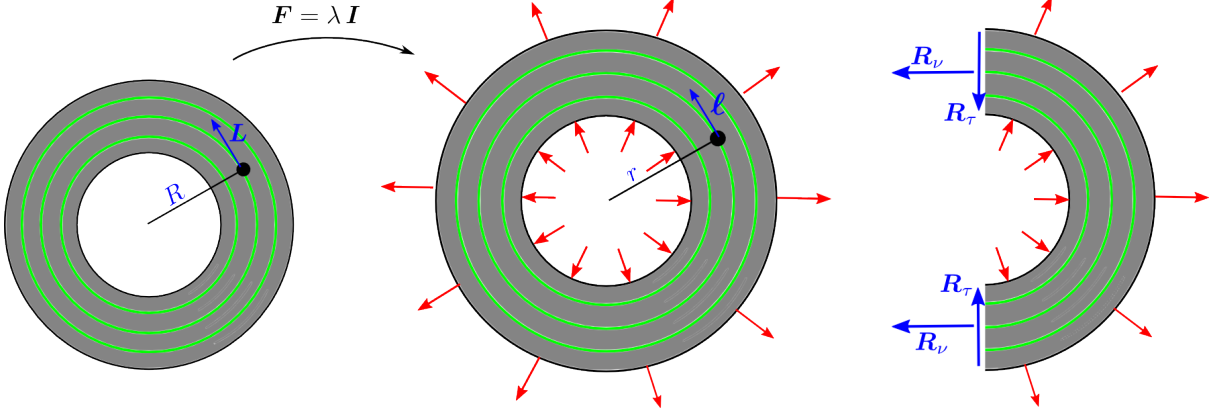


Figure 6: Annulus expansion: An annulus containing matrix (grey color) and distributed circular fibers (green color) is expanded homogeneously from initial configuration (left) by applying Dirichlet boundary condition on both inner and outer surfaces (middle). The expansion causes the resultant interface forces \mathbf{R}_ν and \mathbf{R}_τ on the cut through a symmetry plane (right).

7.4.1 Kinematical quantities

According to Fig. 6, the initial and current configurations as well as the initial fiber direction can be described by

$$\begin{aligned}
 \mathbf{X} &= \mathbf{X}(R, \phi) := R \cos \phi \mathbf{e}_1 + R \sin \phi \mathbf{e}_2 , \\
 \mathbf{x} &= \mathbf{x}(R, \phi) := r \cos \phi \mathbf{e}_1 + r \sin \phi \mathbf{e}_2 , \\
 \mathbf{L} &= \mathbf{L}(\phi) := -\sin \phi \mathbf{e}_1 + \cos \phi \mathbf{e}_2 .
 \end{aligned} \tag{168}$$

Here $r = \lambda R$, due to the homogeneous deformation, with λ being the fiber stretch. From this, we find the covariant tangent vectors

$$\begin{aligned}
 \mathbf{A}_1 &= \frac{\partial \mathbf{X}}{\partial R} = \cos \phi \mathbf{e}_1 + \sin \phi \mathbf{e}_2 , \\
 \mathbf{A}_2 &= \frac{\partial \mathbf{X}}{\partial \phi} = -R \sin \phi \mathbf{e}_1 + R \cos \phi \mathbf{e}_2 , \\
 \mathbf{a}_1 &= \frac{\partial \mathbf{x}}{\partial R} = \lambda \cos \phi \mathbf{e}_1 + \lambda \sin \phi \mathbf{e}_2 , \\
 \mathbf{a}_2 &= \frac{\partial \mathbf{x}}{\partial \phi} = -r \sin \phi \mathbf{e}_1 + r \cos \phi \mathbf{e}_2 ,
 \end{aligned} \tag{169}$$

and the constant surface normal $\mathbf{n} = \mathbf{N} = \mathbf{e}_3$ during deformation. From the tangent vectors, we get

$$\begin{aligned}
 [A_{\alpha\beta}] &= \begin{bmatrix} 1 & 0 \\ 0 & R^2 \end{bmatrix} , & [A^{\alpha\beta}] &= \begin{bmatrix} 1 & 0 \\ 0 & 1/R^2 \end{bmatrix} , \\
 [a_{\alpha\beta}] &= \begin{bmatrix} \lambda^2 & 0 \\ 0 & r^2 \end{bmatrix} , & [a^{\alpha\beta}] &= \begin{bmatrix} 1/\lambda^2 & 0 \\ 0 & 1/r^2 \end{bmatrix} ,
 \end{aligned} \tag{170}$$

and thus the contravariant tangent vectors take the form

$$\begin{aligned}
\mathbf{A}^1 &= \cos \phi \mathbf{e}_1 + \sin \phi \mathbf{e}_2 , \\
\mathbf{A}^2 &= -\frac{1}{R} \sin \phi \mathbf{e}_1 + \frac{1}{R} \cos \phi \mathbf{e}_2 , \\
\mathbf{a}^1 &= \frac{1}{\lambda} \cos \phi \mathbf{e}_1 + \frac{1}{\lambda} \sin \phi \mathbf{e}_2 , \\
\mathbf{a}^2 &= -\frac{1}{r} \sin \phi \mathbf{e}_1 + \frac{1}{r} \cos \phi \mathbf{e}_2 .
\end{aligned} \tag{171}$$

The initial and current fiber direction thus can be expressed as

$$\begin{aligned}
\mathbf{L} &= L^\alpha \mathbf{A}_\alpha , \\
\boldsymbol{\ell} &= \frac{1}{\lambda} \mathbf{F} \mathbf{L} = \ell^\alpha \mathbf{a}_\alpha ,
\end{aligned} \tag{172}$$

with

$$[L^\alpha] := [\mathbf{L} \cdot \mathbf{A}^\alpha] = \begin{bmatrix} 0 \\ 1/R \end{bmatrix} , \quad \text{and} \quad [\ell^\alpha] := [L^\alpha/\lambda] = \begin{bmatrix} 0 \\ 1/r \end{bmatrix} . \tag{173}$$

The components of the structural tensors $\mathbf{L} \otimes \mathbf{L}$ and $\boldsymbol{\ell} \otimes \boldsymbol{\ell}$ thus read

$$[L^{\alpha\beta}] = \begin{bmatrix} 0 & 0 \\ 0 & 1/R^2 \end{bmatrix} , \quad [\ell^{\alpha\beta}] = \begin{bmatrix} 0 & 0 \\ 0 & 1/r^2 \end{bmatrix} , \quad [\ell_\beta^\alpha] = \begin{bmatrix} 0 & 0 \\ 0 & 1 \end{bmatrix} . \tag{174}$$

Further, the fiber director is obtained as

$$\mathbf{c} = \mathbf{n} \times \boldsymbol{\ell} = -\cos \phi \mathbf{e}_1 - \sin \phi \mathbf{e}_2 = c_\alpha \mathbf{a}^\alpha , \tag{175}$$

with

$$[c_\alpha] := [\mathbf{c} \cdot \mathbf{a}_\alpha] = \begin{bmatrix} -\lambda \\ 0 \end{bmatrix} . \tag{176}$$

Therefore, its derivatives read

$$\begin{aligned}
\mathbf{c}_{,1} &:= \frac{\partial \mathbf{c}}{\partial R} = \mathbf{0} , \\
\mathbf{c}_{,2} &:= \frac{\partial \mathbf{c}}{\partial \phi} = \sin \phi \mathbf{e}_1 - \cos \phi \mathbf{e}_2 .
\end{aligned} \tag{177}$$

From Eq. (35) then follows the components of the in-plane curvature tensor in the current configuration as

$$[\bar{b}_{\alpha\beta}] = -\frac{1}{2} [\mathbf{c}_{,\alpha} \cdot \mathbf{a}_\beta + \mathbf{c}_{,\beta} \cdot \mathbf{a}_\alpha] = \begin{bmatrix} 0 & 0 \\ 0 & r \end{bmatrix} . \tag{178}$$

Similarly, we find the in-plane curvature tensor in the initial configuration as

$$[\bar{B}_{\alpha\beta}] = \begin{bmatrix} 0 & 0 \\ 0 & R \end{bmatrix} . \tag{179}$$

Accordingly, the current geodesic curvature can be computed from Eq. (32) as

$$\kappa_g = \bar{b}_{\alpha\beta} \ell^{\alpha\beta} = 1/r . \tag{180}$$

Similarly, we can verify the initial geodesic curvature $\kappa_g^0 = 1/R$. These results lead to $k_g = \kappa_g \lambda - \kappa_g^0 = 0$, and thus $W_{\text{fib-bend}} = 0$ due to the particular choice of strain energy (167.2). This means that the change in the geodesic curvature κ_g in this example is purely due to fiber stretching and not due to fiber bending.

7.4.2 Analytical expression for the reaction forces

From Eq. (166), we find the effective membrane stress

$$J \sigma^{\alpha\beta} = 2 \frac{\partial W}{\partial a_{\alpha\beta}} = K (J - 1) J a^{\alpha\beta} + \frac{1}{2} \epsilon_L (\lambda^2 - 1) L^{\alpha\beta} . \quad (181)$$

Here, the component of the Cauchy stress tensor is $N^{\alpha\beta} = \sigma^{\alpha\beta}$ since $M^{\alpha\beta} = \bar{M}^{\alpha\beta} = 0$ (see Eq. (112) with (93)). Its mixed components thus read

$$[N_{\beta}^{\alpha}] = K (J - 1) \begin{bmatrix} 1 & 0 \\ 0 & 1 \end{bmatrix} + \frac{\epsilon_L}{2J} (\lambda^2 - 1) \begin{bmatrix} 0 & 0 \\ 0 & \lambda^2 \end{bmatrix} , \quad (182)$$

where we have inserted $A^{\alpha\beta}$ and $L^{\alpha\beta}$ from (170) and (174), respectively. It can be verified that with a homogeneous deformation $J = \lambda^2$, the local equilibrium equation $\text{div}_s \boldsymbol{\sigma} = \text{div}_s (N^{\alpha\beta} \mathbf{a}_{\alpha} \otimes \mathbf{a}_{\beta}) = \mathbf{0}$ is satisfied for the functionally graded surface bulk modulus

$$K(R) = \frac{1}{2} \epsilon_L \ln R . \quad (183)$$

Further, the resultant reaction force at the cut in Fig. 6 (right) can be computed by

$$\begin{aligned} \mathbf{R}_{\nu} &= \int_{r_i}^{r_o} (\boldsymbol{\nu} \otimes \boldsymbol{\nu}) \mathbf{T} \, dr = R_{\nu} \boldsymbol{\ell} , \\ \mathbf{R}_{\tau} &= \int_{r_i}^{r_o} (\boldsymbol{\tau} \otimes \boldsymbol{\tau}) \mathbf{T} \, dr = R_{\tau} \mathbf{c} , \end{aligned} \quad (184)$$

since $\boldsymbol{\nu} = \boldsymbol{\ell}$ and $\boldsymbol{\tau} = \mathbf{c}$. Here, $\mathbf{T} = N^{\alpha\beta} \nu_{\beta} \mathbf{a}_{\alpha}$ denotes the traction acting on the cut. Therefore, we get

$$\begin{aligned} \mathbf{T} \cdot \boldsymbol{\ell} &= N_{\beta}^{\alpha} \ell_{\alpha}^{\beta} = \left(\frac{1}{2} \epsilon_L + K \right) (J - 1) , \\ \mathbf{T} \cdot \mathbf{c} &= N_{\beta}^{\alpha} c_{\alpha} \ell^{\beta} = 0 . \end{aligned} \quad (185)$$

Inserting this into (184) and taking (183) into account, finally results in

$$\begin{aligned} R_{\nu} &= \frac{1}{2} \epsilon_L (J - 1) \bar{\lambda} (R_o \ln R_o - R_i \ln R_i) , \\ R_{\tau} &= 0 . \end{aligned} \quad (186)$$

7.5 Pure bending of a flat rectangular sheet

The last example presents the analytical solution for the pure bending of a flat rectangular sheet \mathcal{S}_0 with dimension $S \times L$, subjected to an external bending moment M_{ext} along the two shorter edges, as shown in Fig. 7. This problem was solved by [Sauer and Duong \(2017\)](#) for an isotropic material, and here we additionally consider the influence of fiber bending. For simplicity the fibers are aligned along the bending direction. The strain energy function is taken from (129), which reduces to

$$W = \frac{\mu}{2} (I_1 - 2 - \ln J) + \frac{\beta}{2} K_n^2 \quad (187)$$

in this example.

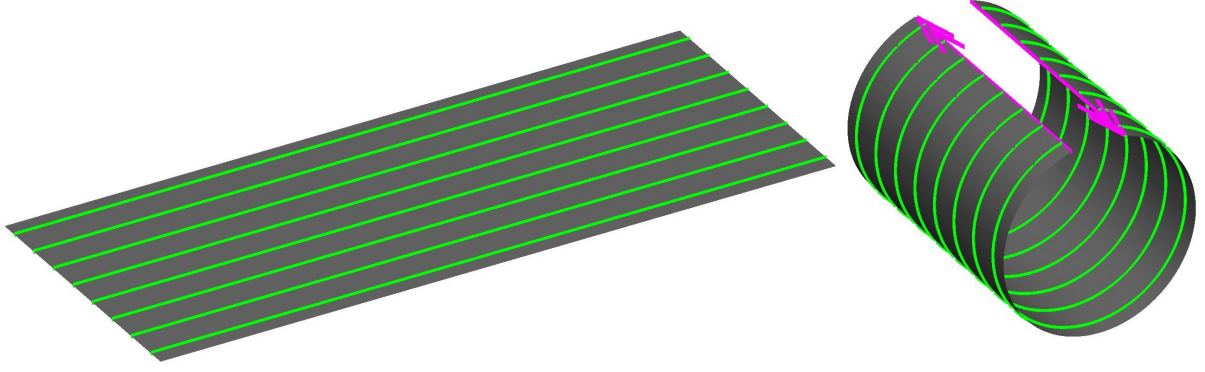


Figure 7: Pure bending: Deformation of a rectangular sheet (left) into a circular arc (right).

7.5.1 Kinematical quantities

We extend the kinematical quantities derived in [Sauer and Duong \(2017\)](#) to account for embedded fibers. The sheet is parametrized by $\xi^1 \in [0, S]$ and $\xi^2 \in [0, L]$. Bending induces (high-order) in-plane deformation, such that the current configuration \mathcal{S} has dimension $s \times \ell$. The stretches along the longer and shorter edges are $\lambda_\ell = \ell/L$ and $\lambda_s = s/S$, respectively, and we have relations $\theta := \kappa_\ell \lambda_\ell \xi$ and $r := 1/\kappa_\ell$, where κ_ℓ is the homogenous curvature of the sheet.

With this, the sheet in the initial and current configurations, and the initial fiber direction can be described by

$$\begin{aligned} \mathbf{X}(\xi, \eta) &= \xi \mathbf{e}_1 + \eta \mathbf{e}_2, \\ \mathbf{x}(\xi, \eta) &= r \sin \theta \mathbf{e}_1 + \lambda_s \eta \mathbf{e}_2 + r(1 - \cos \theta) \mathbf{e}_3, \\ \mathbf{L} &= \mathbf{e}_1. \end{aligned} \quad (188)$$

Therefore, the initial and current tangent vectors, and current normal vector are

$$\begin{aligned} \mathbf{A}_1 &= \frac{\partial \mathbf{X}}{\partial \xi} = \mathbf{e}_1, & \mathbf{A}_2 &= \frac{\partial \mathbf{X}}{\partial \eta} = \mathbf{e}_2, \\ \mathbf{a}_1 &= \frac{\partial \mathbf{x}}{\partial \xi} = \lambda_\ell (\cos \theta \mathbf{e}_1 + \sin \theta \mathbf{e}_3), & \mathbf{a}_2 &= \frac{\partial \mathbf{x}}{\partial \eta} = \lambda_s \mathbf{e}_2, \\ \mathbf{n} &= -\sin \theta \mathbf{e}_1 + \cos \theta \mathbf{e}_3. \end{aligned} \quad (189)$$

From these, we find the components of the structural tensor

$$[L^{\alpha\beta}] = [\mathbf{A}^\alpha (\mathbf{L} \otimes \mathbf{L}) \mathbf{A}^\beta] = \begin{bmatrix} 1 & 0 \\ 0 & 0 \end{bmatrix}, \quad (190)$$

the surface metrics

$$[A_{\alpha\beta}] = \begin{bmatrix} 1 & 0 \\ 0 & 1 \end{bmatrix}, \quad [A^{\alpha\beta}] = \begin{bmatrix} 1 & 0 \\ 0 & 1 \end{bmatrix}, \quad (191)$$

$$[a_{\alpha\beta}] = \begin{bmatrix} \lambda_\ell^2 & 0 \\ 0 & \lambda_s^2 \end{bmatrix}, \quad [a^{\alpha\beta}] = \begin{bmatrix} \lambda_\ell^{-2} & 0 \\ 0 & \lambda_s^{-2} \end{bmatrix}, \quad (192)$$

the surface stretch $J = \lambda_\ell \lambda_s$, and the components of the curvature tensor

$$[b_{\alpha\beta}] = \begin{bmatrix} \kappa_\ell \lambda_\ell^2 & 0 \\ 0 & 0 \end{bmatrix}, \quad [b_\beta^\alpha] = \begin{bmatrix} \kappa_\ell & 0 \\ 0 & 0 \end{bmatrix}, \quad [b^{\alpha\beta}] = \begin{bmatrix} \kappa_\ell \lambda_\ell^{-2} & 0 \\ 0 & 0 \end{bmatrix}, \quad H = \frac{\kappa_\ell}{2}. \quad (193)$$

Therefore, the nominal change in the normal curvature is

$$K_n = b_{\alpha\beta} L^{\alpha\beta} = \kappa_\ell \lambda_\ell^2 \quad (194)$$

7.5.2 Analytical relation between external moment and mean curvature

From Eq. (187), we find

$$\begin{aligned} J \sigma^{\alpha\beta} &= 2 \frac{\partial W}{\partial a_{\alpha\beta}} = \mu (A^{\alpha\beta} - a^{\alpha\beta}) , \\ J M^{\alpha\beta} &= \frac{\partial W}{\partial b_{\alpha\beta}} = \beta K_n L^{\alpha\beta} . \end{aligned} \quad (195)$$

According to Eqs. (93) and (112) with $\bar{M}^{\alpha\beta} = \bar{m}_{;\alpha}^{\alpha} = 0$, the components of the Cauchy stress tensors read

$$N_{\beta}^{\alpha} = \sigma^{\alpha\gamma} a_{\gamma\beta} + M^{\alpha\gamma} b_{\gamma\beta} . \quad (196)$$

Inserting here $A^{\alpha\beta}$, $a^{\alpha\beta}$, and $L^{\alpha\beta}$ from Eqs. (191), (192), and (190) gives

$$[N_{\beta}^{\alpha}] = \frac{\mu}{J} \begin{bmatrix} \lambda_{\ell}^2 - 1 & 0 \\ 0 & \lambda_s^2 - 1 \end{bmatrix} + \frac{\beta}{J} \kappa_{\ell}^2 \lambda_{\ell}^4 \begin{bmatrix} 1 & 0 \\ 0 & 0 \end{bmatrix} . \quad (197)$$

By assuming free edges, we have $N_1^1 = N_2^2 = 0$. That is

$$\begin{aligned} N_1^1 &= \frac{\mu}{J} (\lambda_{\ell}^2 - 1) + \frac{\beta}{J} \kappa_{\ell}^2 \lambda_{\ell}^4 = 0 , \\ N_2^2 &= \frac{\mu}{J} (\lambda_s^2 - 1) = 0 . \end{aligned} \quad (198)$$

From the second equation follows $\lambda_s = 1$. The distributed external moment M_{ext} is in equilibrium to the distributed internal moment m_{τ} – see Eq. (79.2) – on any cut parallel to the shorter edge. We therefore have

$$M_{\text{ext}} = -m_{\tau} = M^{\alpha\beta} \nu_{\alpha} \nu_{\beta} = \frac{\beta}{J} \kappa_{\ell} \lambda_{\ell}^4 , \quad (199)$$

where $\boldsymbol{\nu} = \mathbf{a}_1/\lambda_{\ell}$, $\nu_1 = \lambda_{\ell}$, and $\nu_2 = 0$. By combining Eqs. (199) and (198.1), we get an expression for λ_{ℓ} in terms of M_{ext} ,

$$\lambda_{\ell} = \sqrt{\frac{1}{2} + \sqrt{\frac{1}{4} - \frac{1}{\mu\beta} M_{\text{ext}}^2}} , \quad \text{with the condition } M_{\text{ext}}^2 \leq \frac{1}{4} \mu \beta . \quad (200)$$

With this result and (199), we obtain the relation between external moment and the mean curvature,

$$H = \frac{M_{\text{ext}}}{2 \beta \lambda_{\ell}^4} . \quad (201)$$

8 Conclusion

We have presented a generalized Kirchhoff-Love shell theory capable of capturing in-plane bending of fibers embedded in the surface. The formulation is an extension of classical Kirchhoff-Love shell theory that can handle multiple fiber families, possibly with initial curvature. We use a direct approach to derive our theory assuming Kirchhoff-Love kinematics, plane-stress conditions, and lumped mass at the mid-surface. Like classical Kirchhoff-Love shell theory, no additional degrees-of-freedom are required such as the independent director fields of Cosserat shell theory, and the postulated set of balance laws for the shell only include linear and angular momentum balance.

Our thin shell kinematics is fully characterized by the change of three symmetric tensors: $a_{\alpha\beta}$, $b_{\alpha\beta}$, and the newly added $\bar{b}_{\alpha\beta}$ – denoting the in-plane curvature tensor. These tensors capture the change of the tangent vectors \mathbf{a}_1 , \mathbf{a}_2 , and the in-plane fiber director \mathbf{c} . Tensor $\bar{b}_{\alpha\beta}$ and director vector \mathbf{c} are defined for each fiber family separately. The corresponding stress and moments work-conjugate to $a_{\alpha\beta}$, $b_{\alpha\beta}$, and $\bar{b}_{\alpha\beta}$, are the effective membrane stress $\sigma^{\alpha\beta}$, the out-of-plane stress couple $M^{\alpha\beta}$, and the in-plane stress couple $\bar{M}^{\alpha\beta}$, respectively. The symmetry of $\sigma^{\alpha\beta}$ follows from angular momentum balance. With these work-conjugated pairs, general constitutive equations for hyperelastic materials are derived.

The introduction of $\bar{b}_{\alpha\beta}$ for the in-plane curvature measure is an advantage over existing second-gradient shell theory. Since it is a second order tensor instead of a third order tensor, its induced invariants and their physical meaning can be identified in a straightforward manner from the defined kinematics. Furthermore, it makes in-plane bending fully analogous to out-of-plane bending for both the internal and the external power. These features are advantageous in constructing material models and evaluating Neumann boundary conditions.

Finally this work also provides the weak form, which is required for a finite element formulation based on C^1 -continuous surface discretizations that are presented in future work (Duong et al., 2022). Several analytical examples are presented to serve as useful elementary test cases for the verification of nonlinear computational formulations. The presented analytical examples also confirm that the model correctly describes the mechanics of shells with initially curved fibers.

A Variation of various kinematical quantities

This section provides the variation of several kinematical quantities defined in Sec. 2. They are required for the derivation of the mechanical work balance (Sec. 4), the stresses and moments from a stored energy function (Sec. 5), the weak form (Sec. 6), and the linearization of the weak form (Duong et al., 2022).¹³ We focus here mostly on the new variables introduced above, while the expressions for existing ones can be found elsewhere, e.g. in Sauer and Duong (2017).

Consider a variation of position \mathbf{x} by $\delta\mathbf{x}$. Accordingly, the variation of the tangent vectors reads $\delta\mathbf{a}_\alpha = \delta\mathbf{x}_{,\alpha}$. From Eq. (5), the variation of $\delta a_{\alpha\beta}$ is

$$\delta a_{\alpha\beta} = \delta\mathbf{a}_\alpha \cdot \mathbf{a}_\beta + \mathbf{a}_\alpha \cdot \delta\mathbf{a}_\beta . \quad (202)$$

Further, from Eq. (15.2), we find

$$\delta\mathbf{a}_{\beta;\alpha} = \mathbf{n} \otimes \mathbf{n} (\delta\mathbf{a}_{\alpha,\beta} - \Gamma_{\alpha\beta}^\gamma \delta\mathbf{a}_\gamma) , \quad (203)$$

where we have used the variation (see e.g. Wriggers (2006)),

$$\delta\mathbf{n} = -\mathbf{a}^\alpha (\mathbf{n} \cdot \delta\mathbf{a}_\alpha) . \quad (204)$$

From Eq. (41) we have $\lambda^2 = (\mathbf{F}\mathbf{L}) \cdot (\mathbf{F}\mathbf{L}) = L^{\alpha\beta} a_{\alpha\beta}$. It then follows that,

$$\delta\lambda = \frac{1}{2\lambda} L^{\alpha\beta} \delta a_{\alpha\beta} . \quad (205)$$

With $\delta\lambda$, the variation of ℓ can be derived from Eq. (41) as

$$\delta\ell = (\mathbf{1} - \ell \otimes \ell) \ell^\alpha \delta\mathbf{a}_\alpha . \quad (206)$$

¹³The material time derivative and the linearization of a given quantity \bullet follow directly from its variation $\delta\bullet$, by replacing $\delta\bullet$ by either $\dot{\bullet}$ or $\Delta\bullet$, respectively.

The variation of components $\ell_\alpha = \boldsymbol{\ell} \cdot \mathbf{a}_\alpha$ and $\ell^\alpha = \boldsymbol{\ell} \cdot \mathbf{a}^\alpha$ read

$$\delta \ell_\alpha = \ell^\beta c_\alpha \mathbf{c} \cdot \delta \mathbf{a}_\beta + \boldsymbol{\ell} \cdot \delta \mathbf{a}_\alpha , \quad (207)$$

and

$$\delta \ell^\alpha = -\ell^{\alpha\beta} \boldsymbol{\ell} \cdot \delta \mathbf{a}_\beta , \quad (208)$$

where we have used (206) and (see e.g. [Sauer and Duong \(2017\)](#))

$$\delta \mathbf{a}^\alpha = (a^{\alpha\beta} \mathbf{n} \otimes \mathbf{n} - \mathbf{a}^\beta \otimes \mathbf{a}^\alpha) \delta \mathbf{a}_\beta . \quad (209)$$

With $\ell^{\alpha\beta} = \ell^\alpha \ell^\beta$ and Eq. (208), we further find

$$\delta \ell^{\alpha\beta} = -\ell^{\alpha\beta} \ell^{\gamma\delta} \delta a_{\gamma\delta} . \quad (210)$$

The variation of the in-plane director \mathbf{c} is

$$\delta \mathbf{c} = -(\mathbf{n} \otimes \mathbf{c}) \delta \mathbf{n} - (\boldsymbol{\ell} \otimes \mathbf{c}) \delta \boldsymbol{\ell} , \quad (211)$$

which follows from identities $\mathbf{c} \cdot \mathbf{n} = 0$ and $\boldsymbol{\ell} \cdot \mathbf{n} = 0$. Inserting Eq. (204) and (206) into Eq. (211) gives

$$\delta \mathbf{c} = (c^\alpha \mathbf{n} \otimes \mathbf{n} - \ell^\alpha \boldsymbol{\ell} \otimes \mathbf{c}) \delta \mathbf{a}_\alpha . \quad (212)$$

Using this result and Eq. (209), the variation of the components of \mathbf{c} read

$$\delta c_\alpha = -\ell_\alpha^\beta \mathbf{c} \cdot \delta \mathbf{a}_\beta + \mathbf{c} \cdot \delta \mathbf{a}_\alpha , \quad (213)$$

and

$$\delta c^\alpha = -\ell^{\alpha\beta} \mathbf{c} \cdot \delta \mathbf{a}_\beta - c^\beta \mathbf{a}^\alpha \cdot \delta \mathbf{a}_\beta . \quad (214)$$

From Eq. (19) follows

$$\delta \Gamma_{\alpha\beta}^c = \mathbf{c} \cdot \delta \mathbf{a}_{\alpha,\beta} + \mathbf{a}_{\alpha,\beta} \cdot \delta \mathbf{c} . \quad (215)$$

Further, taking the variation of $\hat{L}_{,\beta}^\alpha$ (see Eq. (44)) and using result (205) gives

$$\delta \hat{L}_{,\beta}^\alpha = -\hat{L}_{,\beta}^\alpha \ell^\gamma \boldsymbol{\ell} \cdot \delta \mathbf{a}_\gamma = \hat{L}_{,\beta}^\alpha \ell_\gamma \delta \ell^\gamma . \quad (216)$$

From Eq. (45.2), the variation of $c_{;\alpha}^\beta$ reads

$$\delta c_{;\alpha}^\beta = -\ell^{\beta\gamma} \delta \Gamma_{\alpha\gamma}^c - \ell^\beta (\Gamma_{\alpha\gamma}^c + \ell_\gamma c_\delta \hat{L}_{,\alpha}^\delta) \delta \ell^\gamma - (c_\gamma \hat{L}_{,\alpha}^\gamma + \ell^\gamma \Gamma_{\gamma\alpha}^c) \delta \ell^\beta - \ell^\beta \hat{L}_{,\alpha}^\gamma \delta c_\gamma . \quad (217)$$

From Eq. (36.1) follows

$$\delta c_{,\alpha} = \mathbf{a}_\beta \delta c_{;\alpha}^\beta + c_{;\alpha}^\beta \delta \mathbf{a}_\beta + c^\beta \delta \mathbf{a}_{\beta;\alpha} + \mathbf{a}_{\beta;\alpha} \delta c^\beta . \quad (218)$$

The variation of the out-of-plane curvature is (see e.g. [Sauer and Duong \(2017\)](#))

$$\delta b_{\alpha\beta} = \mathbf{n} \cdot \delta \mathbf{a}_{\alpha,\beta} - \Gamma_{\alpha\beta}^\gamma \mathbf{n} \cdot \delta \mathbf{a}_\gamma . \quad (219)$$

The variation of the in-plane curvature follows from Eq. (35) as

$$\delta \bar{b}_{\alpha\beta} = -\frac{1}{2} (\delta \mathbf{a}_\alpha \cdot \mathbf{c}_{,\beta} + \mathbf{a}_\alpha \cdot \delta \mathbf{c}_{,\beta} + \delta \mathbf{a}_\beta \cdot \mathbf{c}_{,\alpha} + \mathbf{a}_\beta \cdot \delta \mathbf{c}_{,\alpha}) . \quad (220)$$

The variation of the normal curvature follows from Eq. (21) and (210) as

$$\delta \kappa_n = \frac{\partial \kappa_n}{\partial a_{\alpha\beta}} \delta a_{\alpha\beta} + \frac{\partial \kappa_n}{\partial b_{\alpha\beta}} \delta b_{\alpha\beta} + \frac{\partial \kappa_n}{\partial \bar{b}_{\alpha\beta}} \delta \bar{b}_{\alpha\beta} , \quad (221)$$

with

$$\frac{\partial \kappa_n}{\partial a_{\alpha\beta}} = -\kappa_n \ell^{\alpha\beta} , \quad \frac{\partial \kappa_n}{\partial b_{\alpha\beta}} = \ell^{\alpha\beta} , \quad \text{and} \quad \frac{\partial \kappa_n}{\partial \bar{b}_{\alpha\beta}} = 0 . \quad (222)$$

Similarly, from Eqs. (50.1) and (210), the variation of the geodesic curvature gives

$$\delta \kappa_g = \frac{\partial \kappa_g}{\partial a_{\alpha\beta}} \delta a_{\alpha\beta} + \frac{\partial \kappa_g}{\partial b_{\alpha\beta}} \delta b_{\alpha\beta} + \frac{\partial \kappa_g}{\partial \bar{b}_{\alpha\beta}} \delta \bar{b}_{\alpha\beta} , \quad (223)$$

with

$$\frac{\partial \kappa_g}{\partial a_{\alpha\beta}} = -\kappa_g \ell^{\alpha\beta} , \quad \frac{\partial \kappa_g}{\partial b_{\alpha\beta}} = 0 , \quad \text{and} \quad \frac{\partial \kappa_g}{\partial \bar{b}_{\alpha\beta}} = \ell^{\alpha\beta} . \quad (224)$$

From Eq. (22), (208), and (214), the variation of the geodesic torsion reads

$$\delta \tau_g = \frac{\partial \tau_g}{\partial a_{\alpha\beta}} \delta a_{\alpha\beta} + \frac{\partial \tau_g}{\partial b_{\alpha\beta}} \delta b_{\alpha\beta} + \frac{\partial \tau_g}{\partial \bar{b}_{\alpha\beta}} \delta \bar{b}_{\alpha\beta} , \quad (225)$$

with $\frac{\partial \tau_g}{\partial \bar{b}_{\alpha\beta}} = 0$, and

$$\begin{aligned} \frac{\partial \tau_g}{\partial a_{\alpha\beta}} &= -\frac{1}{2} \kappa_n (\ell^\alpha c^\beta + \ell^\beta c^\alpha) - \frac{1}{2} \tau_g (c^{\alpha\beta} + \ell^{\alpha\beta}), \\ \frac{\partial \tau_g}{\partial b_{\alpha\beta}} &= \frac{1}{2} (\ell^\alpha c^\beta + \ell^\beta c^\alpha) . \end{aligned} \quad (226)$$

Therefore, from Eqs. (31), (221) and (223), the variation of the principal curvature of the fiber is

$$\delta \kappa_p = \frac{\partial \kappa_p}{\partial a_{\alpha\beta}} \delta a_{\alpha\beta} + \frac{\partial \kappa_p}{\partial b_{\alpha\beta}} \delta b_{\alpha\beta} + \frac{\partial \kappa_p}{\partial \bar{b}_{\alpha\beta}} \delta \bar{b}_{\alpha\beta} , \quad (227)$$

with

$$\frac{\partial \kappa_p}{\partial a_{\alpha\beta}} = -\kappa_p \ell^{\alpha\beta} , \quad \kappa_p \frac{\partial \kappa_p}{\partial b_{\alpha\beta}} = \kappa_n \ell^{\alpha\beta} , \quad \text{and} \quad \kappa_p \frac{\partial \kappa_p}{\partial \bar{b}_{\alpha\beta}} = \kappa_g \ell^{\alpha\beta} . \quad (228)$$

B Frame invariance of various strain measures

In this appendix, we show that the strain measures presented in our theory, such as $a_{\alpha\beta}$, $b_{\alpha\beta}$, $c^\beta \ell_{\beta;\alpha}$, κ_g , $\bar{b}_{\alpha\beta}$, together with the components of the structural tensors $c^{\alpha\beta}$, $\ell^{\alpha\beta}$, and $c^\alpha \ell^\beta$, are invariant under superimposed rigid body motions of shell surface \mathcal{S} . To this end, let the shell surface (1) be translated and rigidly rotated by

$$\mathbf{x}^+ = \mathbf{x}_0 + \mathbf{Q} \mathbf{x} , \quad \text{with} \quad \mathbf{Q}^T \mathbf{Q} = \mathbf{1} , \quad (229)$$

where $\mathbf{x}_0 \in \mathbb{E}^3$ and $\mathbf{Q} \in SO(3)$ are a constant translation vector and a rotation tensor. From (229.1), (15.1), (2) and (6), we have

$$\begin{aligned} \mathbf{a}_\alpha^+ &= \mathbf{x}_{,\alpha}^+ = \mathbf{Q} \mathbf{a}_\alpha , \\ \mathbf{a}_{\alpha,\beta}^+ &= \mathbf{x}_{,\alpha\beta}^+ = \mathbf{Q} \mathbf{a}_{\alpha,\beta} , \\ \ell^+ &= \mathbf{x}_{,s}^+ = \mathbf{Q} \ell , \\ \ell_{,\alpha}^+ &= \mathbf{Q} \ell_{,\alpha} . \end{aligned} \quad (230)$$

Here, Eq. (230.4) follows from Eq. (230.3). Using the identity $\mathbf{Q} \mathbf{a} \times \mathbf{Q} \mathbf{b} = \mathbf{Q} (\mathbf{a} \times \mathbf{b})$, together with (3) and (7), we further obtain the following relations

$$\begin{aligned} \mathbf{n}^+ &= \mathbf{Q} \mathbf{n} , \\ \mathbf{c}^+ &= \mathbf{Q} \mathbf{c} , \\ \mathbf{c}_{,\alpha}^+ &= \mathbf{Q} \mathbf{c}_{,\alpha} , \end{aligned} \quad (231)$$

where the last equation follows directly from the second one. The strain measure $a_{\alpha\beta}$ (see Eq. (5.1)) is frame invariant since

$$a_{\alpha\beta}^+ = \mathbf{a}_\alpha^+ \cdot \mathbf{a}_\beta^+ = (\mathbf{Q} \mathbf{a}_\alpha) \cdot (\mathbf{Q} \mathbf{a}_\beta) = \mathbf{a}_\alpha \cdot (\mathbf{Q}^T \mathbf{Q} \mathbf{a}_\beta) = \mathbf{a}_\alpha \cdot \mathbf{a}_\beta = a_{\alpha\beta} , \quad (232)$$

where we have employed Eq. (230.1) and (229.2). Similarly, the frame invariance of $b_{\alpha\beta}$, the strain measure for out-of-plane curvature from Eq. (14), follows as

$$b_{\alpha\beta}^+ = \mathbf{n}^+ \cdot \mathbf{a}_{\alpha,\beta}^+ = (\mathbf{Q} \mathbf{n}) \cdot (\mathbf{Q} \mathbf{a}_{\alpha,\beta}) = \mathbf{n} \cdot (\mathbf{Q}^T \mathbf{Q} \mathbf{a}_{\alpha,\beta}) = \mathbf{n} \cdot \mathbf{a}_{\alpha,\beta} = b_{\alpha\beta} . \quad (233)$$

The frame invariance is also true for the in-plane curvature measure $\bar{b}_{\alpha\beta}$ (see Eq. (35)), i.e.

$$\bar{b}_{\alpha\beta}^+ = -\frac{1}{2}(c_{\beta;\alpha}^+ + c_{\alpha;\beta}^+) = \bar{b}_{\alpha\beta} , \quad (234)$$

since

$$c_{\beta;\alpha}^+ = \mathbf{a}_\beta^+ \cdot \mathbf{c}_{,\alpha}^+ = (\mathbf{Q} \mathbf{a}_\beta) \cdot (\mathbf{Q} \mathbf{c}_{,\alpha}) = \mathbf{a}_\beta \cdot (\mathbf{Q}^T \mathbf{Q} \mathbf{c}_{,\alpha}) = c_{\beta;\alpha} , \quad (235)$$

which follows from (39), (230.1), and (231.3).

Similarly, the covariant derivative $\ell_{\beta;\alpha}$ from Eq. (25) is frame invariant, since

$$\ell_{\beta;\alpha}^+ = \mathbf{a}_\beta^+ \cdot \boldsymbol{\ell}_{,\alpha}^+ = (\mathbf{Q} \mathbf{a}_\beta) \cdot (\mathbf{Q} \boldsymbol{\ell}_{,\alpha}) = \mathbf{a}_\beta \cdot (\mathbf{Q}^T \mathbf{Q} \boldsymbol{\ell}_{,\alpha}) = \ell_{\beta;\alpha} , \quad (236)$$

due to (230.1) and (230.4).

Furthermore, following result (232), it can be shown that $\mathbf{a}_+^\alpha = \mathbf{Q} \mathbf{a}^\alpha$. With this, Eq. (230.3) and (231.2), we can easily show the frame invariance is also true for components $\ell^\alpha = \boldsymbol{\ell} \cdot \mathbf{a}^\alpha = \ell_+^\alpha$ and $c^\alpha = \mathbf{c} \cdot \mathbf{a}^\alpha = c_+^\alpha$. Consequently, we have the frame invariance for all the components of the structural tensors as

$$\begin{aligned} c_+^{\alpha\beta} &= c_+^\alpha c_+^\beta = c^{\alpha\beta} , \\ \ell_+^{\alpha\beta} &= \ell_+^\alpha \ell_+^\beta = \ell^{\alpha\beta} , \\ (c^\alpha \ell^\beta)_+ &= c_+^\alpha \ell_+^\beta = c^\alpha \ell^\beta . \end{aligned} \quad (237)$$

This implies that all the invariants, constructed from the strain measures $a_{\alpha\beta}$, $b_{\alpha\beta}$, and $\bar{b}_{\alpha\beta}$ by these structural tensors (see Tab. 1), are frame invariant. Take for example the geodesic curvature (32). We find

$$\kappa_g^+ = -\ell_+^{\alpha\beta} \bar{b}_{\alpha\beta}^+ = -\ell^{\alpha\beta} \bar{b}_{\alpha\beta} = \kappa_g , \quad (238)$$

due to Eq. (234) and (237.2). Also, the strain measure $c^\beta \ell_{\beta;\alpha}$ (used e.g. in Eq. (105)) is frame invariant, i.e.

$$(c^\beta \ell_{\beta;\alpha})^+ = c_+^\beta \ell_{\beta;\alpha}^+ = c^\beta \ell_{\beta;\alpha} , \quad (239)$$

following from $c_+^\beta = c^\beta$ and Eq. (236).

C On deriving Kirchhoff-Love theory from Cosserat theory

In this appendix, we show that the balance equations of our generalized Kirchhoff-Love shell theory with in-plane fiber bending are consistent with the more general balance equations of Cosserat shell theory (Naghdi, 1982).

To this end, we consider a Cosserat shell \mathcal{S} characterized by material point $\mathbf{x} \in \mathcal{S}$ and a single director field \mathbf{d} attached to \mathbf{x} . The global balance equations of \mathcal{S} are postulated as (see e.g. Green and Naghdi (1974); Naghdi (1982); Steigmann (1999b))

$$\begin{aligned} \frac{D}{Dt} \int_{\mathcal{R}} \rho \mathbf{v}_e da &= \int_{\mathcal{R}} \mathbf{f} da + \int_{\partial\mathcal{R}} \mathbf{T} ds , \\ \frac{D}{Dt} \int_{\mathcal{R}} \rho \mathbf{w}_e da &= \int_{\mathcal{R}} (\mathbf{l} + \mathbf{k}) da + \int_{\partial\mathcal{R}} \tilde{\mathbf{M}} ds , \\ \frac{D}{Dt} \int_{\mathcal{R}} \rho (\mathbf{x} \times \mathbf{v}_e + \mathbf{d} \times \mathbf{w}_e) da &= \int_{\mathcal{R}} (\mathbf{x} \times \mathbf{f} + \mathbf{d} \times \mathbf{l}) da + \int_{\partial\mathcal{R}} (\mathbf{x} \times \mathbf{T} + \mathbf{d} \times \tilde{\mathbf{M}}) ds , \end{aligned} \quad (240)$$

where \mathbf{f} , \mathbf{T} , $\tilde{\mathbf{M}}$, \mathbf{l} , and \mathbf{k} denote the body force (per area), the traction vector, the (general) stress couple vector, the assigned director couple (unit force per area), and the intrinsic director couple (unit force per area), respectively, and where

$$\begin{aligned} \mathbf{v}_e &:= \mathbf{v} + \alpha \mathbf{w} , \\ \mathbf{w}_e &:= \alpha \mathbf{v} + \beta \mathbf{w} \end{aligned} \quad (241)$$

are the effective velocities contributing to the material and director momentum, respectively. Here, α and β denote the inertial coefficient associated with the director velocity $\mathbf{w} := \dot{\mathbf{d}}$. The three equations in (240) correspond to the linear momentum balance, the director momentum balance, and the angular momentum balance of the Cosserat shell.

Now we are in a position to verify that the equilibrium equations in our presented theory are consistent with the equations of Cosserat shell theory (240).

First, we apply the kinematics and moment definition of classical Kirchhoff-Love thin shells (without in-plane bending) to Eq. (240). I.e. we set $\mathbf{d} = \mathbf{n}$ and $\tilde{\mathbf{M}} = \mathbf{M}$. As seen in Sec. 3.2, Kirchhoff-Love assumptions together with plane-stress conditions allow us to define the out-of-plane bending vector \mathbf{M} as in Eq. (75.1), which satisfies the condition

$$\mathbf{M} \cdot \mathbf{n} = 0 , \quad (242)$$

due to Eq. (75.1) and (72.1). Further, since we consider thin shells, the mass along the shell thickness can be lumped at the mid-surface. I.e. the inertia associated with the director field is neglected, which implies $\alpha = 0$ and $\beta = 0$. Furthermore, we assume that no external director loads are applied on the thin shell, i.e. $\mathbf{k} = \mathbf{l} = \mathbf{0}$. With these assumptions, Eq. (240) becomes

$$\begin{aligned} \frac{D}{Dt} \int_{\mathcal{R}} \rho \mathbf{v} da &= \int_{\mathcal{R}} \mathbf{f} da + \int_{\partial\mathcal{R}} \mathbf{T} ds , \\ \mathbf{0} &= \int_{\partial\mathcal{R}} \mathbf{M} ds , \\ \frac{D}{Dt} \int_{\mathcal{R}} \rho \mathbf{x} \times \mathbf{v} da &= \int_{\mathcal{R}} \mathbf{x} \times \mathbf{f} da + \int_{\partial\mathcal{R}} (\mathbf{x} \times \mathbf{T} + \mathbf{n} \times \mathbf{M}) ds . \end{aligned} \quad (243)$$

Second, we extend the equilibrium equations (243) in order to describe in-plane bending of fibers embedded within the shell surface. The kinematics and the definitions of stress and moment for in-plane bending of our presented theory in Secs 2 & 3 are directly applied to the extended equations.

To this end, we model a fiber as a beam, where all material points on its cross section follow Euler-Bernoulli kinematics and the mass is lumped at the center line of the beam. This allows us to introduce an additional director field \mathbf{c} associated with in-plane bending, analogous to $\mathbf{n} = \mathbf{d}$, that satisfies $\mathbf{c} \cdot \mathbf{n} = 0$ and contributes no inertia. We assume that the momentum balance of director \mathbf{c} is independent (decoupled) from the surface director field \mathbf{n} . As there is no stress on any cut parallel to the beam center line, we also consider no external director loads – similar to \mathbf{k} and \mathbf{l} – acting on the fiber. Therefore, the set of balance equations in Eq. (243) simply expands to

$$\begin{aligned}
\frac{D}{Dt} \int_{\mathcal{R}} \rho \mathbf{v} da &= \int_{\mathcal{R}} \mathbf{f} da + \int_{\partial\mathcal{R}} \mathbf{T} ds , \\
\mathbf{0} &= \int_{\partial\mathcal{R}} \mathbf{M} ds , \\
\mathbf{0} &= \int_{\partial\mathcal{R}} \bar{\mathbf{M}} ds , \\
\frac{D}{Dt} \int_{\mathcal{R}} \rho \mathbf{x} \times \mathbf{v} da &= \int_{\mathcal{R}} \mathbf{x} \times \mathbf{f} da + \int_{\partial\mathcal{R}} (\mathbf{x} \times \mathbf{T} + \mathbf{n} \times \mathbf{M} + \mathbf{c} \times \bar{\mathbf{M}}) ds
\end{aligned} \tag{244}$$

for in-plane fiber bending. Here the third equation is the linear momentum balance of the director field \mathbf{c} , while vector $\bar{\mathbf{M}}$ denotes the stress couple associated with in-plane bending, which is defined by Eq. (76.3) in our theory, and thus it always points in fiber direction ℓ , i.e.

$$\bar{\mathbf{M}} \cdot \mathbf{c} = 0 . \tag{245}$$

The local balance equations can then be obtained by inserting Eqs. (61) and (78) into (244), considering (58), (75), (72) and mass conservation. This gives

$$\begin{aligned}
\mathbf{T}_{;\alpha}^\alpha + \mathbf{f} &= \rho \dot{\mathbf{v}} , \\
\mathbf{M}_{;\alpha}^\alpha &= \mathbf{0} , \\
\bar{\mathbf{M}}_{;\alpha}^\alpha &= \mathbf{0} , \\
\mathbf{a}_\alpha \times \mathbf{T}^\alpha + \mathbf{n}_{,\alpha} \times \mathbf{M}^\alpha + \mathbf{c}_{,\alpha} \times \bar{\mathbf{M}}^\alpha &= \mathbf{0} .
\end{aligned} \tag{246}$$

Since we can write

$$\begin{aligned}
\mathbf{n}_{,\alpha} \times \mathbf{M}^\alpha &= (\mathbf{n} \times \mathbf{M}^\alpha)_{;\alpha} - \mathbf{n} \times \mathbf{M}_{;\alpha}^\alpha \\
\mathbf{c}_{,\alpha} \times \mathbf{M}^\alpha &= (\mathbf{c} \times \bar{\mathbf{M}}^\alpha)_{;\alpha} - \mathbf{c} \times \bar{\mathbf{M}}_{;\alpha}^\alpha ,
\end{aligned} \tag{247}$$

the last three equations in (246) can be rewritten into

$$\mathbf{a}_\alpha \times \mathbf{T}^\alpha + \hat{\mathbf{m}}_{;\alpha}^\alpha = \mathbf{0} , \tag{248}$$

where $\hat{\mathbf{m}}^\alpha := \mathbf{n} \times \mathbf{M}^\alpha + \mathbf{c} \times \bar{\mathbf{M}}^\alpha$ is known from Eq. (71). Eq. (248) is identical to the local momentum balance Eq. (91), since $\hat{\mathbf{m}}_{;\alpha}^\alpha = \text{div}_s \hat{\boldsymbol{\mu}}^\top$, which follows directly from Eq. (86) when replacing $\boldsymbol{\sigma}$ and \mathbf{T}^α with $\hat{\boldsymbol{\mu}} = \mathbf{a}_\alpha \otimes \hat{\mathbf{m}}^\alpha$ and $\hat{\mathbf{m}}^\alpha$, respectively

Therefore, we can conclude that the linear and angular momentum balance of our presented theory is equivalent to the set of balance equations of Cosserat theory under Kirchhoff-Love kinematics ($\mathbf{d} = \mathbf{n}$), suitable external loads ($\mathbf{l} = \mathbf{k} = \mathbf{0}$), and mass lumping at the mid-surface ($\alpha = 0$ and $\beta = 0$). In other words, the linear and angular momentum balance equations (83) and (87) of our presented theory fully characterize the equilibrium of the generalized Kirchhoff-Love shell with in-plane bending.

Remark C.1: Note here, that the total (equivalent) moment $\hat{\mathbf{m}}$ (see Eq. (74)) can be defined from the couple vectors as $\hat{\mathbf{m}} = \hat{\mathbf{m}}^\alpha \nu_\alpha = \mathbf{n} \times \mathbf{M}^\alpha \nu_\alpha + \mathbf{c} \times \bar{\mathbf{M}}^\alpha \nu_\alpha =: \mathbf{m} + \bar{\mathbf{m}}$, where $\mathbf{m} = \mathbf{n} \times \mathbf{M}$ and $\bar{\mathbf{m}} = \mathbf{c} \times \bar{\mathbf{M}}$ are the moment vectors causing out-of-plane and in-plane bending, respectively. In contrast to the shell theory with in-plane bending of Steigmann (2018), these moment vectors are energetically equivalent to couple vectors \mathbf{M} and $\bar{\mathbf{M}}$ due to (242) and (245). This is due to the fact that \mathbf{M} and $\bar{\mathbf{M}}$ in our theory only do work on local rotations of the normalized vectors \mathbf{n} and \mathbf{c} , respectively. Physically, this implies that \mathbf{M} and $\bar{\mathbf{M}}$ are not doing work when stretching the material along \mathbf{n} and \mathbf{c} , respectively.

D Effective membrane stress in the existing second-gradient theory of Kirchhoff-Love shells

This section presents the intermediate steps to derive the effective membrane stress (122) appearing in the existing second-gradient theory of Kirchhoff-Love shells (121), where the change in the relative Christopher symbol $S_{\alpha\beta}^\gamma$ is used as the strain measure of in-plane bending. It also shows that the resulting effective membrane stress is unsymmetric for general materials, even for initially straight fibers.

To this end, we first take the time derivative of the geodesic curvature (51). This gives

$$\dot{\kappa}_g = \dot{\kappa}_g^\Gamma + \dot{\kappa}_g^L, \quad (249)$$

where

$$\begin{aligned} \dot{\kappa}_g^\Gamma &= \dot{\ell}^{\alpha\beta} c_\gamma S_{\alpha\beta}^\gamma + \ell^{\alpha\beta} \dot{c}_\gamma S_{\alpha\beta}^\gamma + \ell^{\alpha\beta} c_\gamma \dot{S}_{\alpha\beta}^\gamma, \\ \dot{\kappa}_g^L &= \dot{\lambda}^{-1} c_\alpha \ell^\beta L_{;\beta}^\alpha + \lambda^{-1} \dot{c}_\alpha \ell^\beta L_{;\beta}^\alpha + \lambda^{-1} c_\alpha \dot{\ell}^\beta L_{;\beta}^\alpha. \end{aligned} \quad (250)$$

Here, the time derivatives $\dot{\ell}^{\alpha\beta}$, \dot{c}_α , $\dot{\lambda}$, and $\dot{\ell}^\alpha$ can be obtained from replacing $\delta\bullet$ by $\dot{\bullet}$ in expressions (210), (213), (205), and (208), respectively. By taking these into account, Eq. (250) becomes

$$\begin{aligned} \dot{\kappa}_g^\Gamma &= -2 \kappa_g^\Gamma \ell^{\alpha\beta} \mathbf{a}_\beta \cdot \dot{\mathbf{a}}_\alpha + (\ell^{\gamma\delta} S_{\gamma\delta}^\alpha - \ell^{\gamma\delta} \ell_\theta S_{\gamma\delta}^\theta \ell^\alpha) c^\beta \mathbf{a}_\beta \cdot \dot{\mathbf{a}}_\alpha + \ell^{\alpha\beta} c_\gamma \dot{S}_{\alpha\beta}^\gamma, \\ \dot{\kappa}_g^L &= -2 \kappa_g^L \ell^{\alpha\beta} \mathbf{a}_\beta \cdot \dot{\mathbf{a}}_\alpha + \lambda^{-1} (\ell^\gamma L_{;\gamma}^\alpha - \ell_\gamma^\delta L_{;\delta}^\gamma \ell^\alpha) c^\beta \mathbf{a}_\beta \cdot \dot{\mathbf{a}}_\alpha. \end{aligned} \quad (251)$$

With this, inserting (249) into (106) gives

$$\dot{w}_{\text{int}} := \sigma^{\alpha\beta} \mathbf{a}_\beta \cdot \dot{\mathbf{a}}_\alpha + M^{\alpha\beta} \dot{b}_{\alpha\beta} + \bar{\mu} \ell^{\alpha\beta} c_\gamma \dot{S}_{\alpha\beta}^\gamma, \quad (252)$$

where $\sigma^{\alpha\beta}$ is defined by Eq. (122). It is valid for initially curved fibers. For initially straight fibers, $\dot{\kappa}_g^L$ in (249) vanishes, so that $\sigma^{\alpha\beta}$ becomes

$$\sigma^{\alpha\beta} := \tilde{\sigma}^{\alpha\beta} + \bar{\mu} (\kappa_g^L - \kappa_g^\Gamma) \ell^{\alpha\beta} + \bar{\mu} \left[(\ell^{\gamma\delta} S_{\gamma\delta}^\alpha) c^\beta - (\ell^{\gamma\delta} S_{\gamma\delta}^\theta \ell_\theta) \ell^\alpha c^\beta \right], \quad (253)$$

which is unsymmetric for general materials. The asymmetry is due to the fact that the derivative \dot{c}_α of fiber director components c_α appearing in (250.1) contains not only surface stretching, but also in-plane bending. In other words, $\dot{c}_\alpha \neq \frac{\partial c_\alpha}{\partial a_{\beta\gamma}} \dot{a}_{\beta\gamma}$.

Acknowledgements

The authors are grateful to the German Research Foundation (DFG) for supporting this research under grants IT 67/18-1 and SA1822/11-1.

References

- Asmanoglo, T. and Menzel, A. (2017). A multi-field finite element approach for the modelling of fibre-reinforced composites with fibre-bending stiffness. *Comput. Methods Appl. Mech. Engrg.*, **317**:1037–1067.
- Balobanov, V., Kiendl, J., Khakalo, S., and Niiranen, J. (2019). Kirchhoff–Love shells within strain gradient elasticity: Weak and strong formulations and an H3-conforming isogeometric implementation. *Comput. Methods Appl. Mech. Engrg.*, **344**:837–857.
- Barbagallo, G., Madeo, A., Azehaf, I., Giorgio, I., Morestin, F., and Boisse, P. (2017). Bias extension test on an unbalanced woven composite reinforcement: Experiments and modeling via a second-gradient continuum approach. *J. Compos. Mater.*, **51**(2):153–170.
- Boisse, P., Hamila, N., Guzman-Maldonado, E., Madeo, A., Hivet, G., and Dell’Isola, F. (2017). The bias-extension test for the analysis of in-plane shear properties of textile composite reinforcements and prepregs: a review. *Int. J. Mater. Form.*, **10**:473–492.
- Coleman, B. D. and Noll, W. (1964). The thermodynamics of elastic materials with heat conduction and viscosity. *Arch. Ration. Mech. Anal.*, **13**:167–178.
- Dell’Isola, F., Giorgio, I., Pawlikowski, M., and Rizzi, N. L. (2016). Large deformations of planar extensible beams and pantographic lattices: heuristic homogenization, experimental and numerical examples of equilibrium. *Proc. R. Soc. A*, **472**(2185):20150790.
- Dell’Isola, F., Seppecher, P., Spagnuolo, M., Barchiesi, E., Hild, F., Lekszycki, T., Giorgio, I., Placidi, L., Andraus, U., Cuomo, M., Eugster, S. R., Pfaff, A., Hoshcke, K., Langkemper, R., Turco, E., Sarikaya, R., Misra, A., De Angelo, M., D’Annibale, F., Bouterf, A., Pinelli, X., Misra, A., Desmorat, B., Pawlikowski, M., Dupuy, C., Scerrato, D., Peyre, P., Laudato, M., Manzari, L., Göransson, P., Hesch, C., Hesch, S., Franciosi, P., Dirrenberger, J., Maurin, F., Vangelatos, Z., Grigoropoulos, C., Melissinaki, V., Farsari, M., Muller, W., Abali, B. E., Liebold, C., Ganzosch, G., Harrison, P., Drobnicki, R., Igumnov, L., Alzahrani, F., and Hayat, T. (2019). Advances in pantographic structures: design, manufacturing, models, experiments and image analyses. *Continuum Mech. Thermodyn.*, **31**(4):1231–1282.
- Duong, T. X., Itskov, M., and Sauer, R. A. (2022). A general isogeometric finite element formulation for rotation-free shells with in-plane bending of embedded fibers. *Int. J. Numer. Meth. Engrg.*, in press, doi: 10.1002/nme.6937; preprint arXiv:2110.00460.
- Duong, T. X., Roohbakhshan, F., and Sauer, R. A. (2017). A new rotation-free isogeometric thin shell formulation and a corresponding continuity constraint for patch boundaries. *Comput. Methods Appl. Mech. Engrg.*, **316**:43–83.
- Ferretti, M., Madeo, A., Dell’Isola, F., and Boisse, P. (2014). Modeling the onset of shear boundary layers in fibrous composite reinforcements by second-gradient theory. *Z. für Angew. Math. Phys.*, **65**:587–612.

- Gasser, T. C., Ogden, R. W., and Holzapfel, G. A. (2006). Hyperelastic modelling of arterial layers with distributed collagen fibre orientations. *J. R. Soc. Interface*, **3**(6):15–35.
- Germain, P. (1973). The method of virtual power in continuum mechanics. Part 2: Microstructure. *SIAM J. Appl. Math.*, **25**(3):556–575.
- Green, A. E. and Naghdi, P. M. (1974). On the Derivation of Shell Theories by Direct Approach. *J. Appl. Mech.*, **41**(1):173–176.
- Green, A. E. and Rivlin, R. S. (1964). Multipolar continuum mechanics. *Arch. Ration. Mech. Anal.*, **17**:113–147.
- Khiêm, V. N., Krieger, H., Itskov, M., Gries, T., and Stapleton, S. E. (2018). An averaging based hyperelastic modeling and experimental analysis of non-crimp fabrics. *Int. J. Solids Struct.*, **154**:43–54.
- Kiendl, J., Hsu, M.-C., Wu, M. C., and Reali, A. (2015). Isogeometric Kirchhoff–Love shell formulations for general hyperelastic materials. *Comput. Methods Appl. Mech. Engrg.*, **291**:280–303.
- Koiter, W. T. (1963). Couple-stresses in the theory of elasticity. *Philos. Trans. Royal Soc.*, **67**:17–44.
- Libai, A. and Simmonds, J. G. (1998). *The Nonlinear Theory of Elastic Shells*. Cambridge University Press, Cambridge, 2nd edition.
- Madeo, A., Barbagallo, G., D’Agostino, M. V., and Boisse, P. (2016). Continuum and discrete models for unbalanced woven fabrics. *Int. J. Solids Struct.*, **94–95**:263–284.
- Mindlin, R. (1964). Micro-structure in linear elasticity. *Arch. Ration. Mech. Anal.*, **16**:51–78.
- Mindlin, R. (1965). Second gradient of strain and surface-tension in linear elasticity. *Int. J. Solids Struct.*, **1**(4):417–438.
- Mindlin, R. D. and Tiersten, H. F. (1962). Effects of couple-stresses in linear elasticity. *Arch. Rational Mech. Anal.*, **11**:415–488.
- Naghdi, P. M. (1982). Finite deformation of elastic rods and shells. In Carlson, D. E. and Shields, R. T., editors, *Proceedings of the IUTAM Symposium on Finite Elasticity*, pages 47–103, The Hague. Martinus Nijhoff Publishers.
- Pietraszkiewicz, W. (1989). Geometrically nonlinear theories of thin elastic shells. *Advances Mech.*, **12**(1):51–130.
- Placidi, L., Greco, L., Bucci, S., Turco, E., and Rizzi, N. L. (2016). A second gradient formulation for a 2D fabric sheet with inextensible fibres. *Z. Angew. Math. Phys.*, **67**(5):114.
- Roohbakhshan, F. and Sauer, R. A. (2017). Efficient isogeometric thin shell formulations for soft biological materials. *Biomech. Model. Mechanobiol.*, **16**:1569–1597.
- Sauer, R. A. and Duong, T. X. (2017). On the theoretical foundations of solid and liquid shells. *Math. Mech. Solids*, **22**:343–371.
- Sauer, R. A., Duong, T. X., Mandadapu, K. K., and Steigmann, D. J. (2017). A stabilized finite element formulation for liquid shells and its application to lipid bilayers. *J. Comput. Phys.*, **330**:436–466.

- Sauer, R. A., Ghaffari, R., and Gupta, A. (2019). The multiplicative deformation split for shells with application to growth, chemical swelling, thermoelasticity, viscoelasticity and elastoplasticity. *Int. J. Solids Struct.*, **174-175**:53–68.
- Schulte, J., Dittmann, M., Eugster, S., Hesch, S., Reinicke, T., Dell’Isola, F., and Hesch, C. (2020). Isogeometric analysis of fiber reinforced composites using Kirchhoff-Love shell elements. *Comput. Methods Appl. Mech. Engrg.*, **362**:112845.
- Simo, J., Rifai, M., and Fox, D. (1990). On a stress resultant geometrically exact shell model. part iv: Variable thickness shells with through-the-thickness stretching. *Comput. Methods Appl. Mech. Engrg.*, **81**(1):91–126.
- Spencer, A. and Soldatos, K. (2007). Finite deformations of fibre-reinforced elastic solids with fibre bending stiffness. *Int. J. Nonlin. Mech.*, **42**(2):355–368.
- Steigmann, D. J. (1999a). Fluid films with curvature elasticity. *Arch. Rat. Mech. Anal.*, **150**:127–152.
- Steigmann, D. J. (1999b). On the relationship between the Cosserat and Kirchhoff-Love theories of elastic shells. *Math. Mech. Solids*, **4**:275–288.
- Steigmann, D. J. (2012). Theory of elastic solids reinforced with fibers resistant to extension, flexure and twist. *Int. J. Nonlin. Mech.*, **47**(7):734–742.
- Steigmann, D. J. (2018). Equilibrium of elastic lattice shells. *J. Eng. Math*, **109**:47–61.
- Steigmann, D. J. and Dell’Isola, F. (2015). Mechanical response of fabric sheets to three-dimensional bending, twisting, and stretching. *Acta Mech. Sin.*, **31**:373–382.
- Tepole, A. B., Kabaria, H., Bletzinger, K.-U., and Kuhl, E. (2015). Isogeometric Kirchhoff-Love shell formulations for biological membranes. *Comput. Methods Appl. Mech. Engrg.*, **293**:328–347.
- Toupin, R. A. (1964). Theories of elasticity with couple-stress. *Arch. Rational Mech. Anal.*, **17**(2):85–112.
- Wang, W.-B. and Pipkin, A. C. (1986). Inextensible networks with bending stiffness. *Q. J. Mech. Appl. Math.*, **39**(3):343–359.
- Wang, W. B. and Pipkin, A. C. (1987). Plane deformations of nets with bending stiffness. *Acta Mechanica*, **65**:263–279.
- Wriggers, P. (2006). *Computational Contact Mechanics*. Springer-Verlag Berlin Heidelberg, 2nd edition.
- Wu, M. C., Zakerzadeh, R., Kamensky, D., Kiendl, J., Sacks, M. S., and Hsu, M.-C. (2018). An anisotropic constitutive model for immersogeometric fluid-structure interaction analysis of bioprosthetic heart valves. *J. Biomech.*, **74**:23 – 31.